

# **Introduction to Remote Sensing**

## **Chapter 3**

### **Sensor Models**

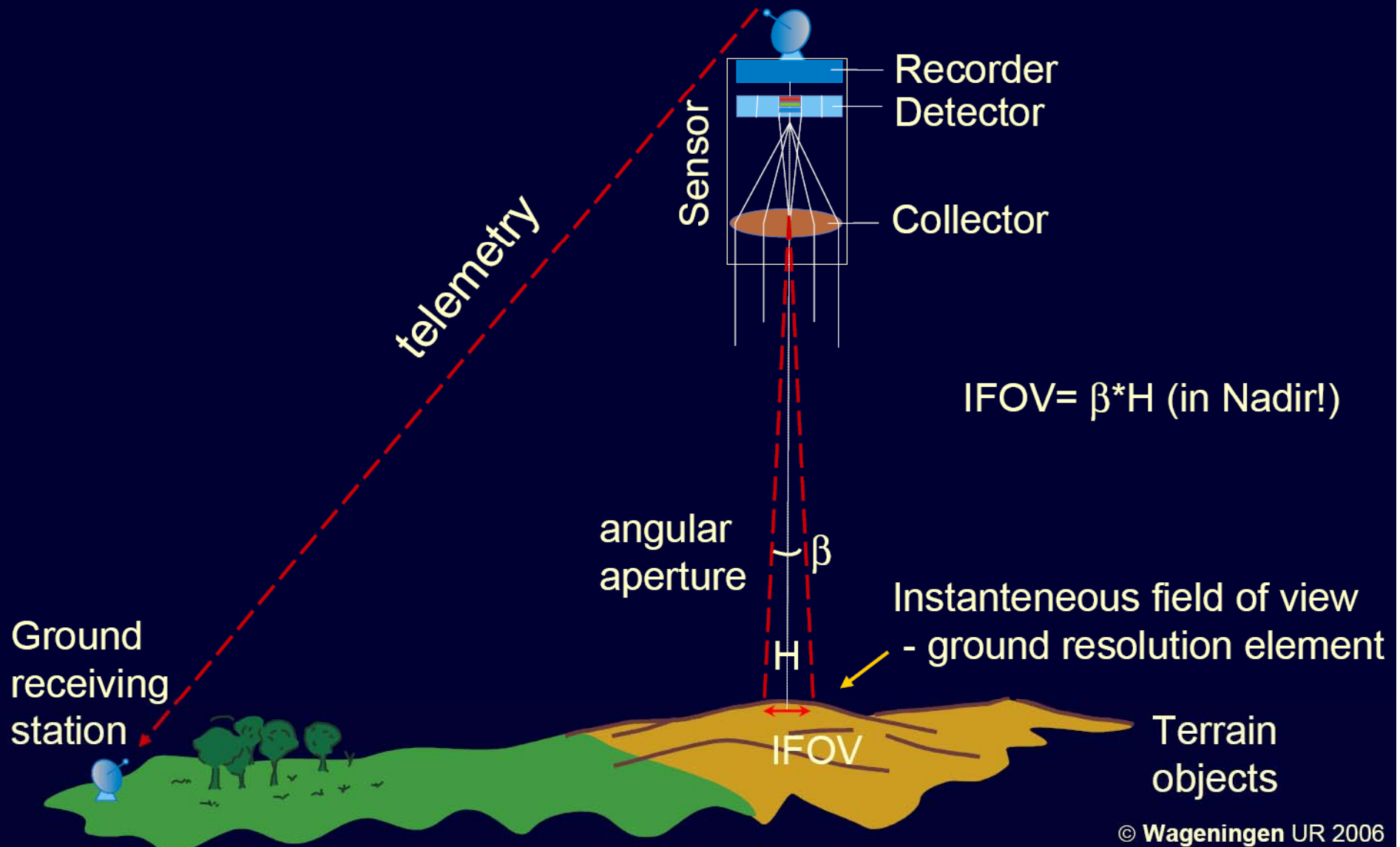
Prof. Vidya Manian  
Dept. of Electrical and Computer  
Engineering

# Overview

- Overall sensor Model
- Spatial Resolution
- Spectral Resolution
- Spatial Response
- Spectral Response
- Signal Amplification
- Simplified Sensor Model
- Geometric Distortion

# Remote Sensing Instrumentation

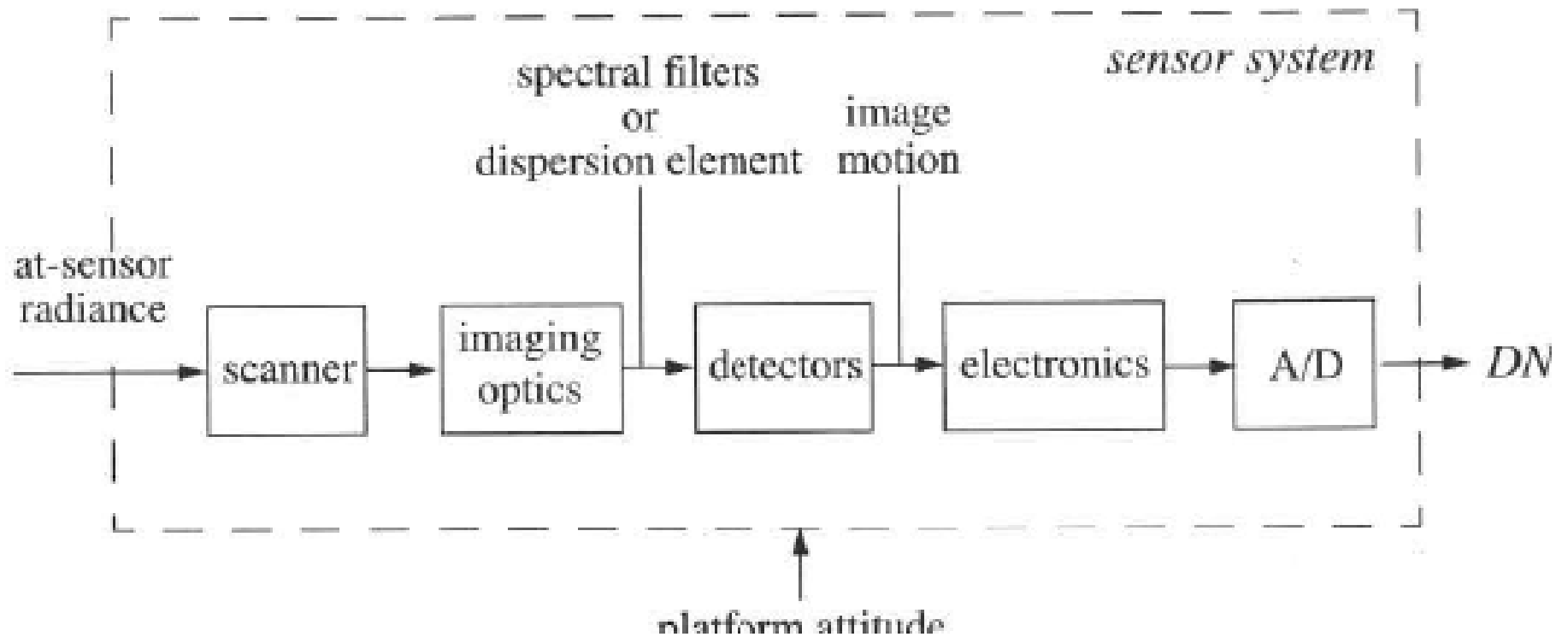
## General concept



- Scanning operation converts spatial at-sensor radiance to a continuous, time-varying optical signal on the detectors
- Detectors convert it to electronic signal
- Signal is sampled and quantized into discrete DN values at the A/D converter

- Several transformations of the data occur
  - Radiometric
  - Spatial
  - Geometric
- The sensor degrades the signal of interest.
- Need to understand degradation to properly design image processing algorithms and interpret their results
- Remote sensors are complex systems of optical, mechanical and electronic components
  - These components determine the quality of the data from the sensor
  - The sensor may be considered a “black-box” that converts at-sensor radiance to DNs

# The primary components in an electro-optical remote sensing systems



# Resolution

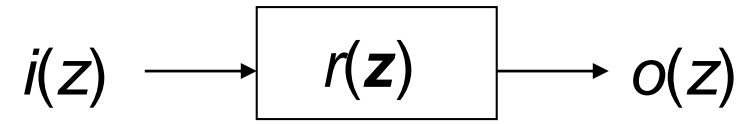
- RS systems have resolution in the spectral, spatial and temporal measurement domains
- Any instrument that measures a physical quantity is limited in the amount of detail it can capture
  - This limit is referred to as the instrument's "resolution"
  - "Resolution" is a term that is widely used, but often misunderstood

# LSI System Model

- Model the various systems as Linear Shift- Invariant (LSI)
  - A linear transformation of the input  $x$  results in a similar transformation of the output  $y$
- Superposition principle
  - If  $T[f_1] = g_1$  and  $T[f_2] = g_2$  , then  $T[a_1f_1 + a_2f_2] = a_1g_1 + a_2g_2$
- Shift invariance: Shifting the input results in a similar shift of the output
  - If  $T[f(x)] = g(x)$  , then  $T[f(x-x_0)] = g(x-x_0)$
- LSI model is generally applicable over the nominal range of operation for these systems
  - Model will break down as performance limits are approached (i.e., system response becomes non-linear)



# Instrument as a LSI System



$$o(\mathbf{z}) = T[i(\mathbf{z})]$$

$$o(\mathbf{z}_0) = \int_W r(\mathbf{z}_0 - \boldsymbol{\alpha}) i(\boldsymbol{\alpha}) d\boldsymbol{\alpha}$$

The instrument weights the input signal in the vicinity ( $W$ ) of  $z$  and integrates the result

$r(\mathbf{z})$  instrument response,  $\mathbf{z}=(x,y)$  or  $\lambda$

- $i(\alpha)$  – input signal
- $R(z_0 - \alpha)$  = instrument response (unit area), inverted and shifted by  $z_0$
- $O(z_0)$  = output signal at  $z = z_0$  and
- $W$  = range over which the instrument response is significant
- Convolution:  $o(z) = i(z) * r(z)$
- Output signal equals the input signal convolved with the response function

# The Ideal Sensor: Infinite Precision

- $r(\mathbf{z}) = \delta(\mathbf{z})$

$$o(\mathbf{z}) = \int_W \delta(\mathbf{z} - \mathbf{a}) i(\mathbf{a}) d\mathbf{a} = i(\mathbf{z})$$

**No instrument can measure a physical signal with infinite precision.**

# Linear Shift-Variant Systems

$$o(\mathbf{z}) = \mathbf{T}[i(\mathbf{z})]$$

$$o(\mathbf{z}) = \int_W r(\mathbf{z}, \boldsymbol{\alpha}) i(\boldsymbol{\alpha}) d\boldsymbol{\alpha}$$

$r(\mathbf{z}, \boldsymbol{\alpha})$  is called the system weighting function.

**The weighting function of the instrument can depend on the “location” being measured.**

# Spatial Resolution

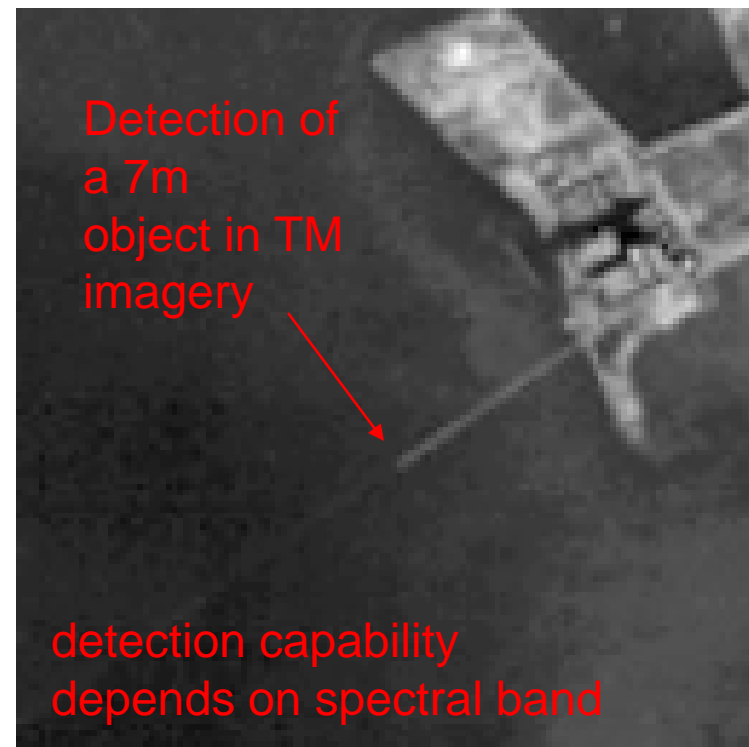
- GSI (ground projected sample interval) or GIFOV (ground projected instantaneous field of view)
- Detect smaller objects if the contrast with the surrounding background is sufficiently high
- Ground area larger than GIFOV with 0 reflectance produces a 0 DN, reflectance of 1 produces maximum DN, say 255
- Area within GIFOV contain two materials 50% each then DN is 128

# Spatial Resolution

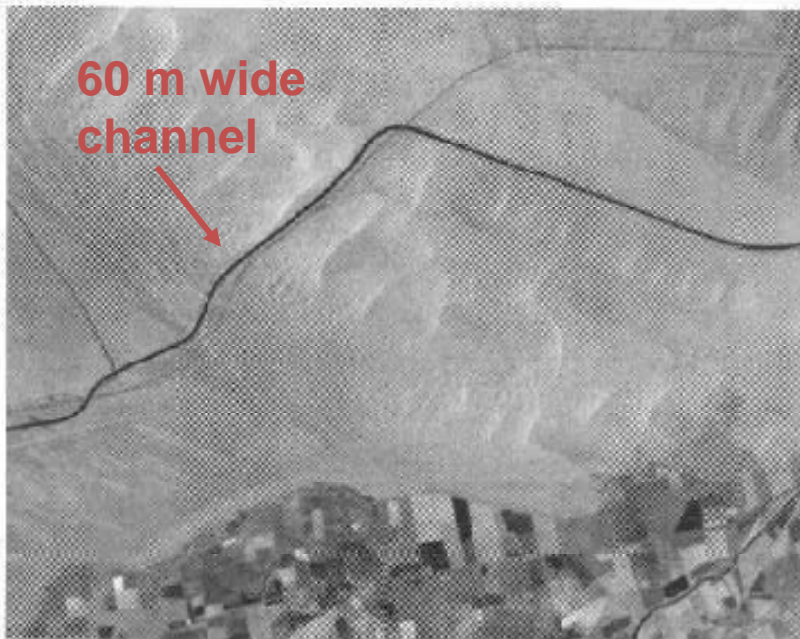
- A “subpixel” object smaller than the GIFOV can be **detected**, but not **resolved**
- Detectability of a subpixel object depends on:
  - object size relative to the sensor GIFOV
  - object radiance contrast to the surrounding background
  - scene noise (“clutter”)
  - sensor noise



Berkeley Pier: 7m wide, concrete and wood

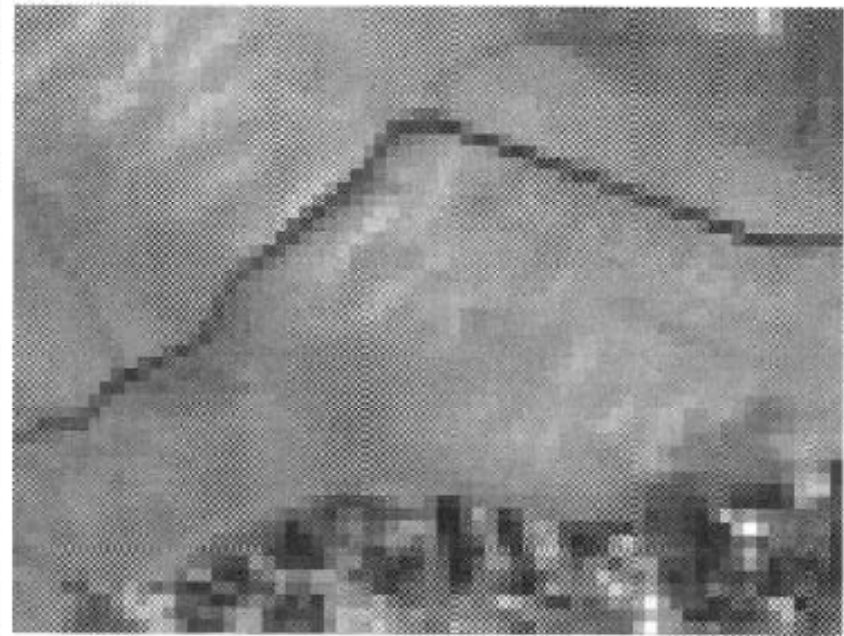


# Another Example of Subpixel Detection



*TM band 4*

**30 m resolution**



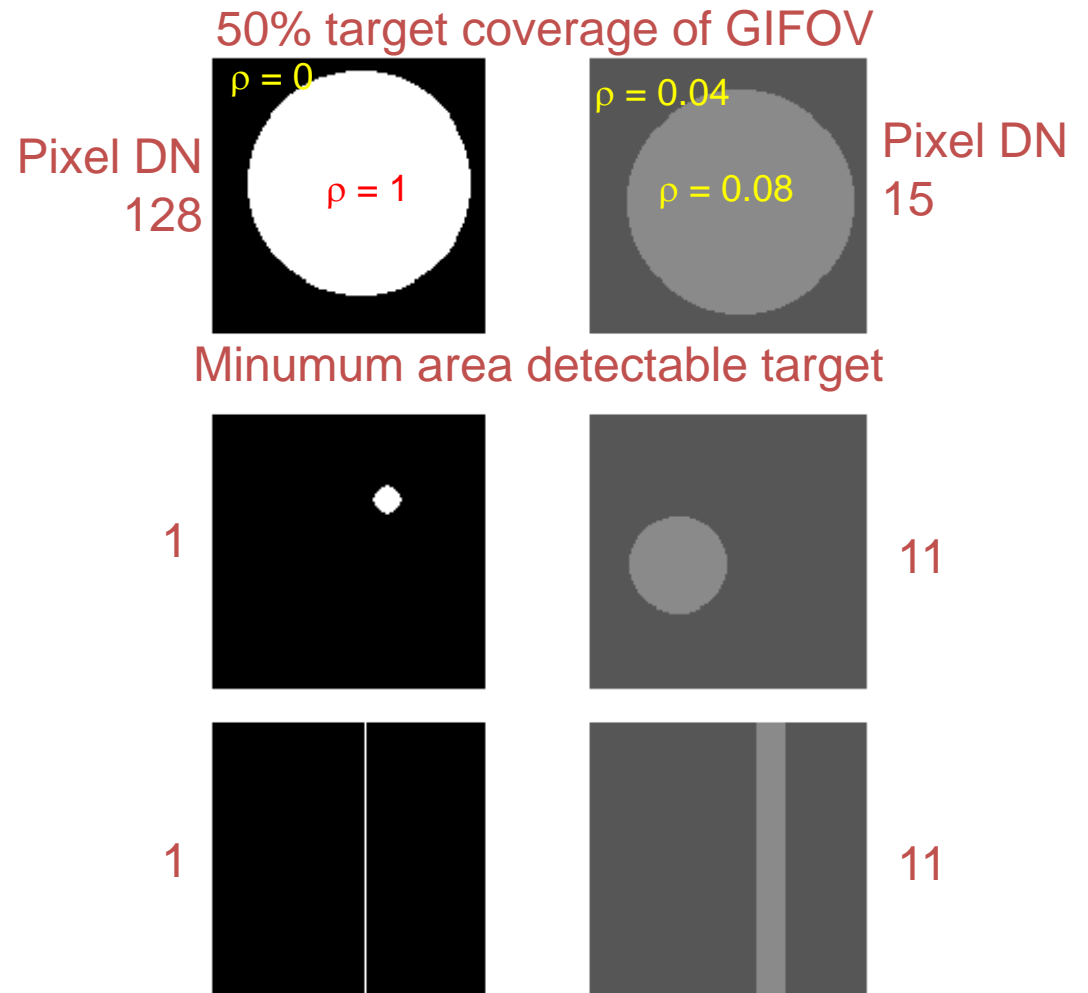
*MODIS band 2*

**250 m resolution**

# Detectability

## Dependence of Object Size and Contrast

- Low-contrast subpixel targets must be bigger than high contrast targets for detection
- Contrast ratio (2:1)

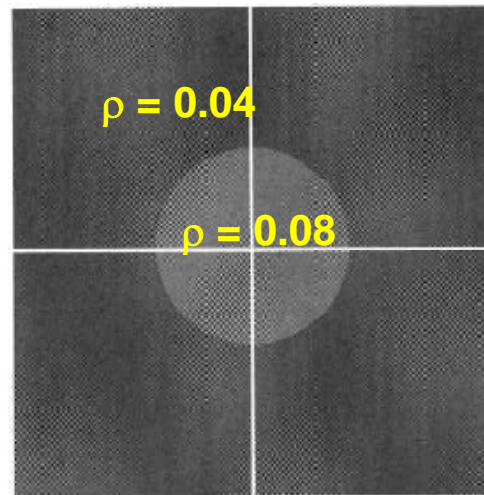




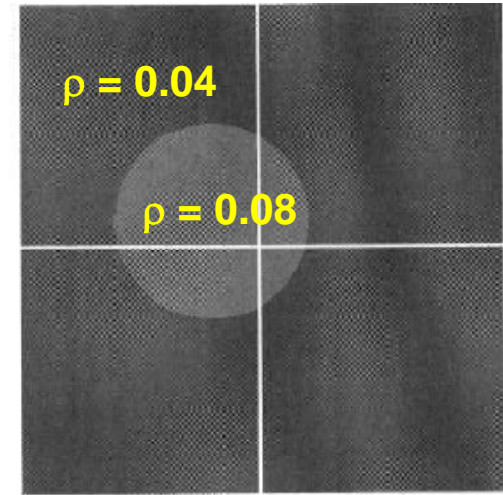
- Size of target  $<10\%$  of a pixel, it falls below threshold (one DN) for detection
- Radiometric quantization, target and background reflectances and sensor GIFOV determine “resolution” of the image
- Sample scene phase: relative location of the pixels and the target, varies from acquisition to acquisition-influences image resolution

# Sample Scene Phase

- The measured radiance of a subpixel object depends on the location of the object relative to the pixel samples



$DN = 11$	$DN = 11$
$DN = 11$	$DN = 11$

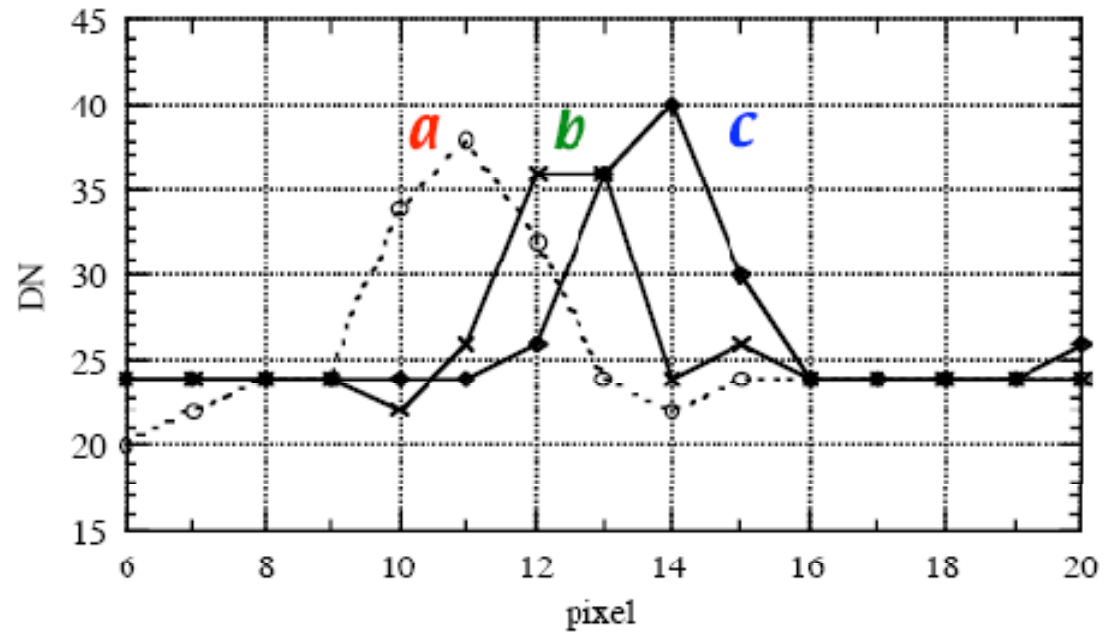
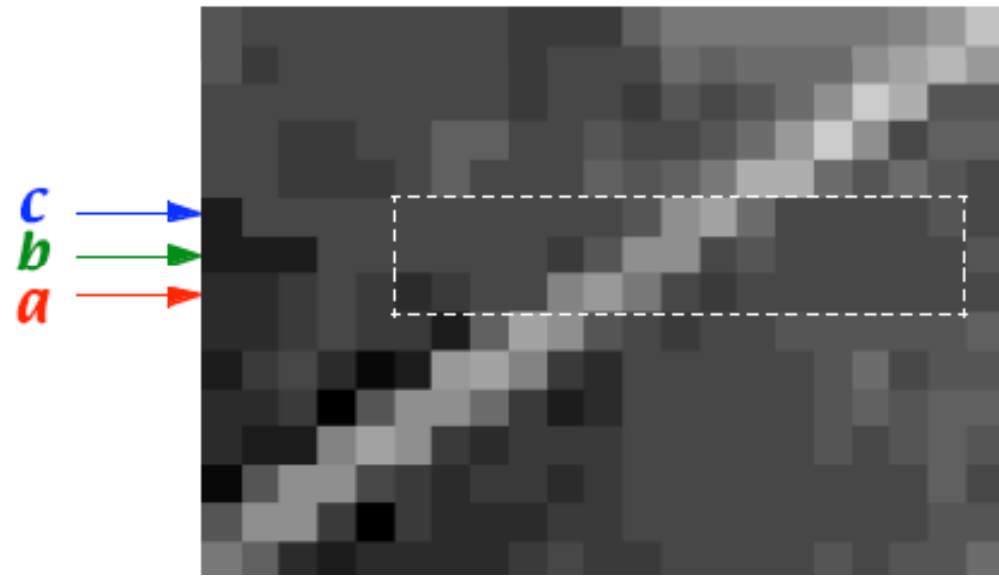


$DN = 13$	$DN = 11$
$DN = 12$	$DN = 10$

- DN profile along each scan line across the pier is different
- It is not oriented at 90 deg to the scan, hence it is one pixel or 2 pixel wide
- To estimate true width of subpixel object, an interleaved composite of many lines should be made, phasing them to fractions of a pixel

More on  
Sample  
Scene Phase

*Three scans across the Berkeley Pier*



# Effects of Atmosphere



a

**Figure 4.4** Poor atmospheric and light conditions can dramatically reduce the effective spatial resolution of a remote sensing system.



b

These images of the same scene were taken by the same sensor system under good (a) and poor (b) atmospheric conditions.

Source: Courtesy of Imagery Resolution Assessments and Reporting Standards Committee.

# Spatial Resolution

- Factors in real images
  - Sensor noise
  - Non-uniform targets and backgrounds
  - Variable solar angle and topography
  - Atmospheric conditions
- Spatial resolution is not so simple!
- In general, the term resolution will refer to the GSI

# Quiz

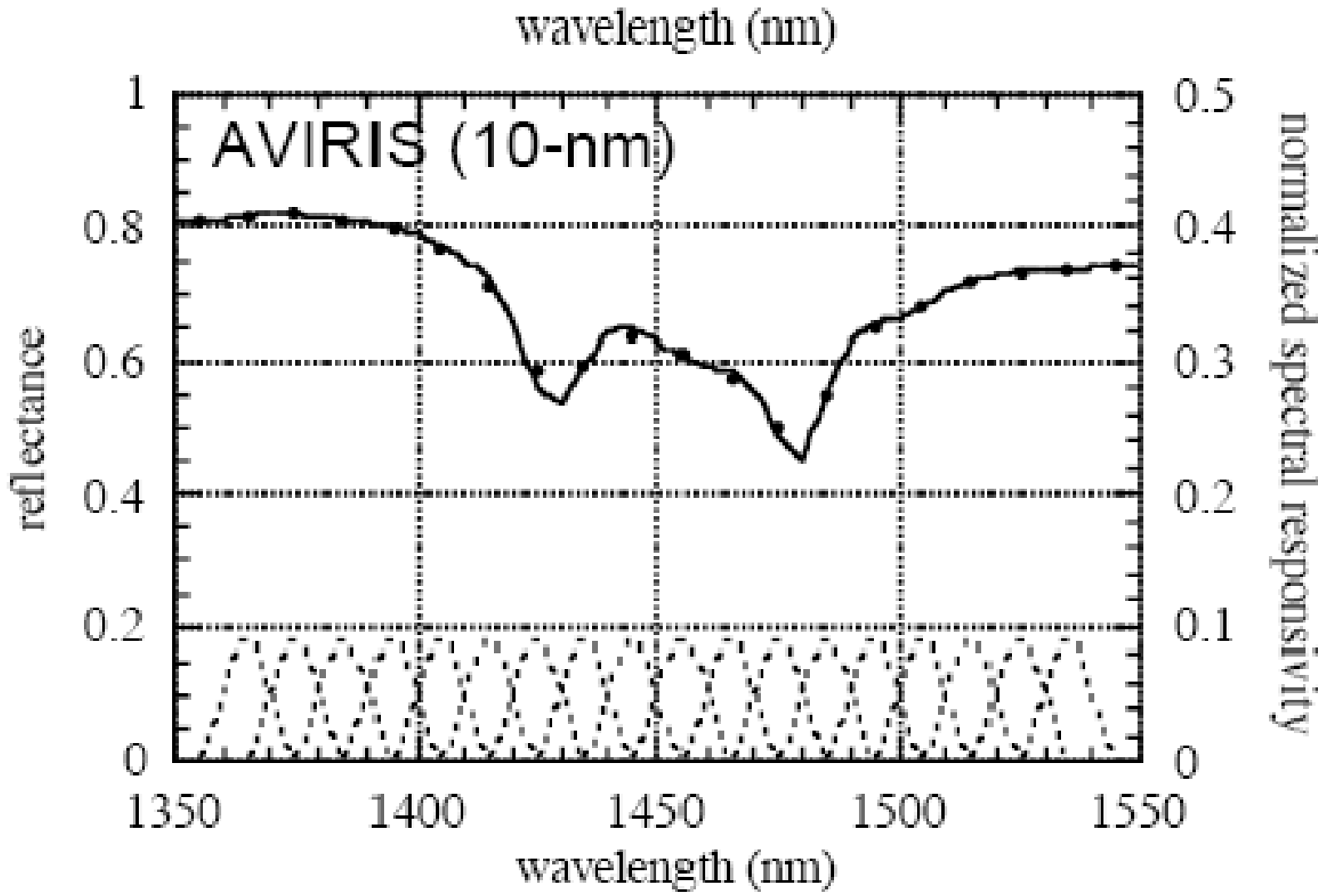
- What are the steps to convert radiance to image DNs
- What is resolution
- What is a LSI system
- What size should the target be with respect to background to be detectable. What DNs should the target pixels have to be detectable

# Spectral resolution

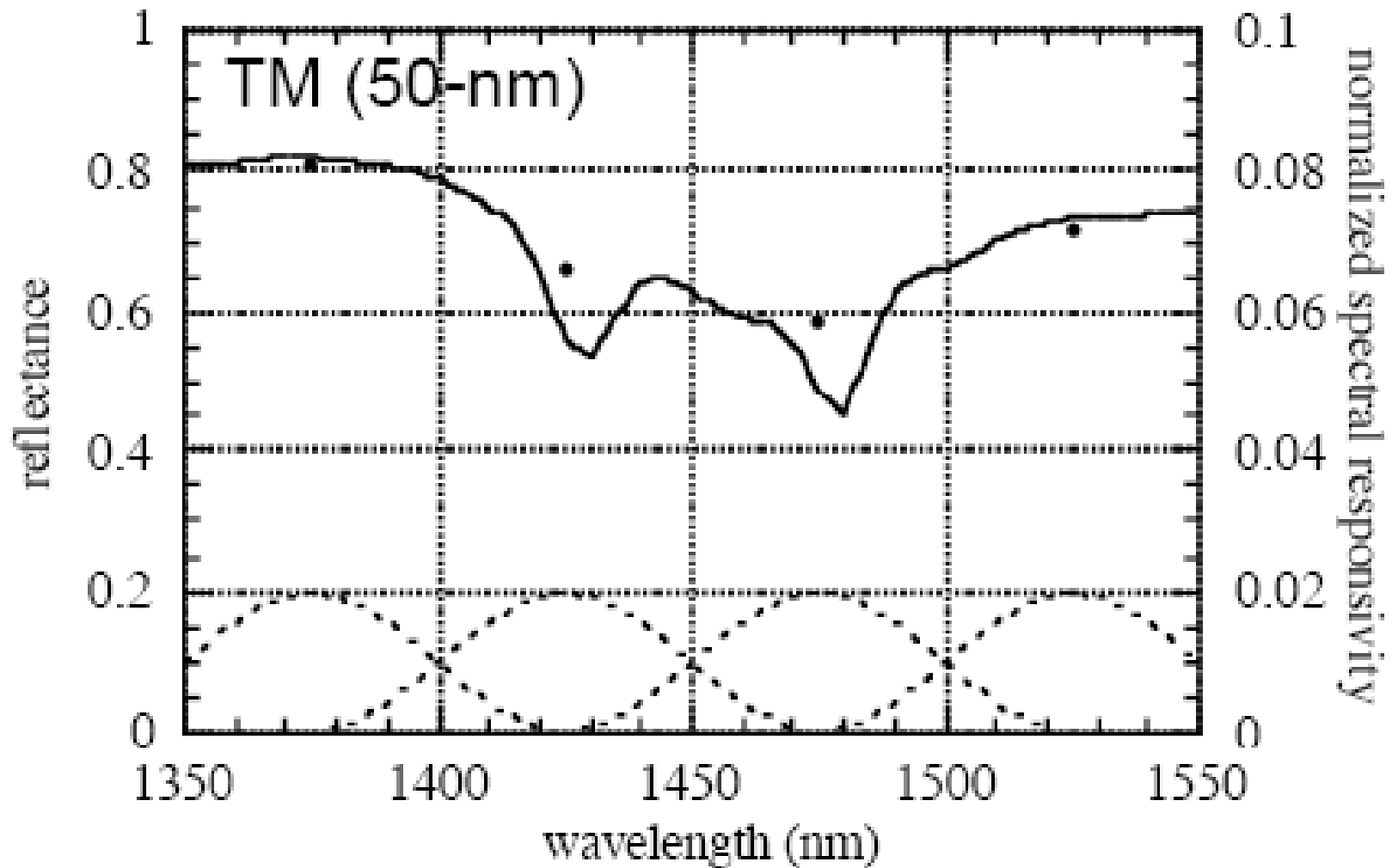
- Total energy measured in each spectral band is a spectrally weighted sum of image irradiance over the spectral passband
- Example –reflectance data for mineral alunite
- Each band sees an effective reflectance which is the weighted reflectance over the band; weighting function is the spectral response of the sensor in each band
- 50nm wide spectral bands-loss of information about the doublet; averaged away by broad spectral bands



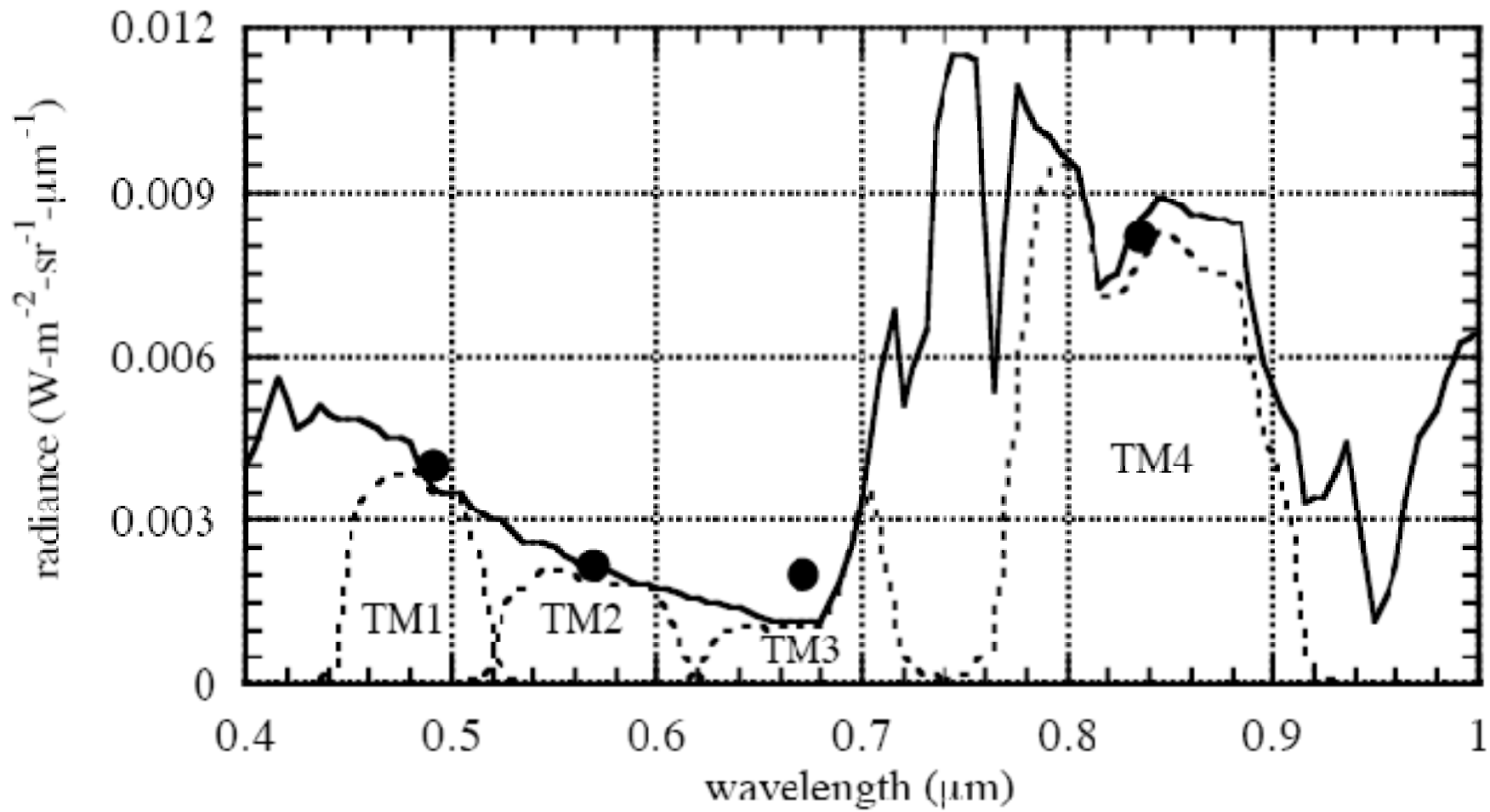
# Reflectance of alunite as measured by a hyperspectral sensor (10nm res)



# Reflectance of alumnite as measured by a multispectral sensor (50nm res.)

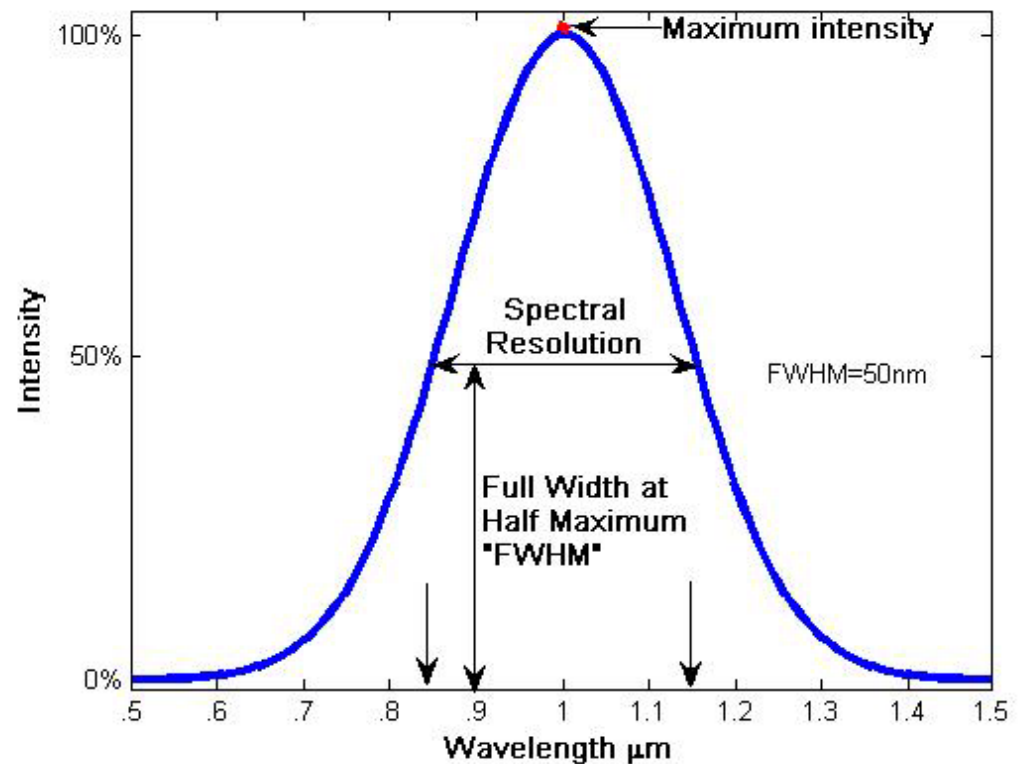


# Simulation of TM band measurements of Kentucky bluegrass



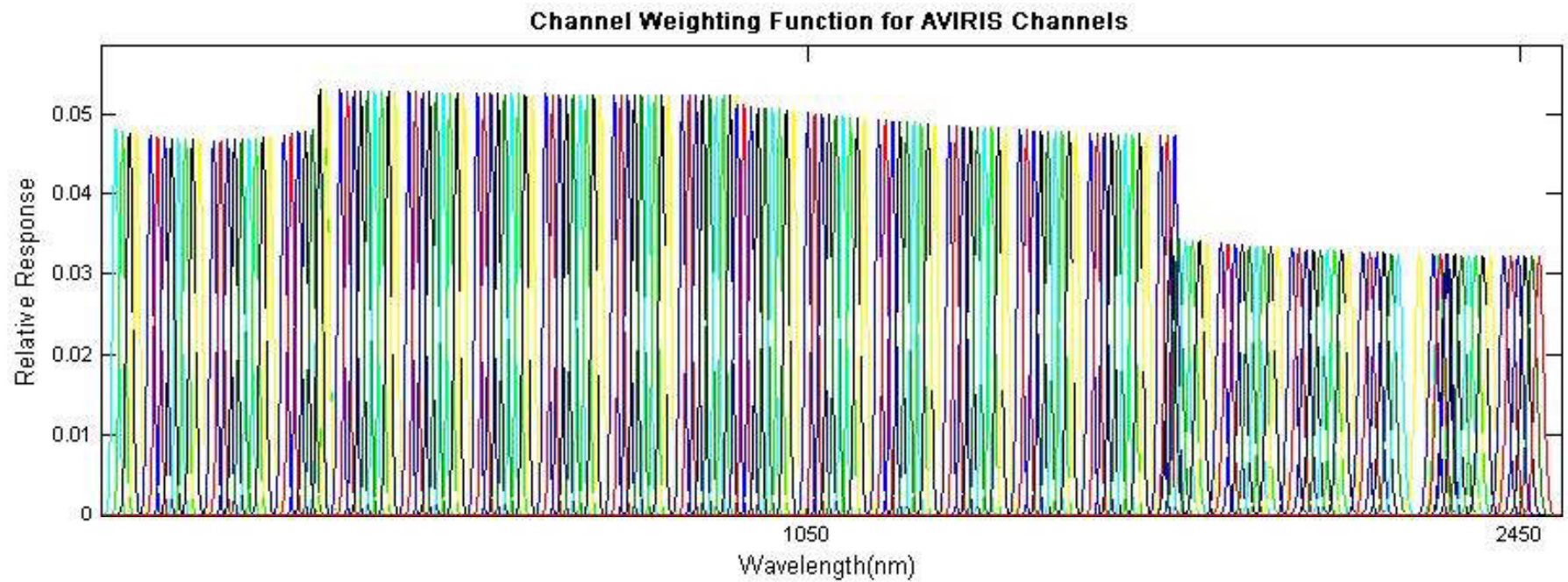
# Spectral Resolution Concepts

- Spectral Resolution
  - Bandwidth in nm or Hz
  - Midvalue
  - Sensitivity curve
- Spectral Range
  - Number and position of the bands

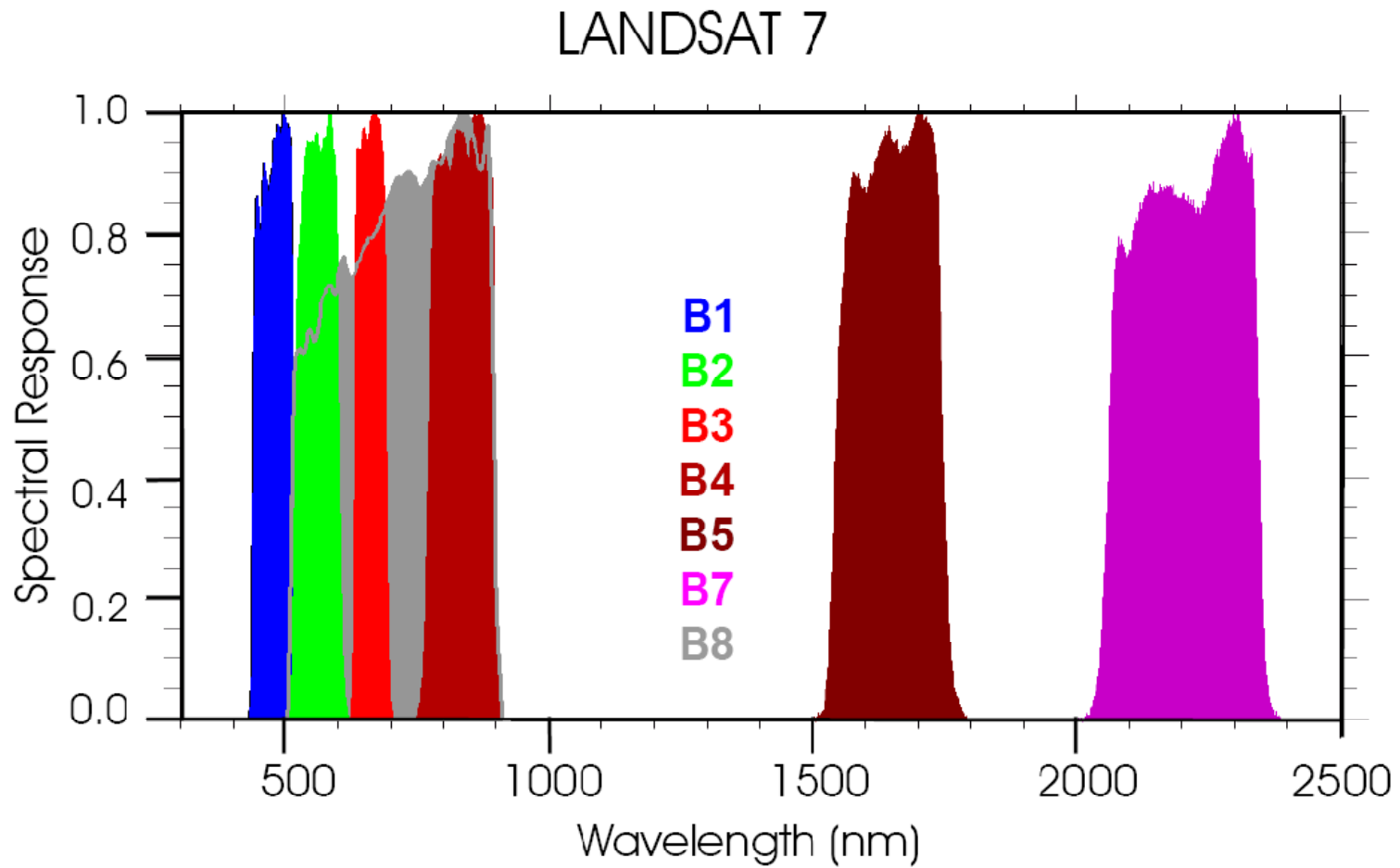


***Spectral Responsivity  $R_b(\lambda)$***

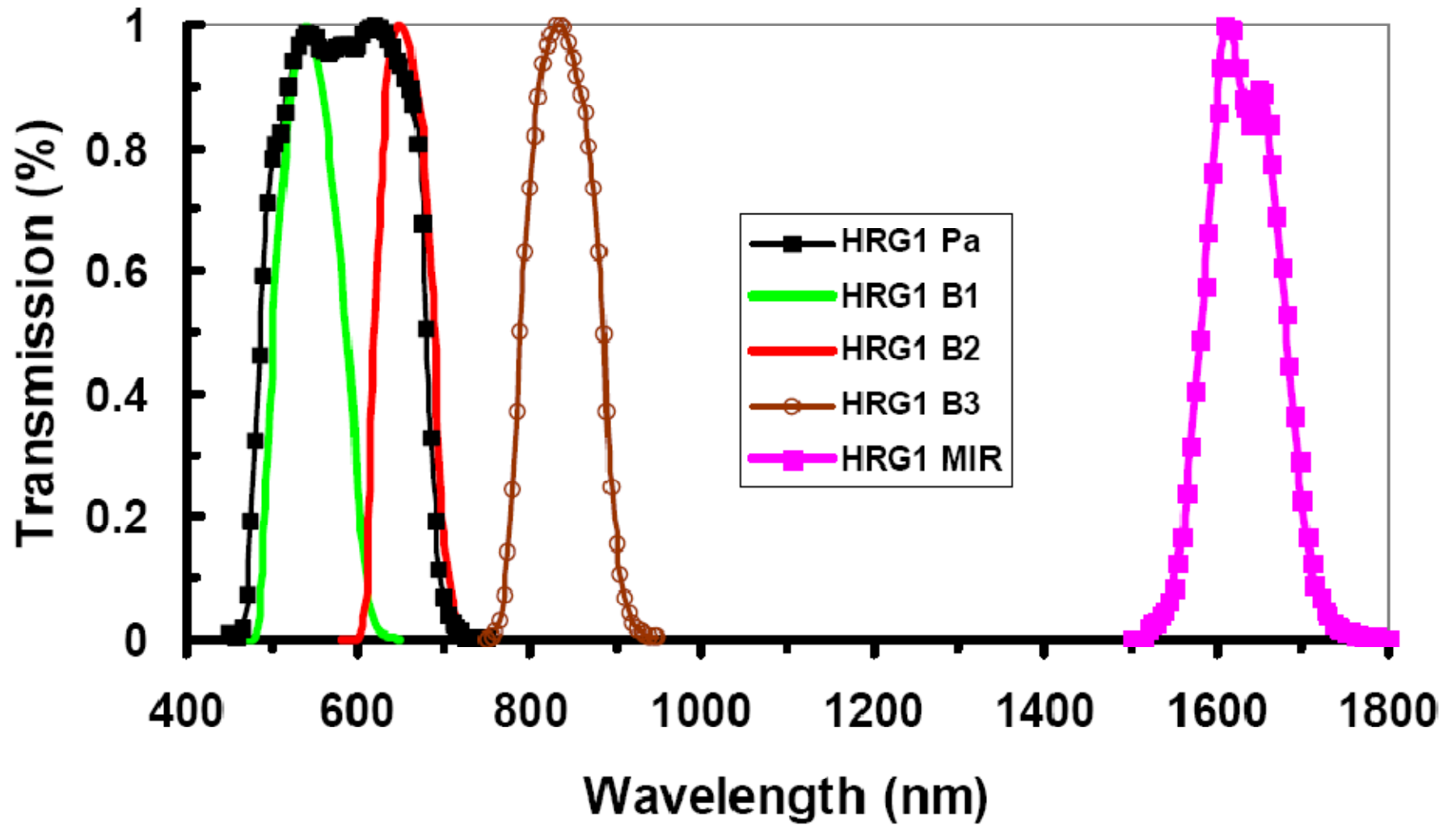
# AVIRIS



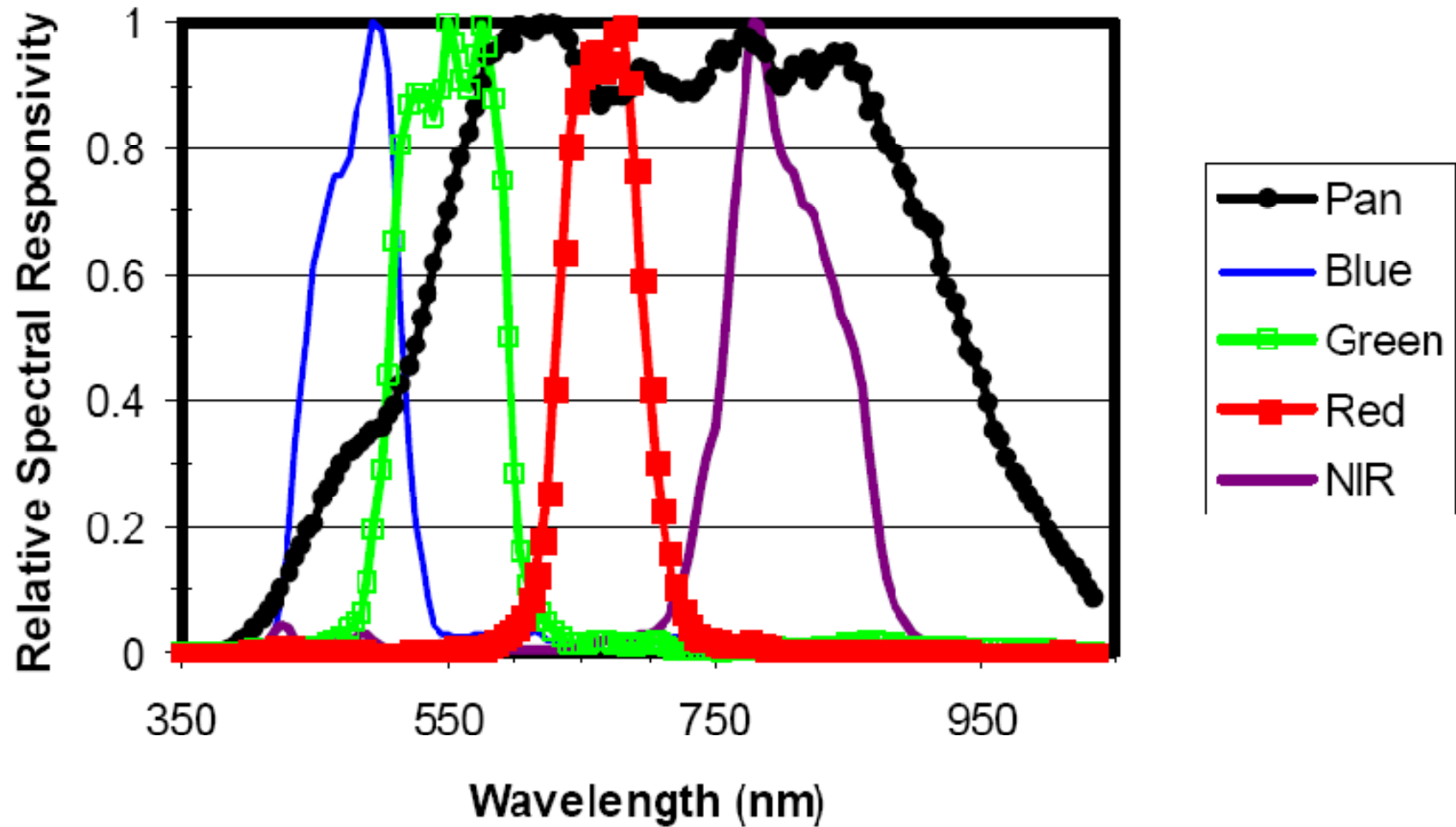
# Landsat 7 ETM+



# SPOT-5 Spectral Response

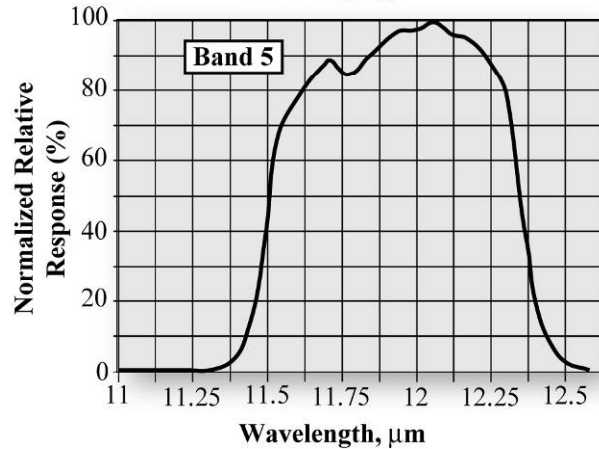
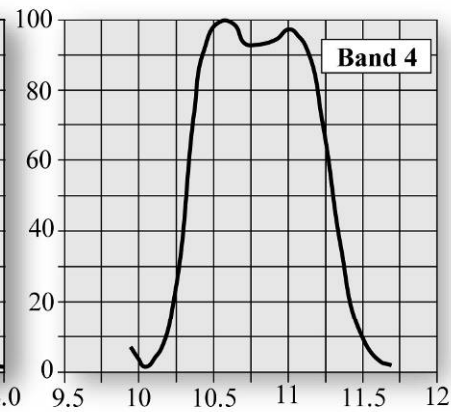
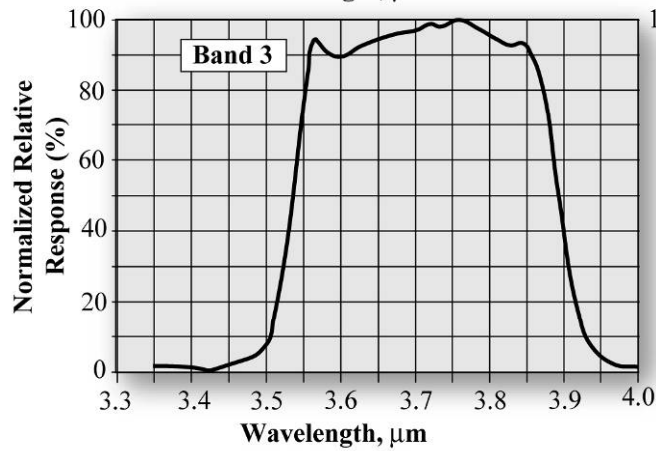
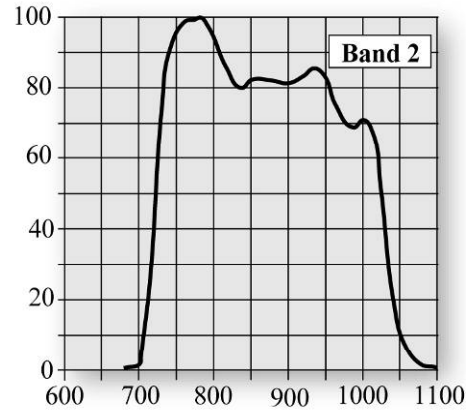
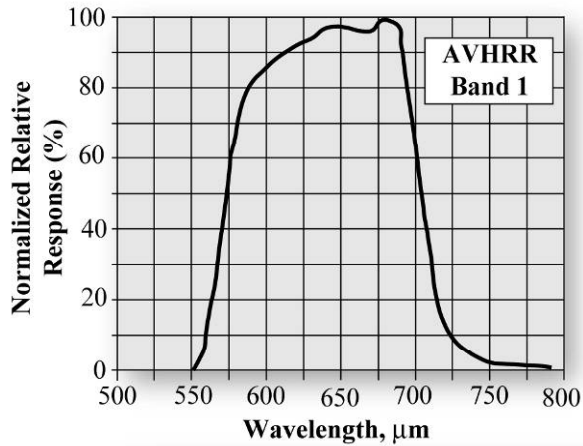


## IKONOS-2 Relative Spectral Response





Advanced Very High  
Resolution Radiometer  
(AVHRR)

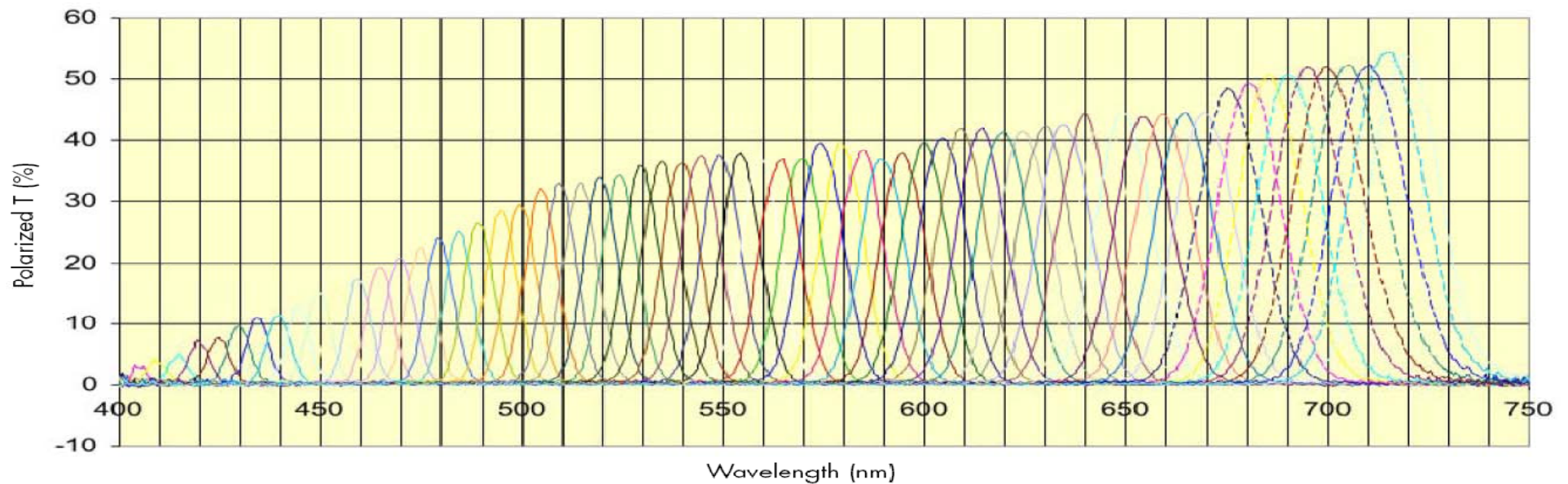


AVHRR-14  
Bandwidths

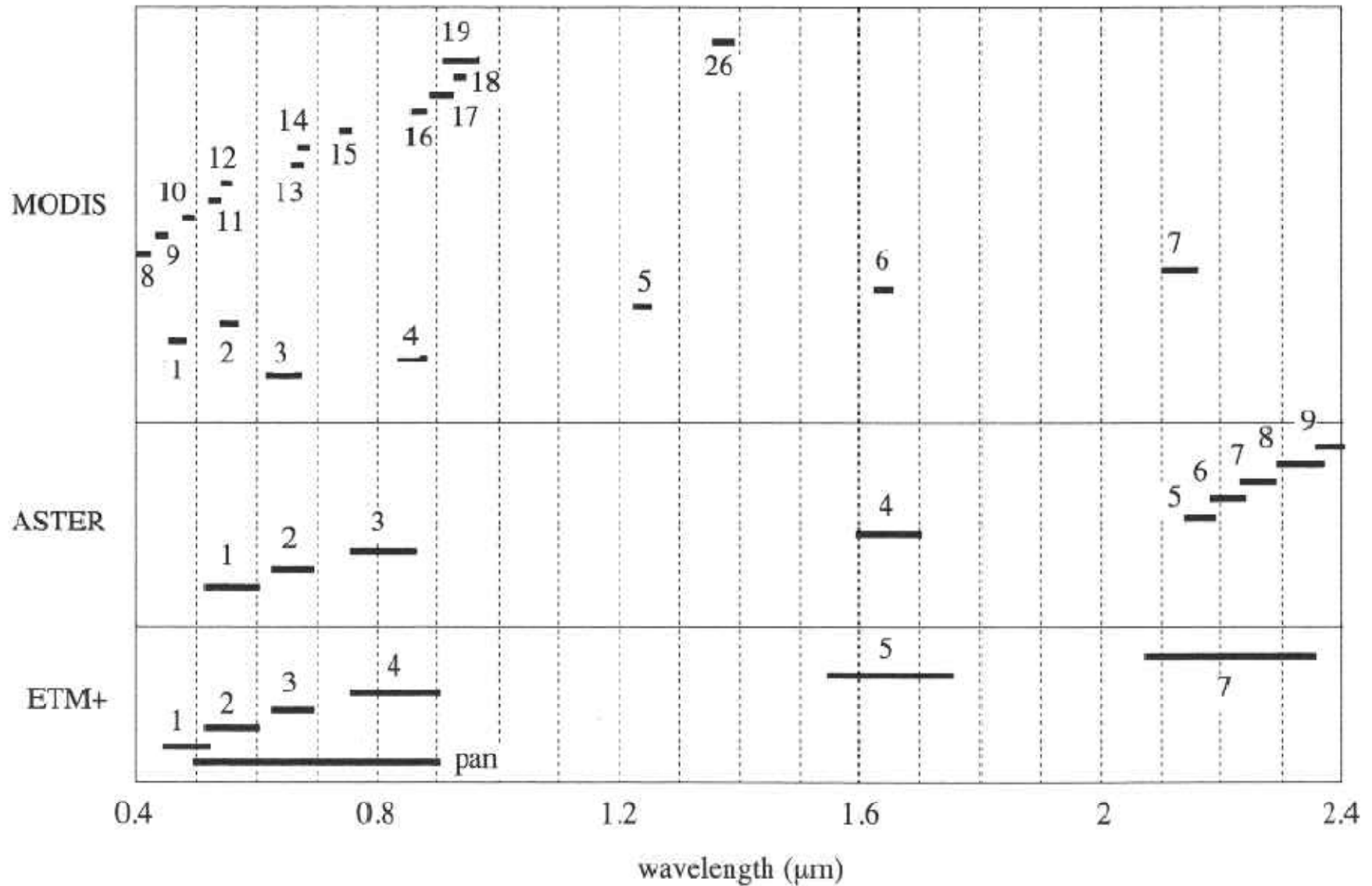
Jensen, 2007

# CRI VariSpec Tunable Imaging Filter

[http://www.cri-inc.com/files/VariSpec\\_Brochure.pdf](http://www.cri-inc.com/files/VariSpec_Brochure.pdf)



# Comparison of the VSWIR spectral bands for MODIS, ASTER and ETM+



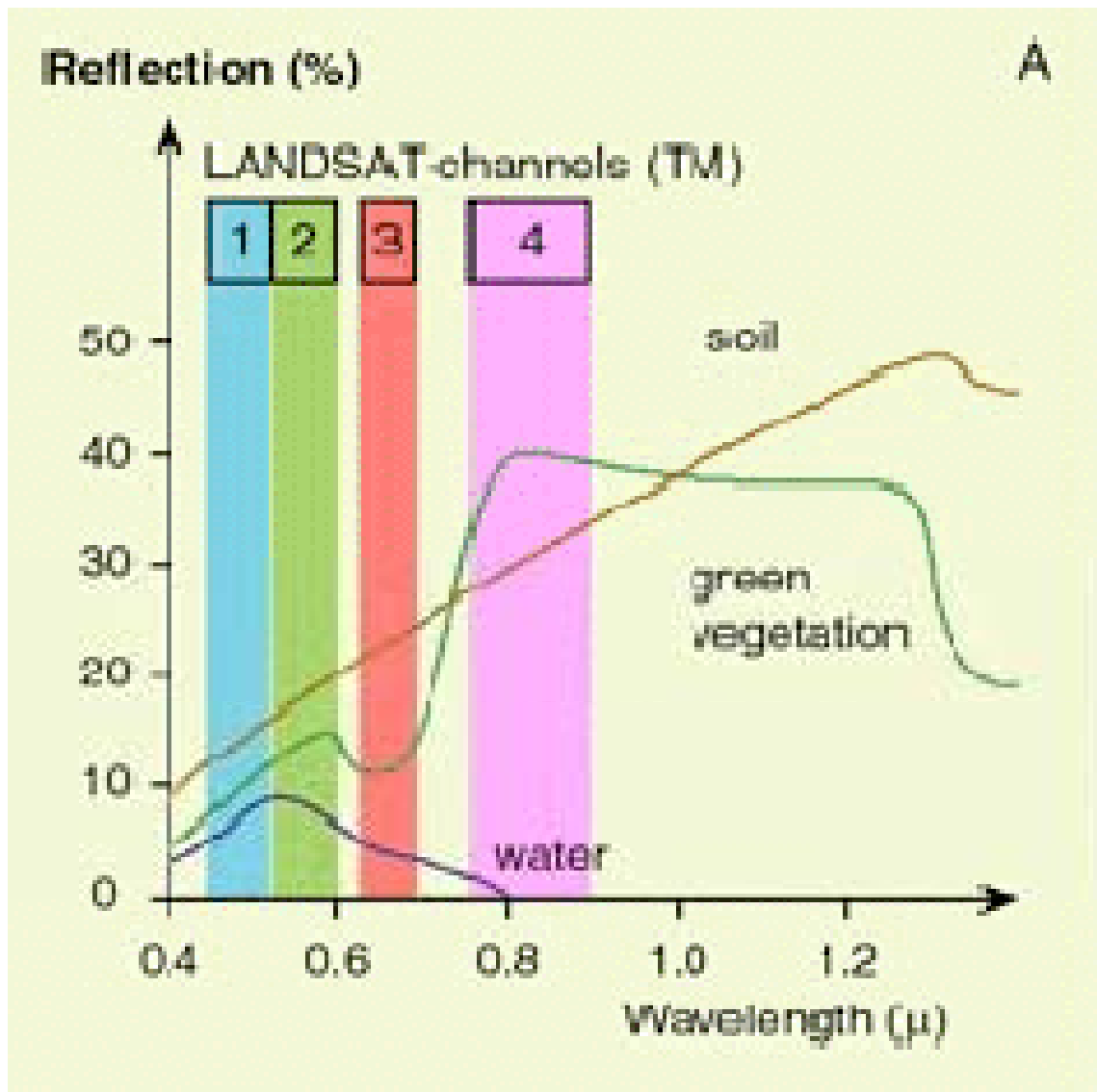
# Spectral Characteristics of AVIRIS vs HYPERION

# Spectral Resolution

- High spectral resolution → imaging spectroscopy
- Multispectral → Placement of bands and spectral bandwidth is important to sensor's ability to resolve spectral features.

# Multispectral is VERY useful

Surface components with very distinct spectral differences can be resolved using broad wavelength ranges



# Spatial response

- The sensor modifies the spatial properties of the scene by(1) blurring due to the sensor's optics, detectors and electronics (2) distortion of geometry
- Small details are blurred relative to larger features characterized by the net sensor Point Spread Function (PSF<sub>net</sub>) – spatial responsivity of sensor

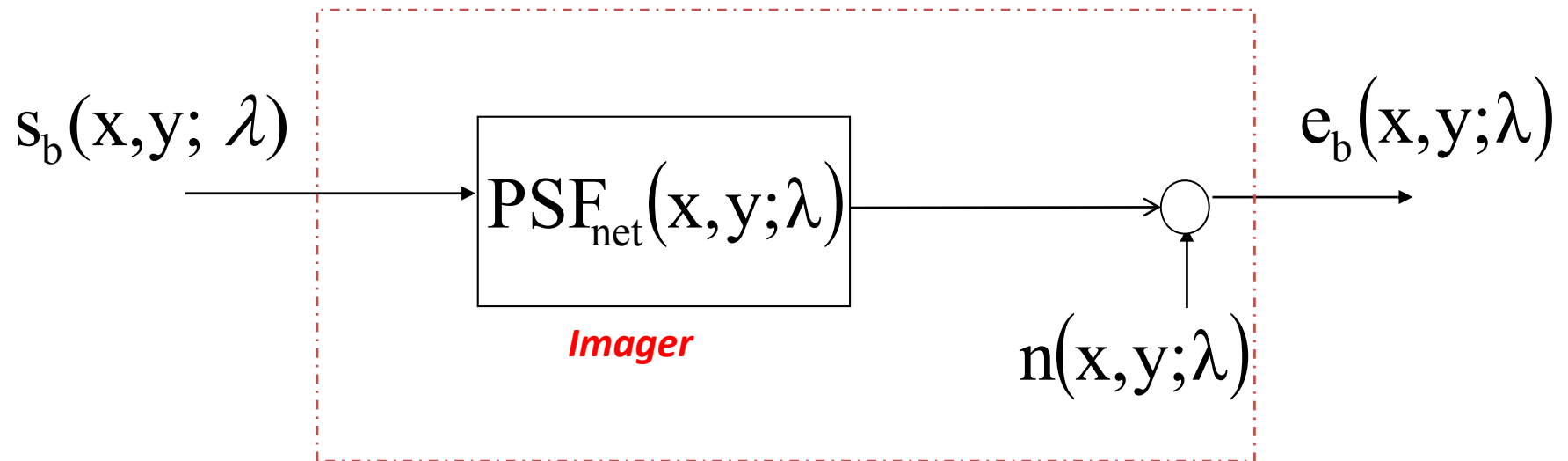
# Quiz

- What is spatial resolution
- What factors affect the objects imaged at a pixel
- What is spectral resolution
- When is it good to have a high or low spectral resolution
- Explain the terms: FOV, GFOV, GSI
- Explain: whiskbroom and pushbroom scanners
- How is at-sensor radiance converted to DN's, give example DN's



# Basic Imaging System Model

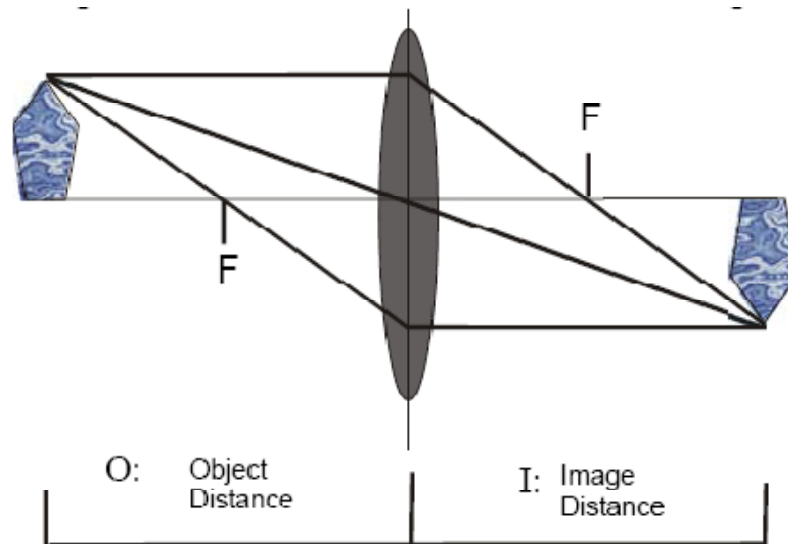
## *Linear Imaging System*



*$\text{PSF}_{\text{net}}(x, y; \lambda)$  is the system point spread function for band centered in  $\lambda$*

# Coordinate System

- The coordinates  $(x,y)$  and all parameters are assumed to be in image space
- Conversion factors
  - Ground distance = image distance / magnification  
= image distance  $\times H/f$
  - Ground velocity = image velocity / magnification  
= image velocity  $\times H/f$



# Spatial Response

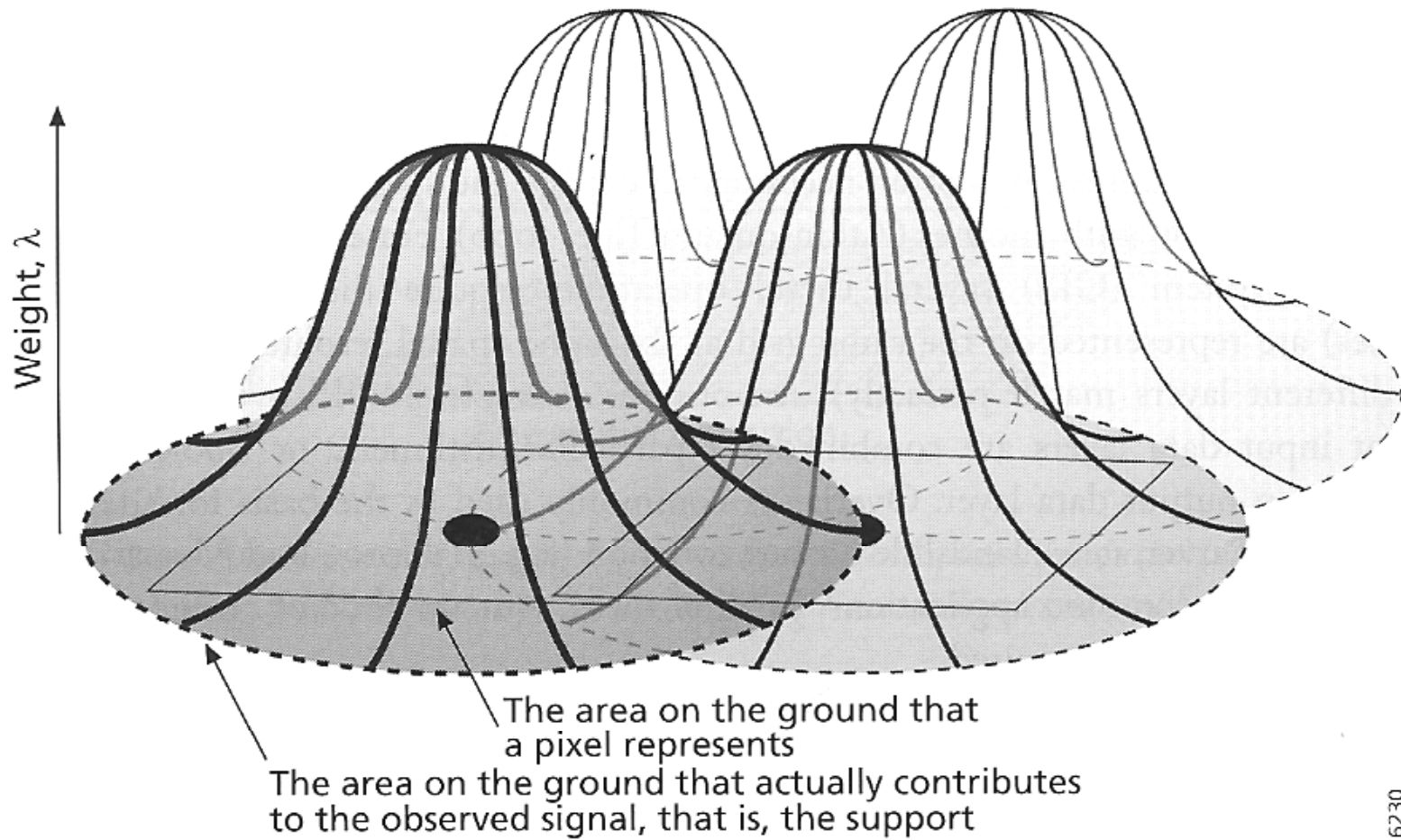
- The spectral signal is convolved with the sensor spatial response

$$e_b(\mathbf{x}, y; \lambda) = \int_{\alpha_{\min}}^{\alpha_{\max}} \int_{\beta_{\min}}^{\beta_{\max}} \text{PSF}_{\text{net}}(\mathbf{x} - \alpha, y - \beta; \lambda) s_b(\alpha, \beta; \lambda) d\alpha d\beta$$

- where the spatial response of an imaging system is now called the Point Spread Function (PSF). Assumes LSI imaging system.
- The net sensor PSF is a convolution of individual responses from:
  - optics  $\text{PSF}_{\text{opt}}$
  - image motion  $\text{PSF}_{\text{IM}}$
  - detector  $\text{PSF}_{\text{det}}$  (defines the geometrical GIFOV)
  - electronics  $\text{PSF}_{\text{el}}$

$$\text{PSF}_{\text{net}}(\mathbf{x}, y) = \text{PSF}_{\text{opt}} * \text{PSF}_{\text{IM}} * \text{PSF}_{\text{det}} * \text{PSF}_{\text{el}}(\mathbf{x}, y)$$

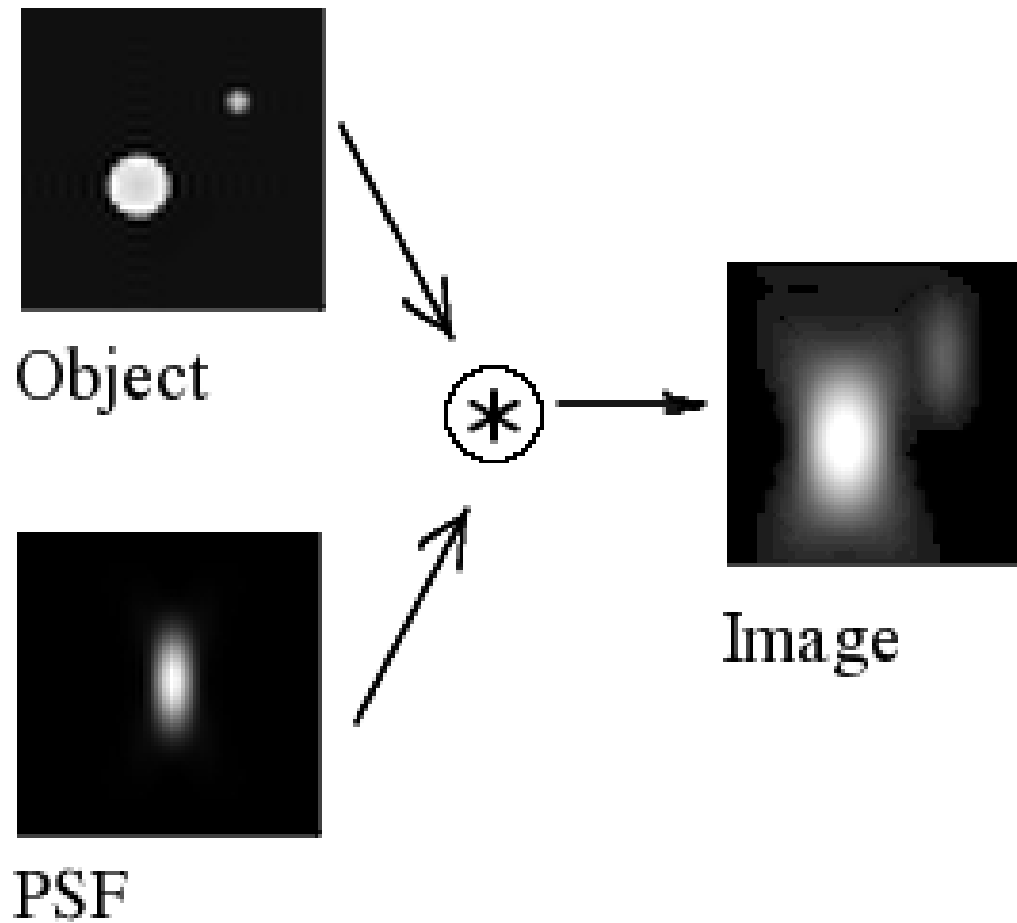
# Spatial Response: Larger than GIFOV



$$\text{PSF}_{\text{net}}(x, y; \lambda)$$

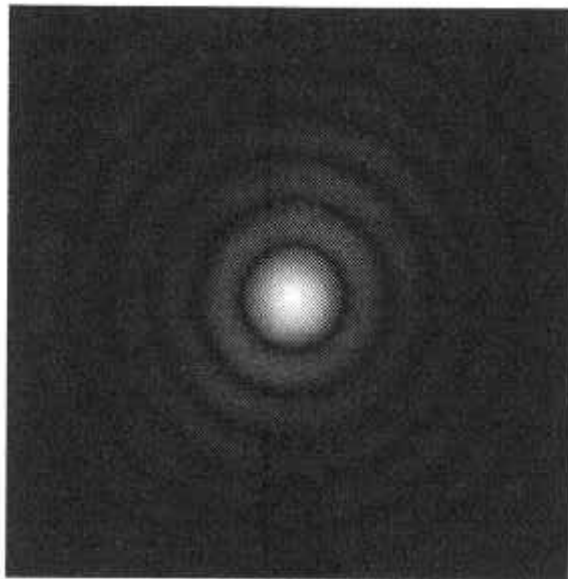
- The total system response to a spatial “impulse” signal
- Larger than geometric GIFOV
  - **time integration smear** (cross-track for whiskbrooms, in-track for pushbrooms)
  - **optics** blur
  - **electronic** filters (cross-track for whiskbrooms; not common for pushbrooms)
  - **detector** electron diffusion, charge transfer inefficiency (pushbrooms)
- The **net spatial response** is the **convolution** of all these factors, converted to a common spatial coordinate system

# Illustration of PSF

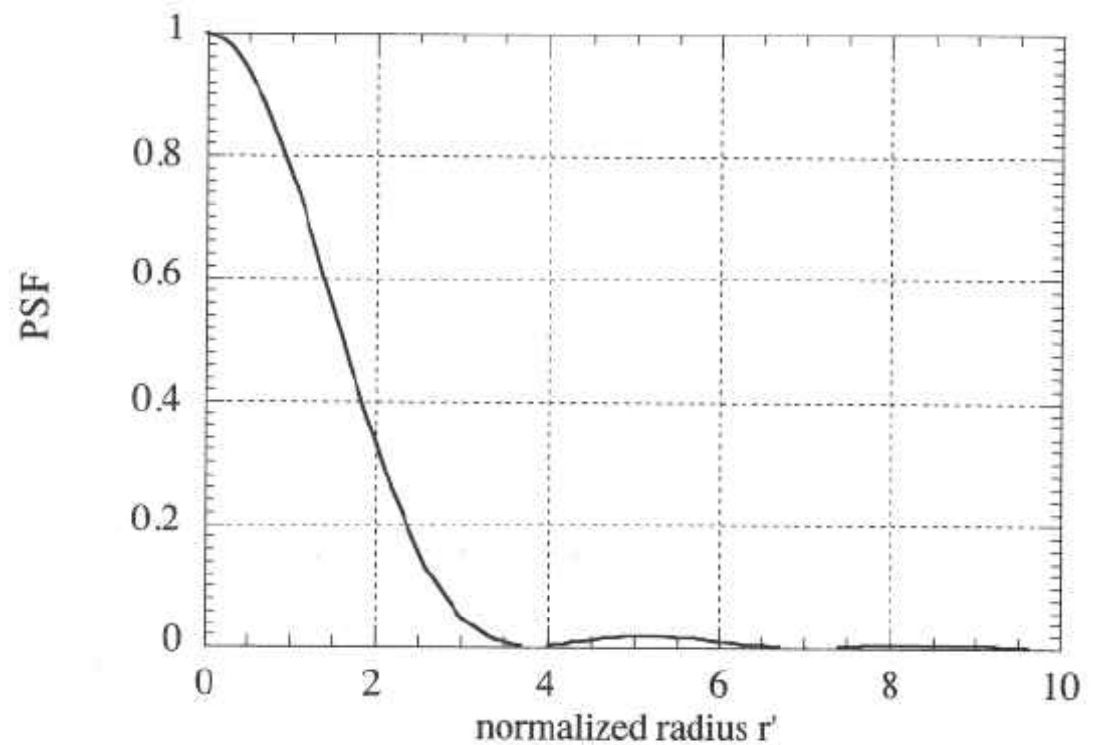


from Wikipedia

Optical PSF  $\rightarrow$  PSF<sub>opt</sub>



*Airy Pattern*



Valid for an optical system with no degradation other than diffraction.

# Optical PSF $\rightarrow$ PSF<sub>opt</sub>

- PSF<sub>opt</sub> is given by

$$PSF(r') = \left[ 2 \frac{J_1(r')}{r'} \right]^2$$

where  $J_1$  is a Bessel function of the first kind and the normalized radius is given by

$$r' = \frac{\pi D}{\lambda f} r = \frac{\pi r}{\lambda N}, \text{ where}$$

$D$  = aperture diameter  
 $f$  = focal length  
 $N$  = f-number  
 $\lambda$  = wavelength of light ,

and the radius to the first dark ring (Airi Disk) is

$$r = 1.22 \left[ \frac{\lambda f}{D} \right] = 1.22 \lambda N,$$

where  $N$  is the optics f-number given by the ratio of the optical focal length  $f$  divided by the aperture stop diameter



# Detector PSF $\rightarrow$ PSF<sub>det</sub>

$$PSF_{det}(x, y) = \text{rect}(x/w)\text{rect}(y/w)$$

*detector PSF<sub>det</sub>*

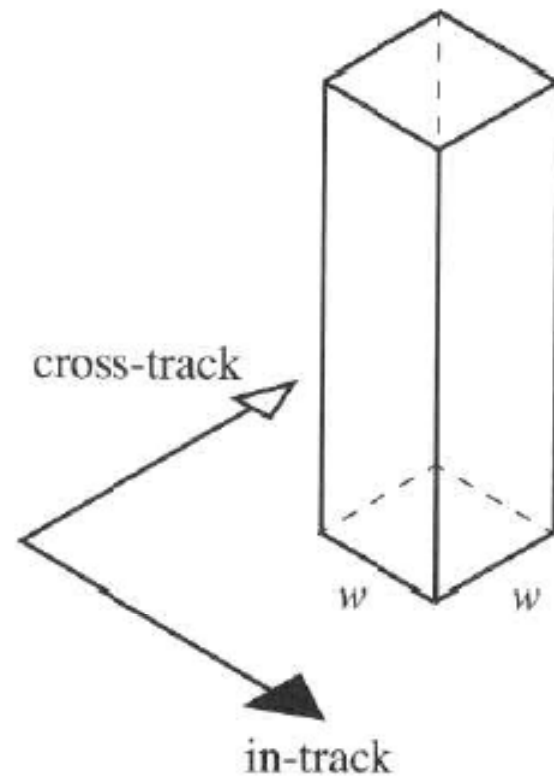
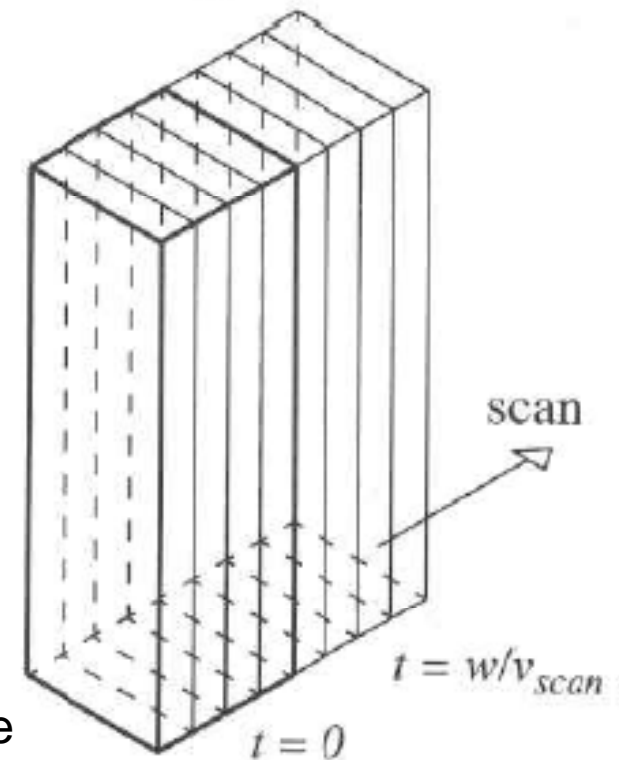


# Image Motion $\rightarrow$ $PSF_{IM}$

*image motion  
during scan*



*whiskbroom scanner:  $PSF_{IM}(x, y) = \text{rect}(x/s)$*

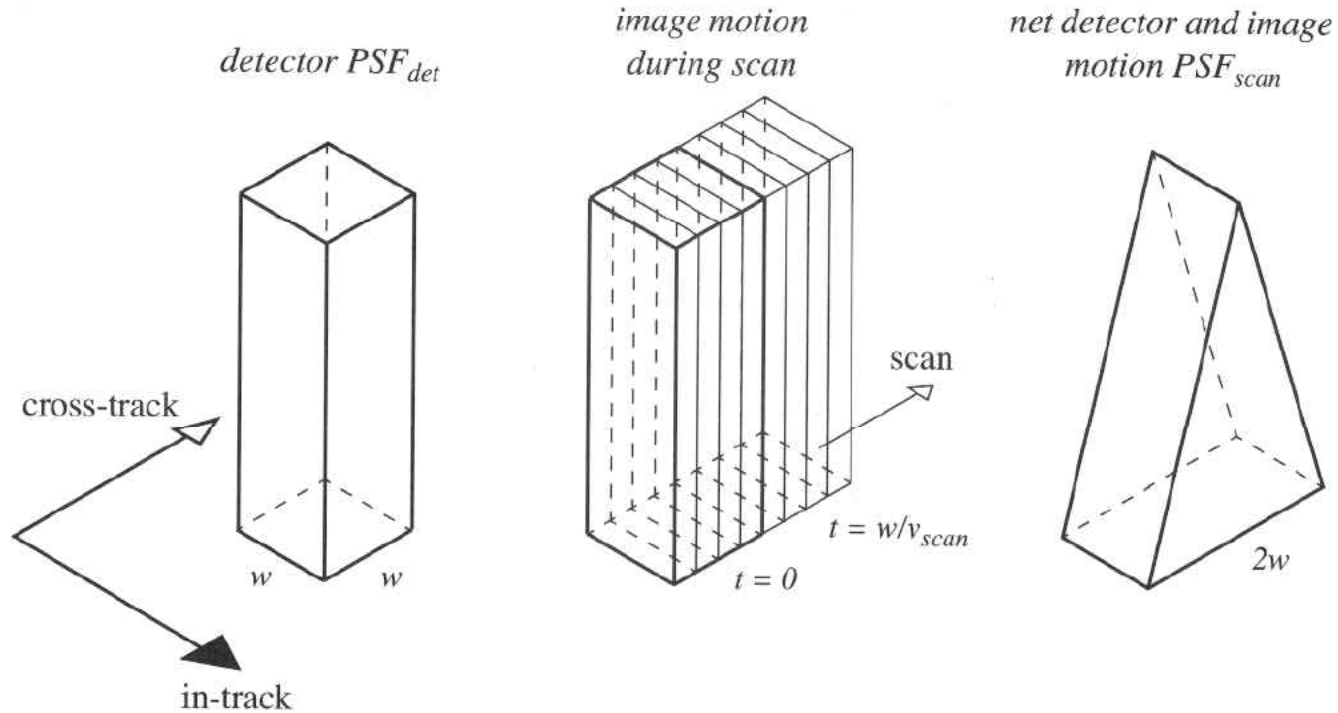
*pushbroom scanner:  $PSF_{IM}(x, y) = \text{rect}(y/s)$*

where  $s$  is the spatial smear of the image in the focal plane

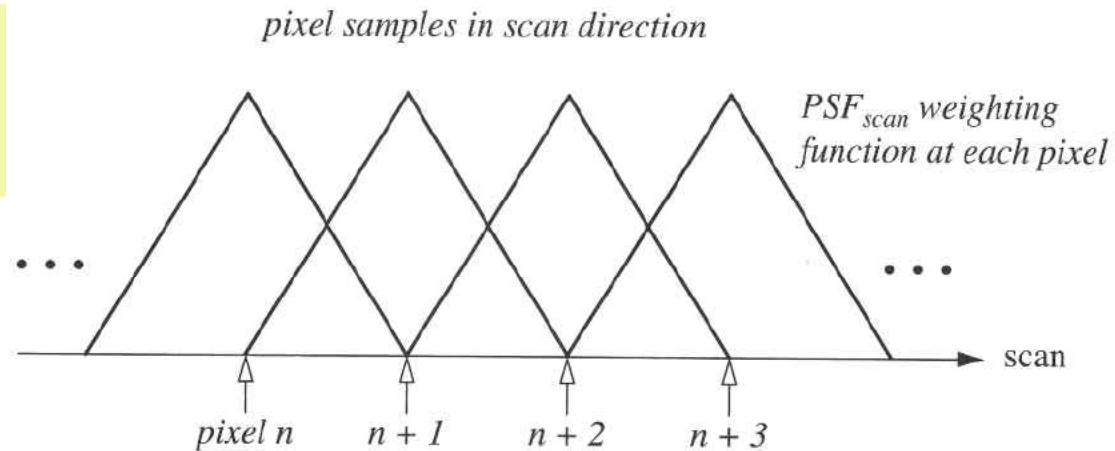
*whiskbroom scanner:  $s = \text{scan velocity} \times \text{integration time}$*

*pushbroom scanner:  $s = \text{platform velocity} \times \text{integration time}$*

# MODIS: $PSF_{det} * PSF_{IM}$



50% overlapping of neighboring pixels!



# Electronics PSF $\rightarrow$ PSF<sub>el</sub>

- Detectors signal is filtered to reduce noise.
  - AVHRR, MSS, TM and ETM+ whiskbroom scanners use a low-pass Butterworth type filter
  - Pushbroom scanners have no filters but introduce PSF due to intrinsic properties
- Time domain  $\rightarrow$  Equivalent to a spatial dependence

*whiskbroom scanner:*  $x = \text{scan velocity} \times \text{sample time interval}$

*pushbroom scanner:*  $y = \text{platform velocity} \times \text{sample time interval}$

Net PSF  $\rightarrow$  PSF<sub>net</sub>

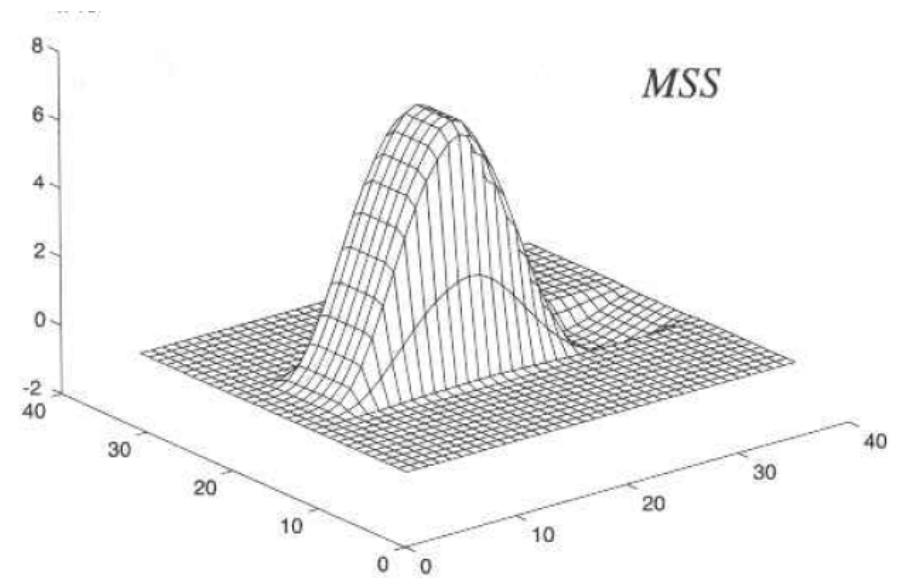
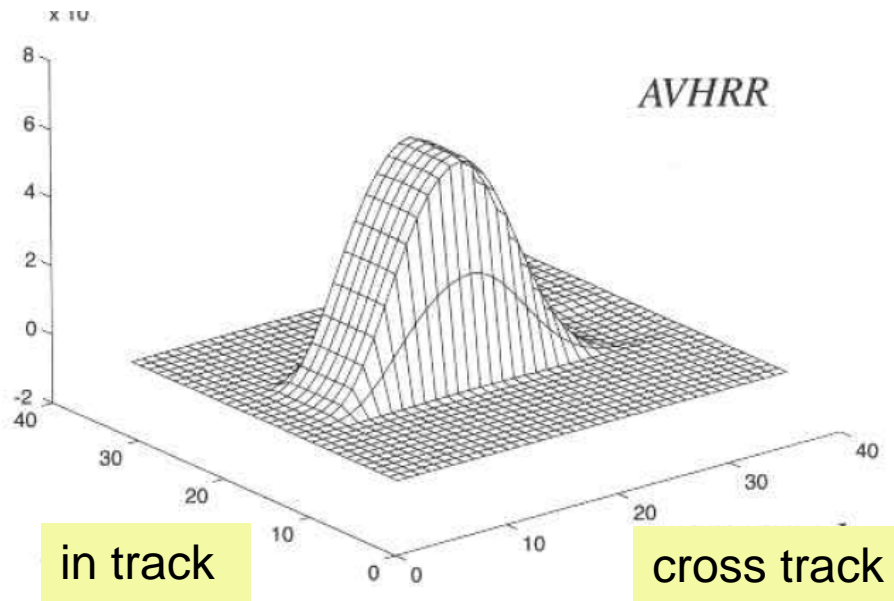
$$\text{PSF}_{\text{net}}(x, y) = \text{PSF}_{\text{opt}} * \text{PSF}_{\text{IM}} * \text{PSF}_{\text{det}} * \text{PSF}_{\text{el}}(x, y)$$

# PSF Properties

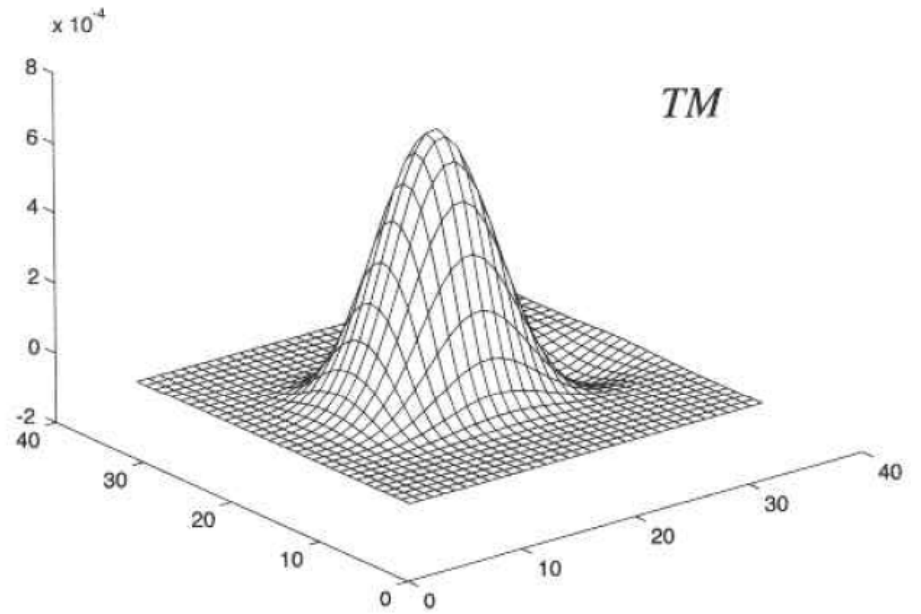
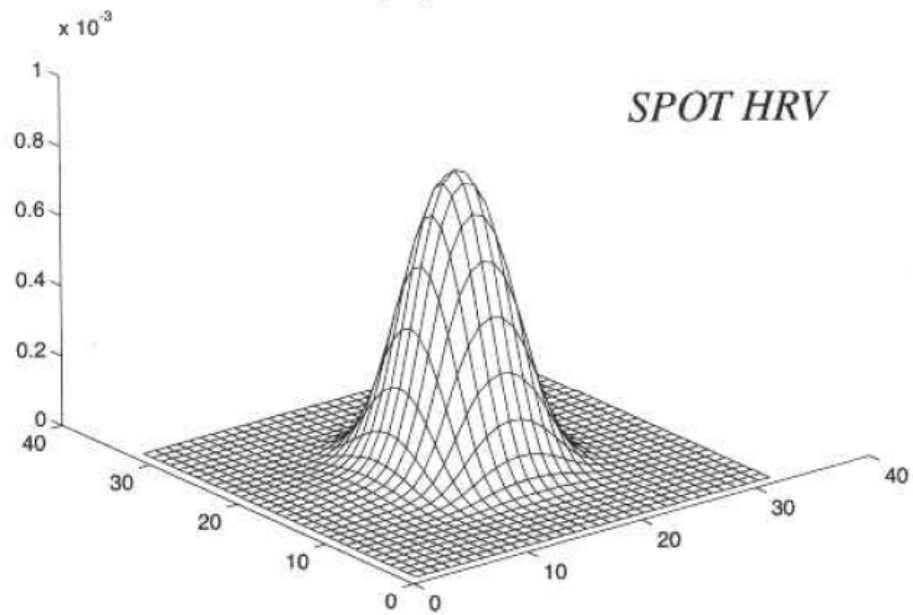
- The net sensor PSF is wider than the GIFOV because of
  - $\text{PSF}_{\text{opt}}$  in both directions
  - $\text{PSF}_{\text{IM}}$ 
    - cross-track for whiskbroom scanners
    - in-track for pushbroom scanners
  - $\text{PSF}_{\text{el}}$  cross-track for whiskbroom scanners
- Reasonable assumption in many cases is that the PSF is **separable** in the cross-track and intrack directions

$$\text{PSF}_{\text{net}}(x, y) = \text{PSF}_i(x)\text{PSF}_c(y)$$

# PSF for AVHRR and MSS

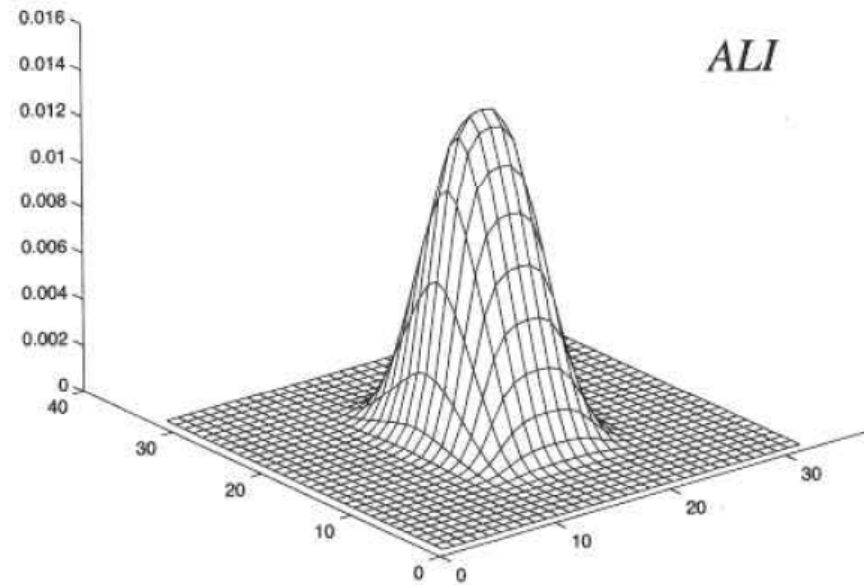
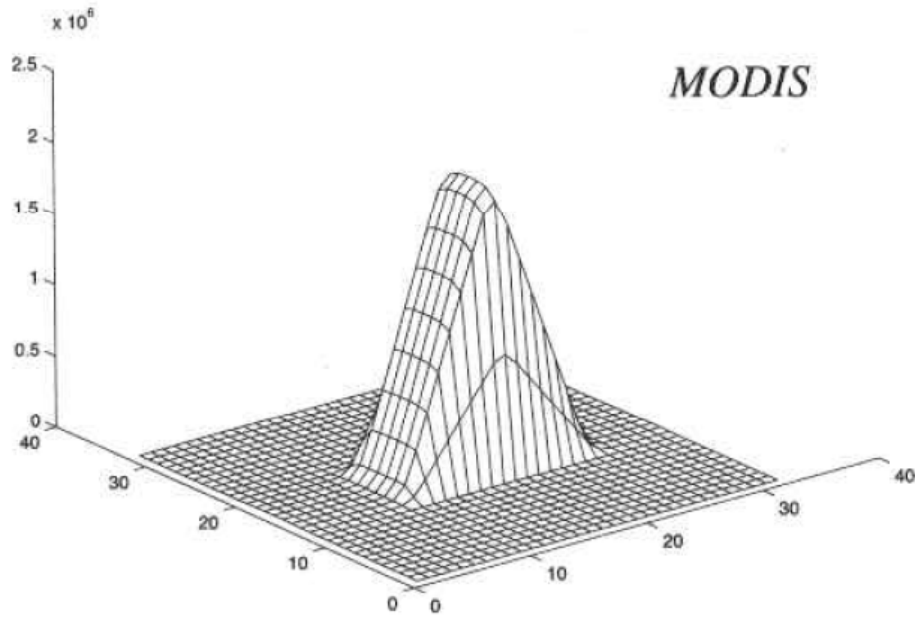


# PSF for SPOT and TM





# PSF for MODIS and ALI



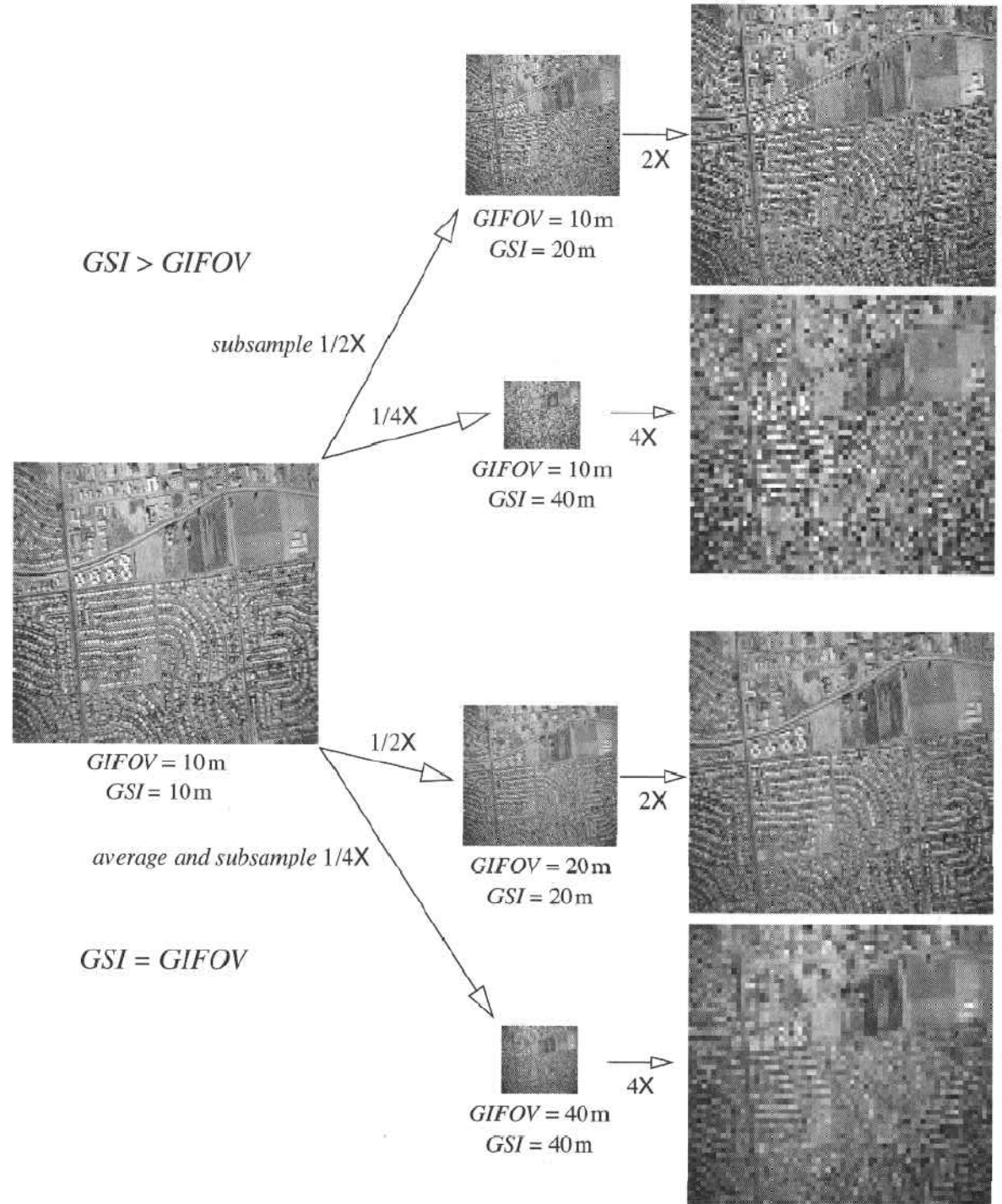
- PSF is normalized to same GSI
- For AVHRR and MSS, the amount of sensor blur is about twice as great in the cross-track direction than in the in-track direction
- Cross-track response is considerably broader than that of the detector.
- Effective GIFOV of RS systems is larger than the quoted geometric GIFOV

Visualizing imaging system effect  
using simulation

Simulation of the effect of GSI and GIFOV on visual image quality.

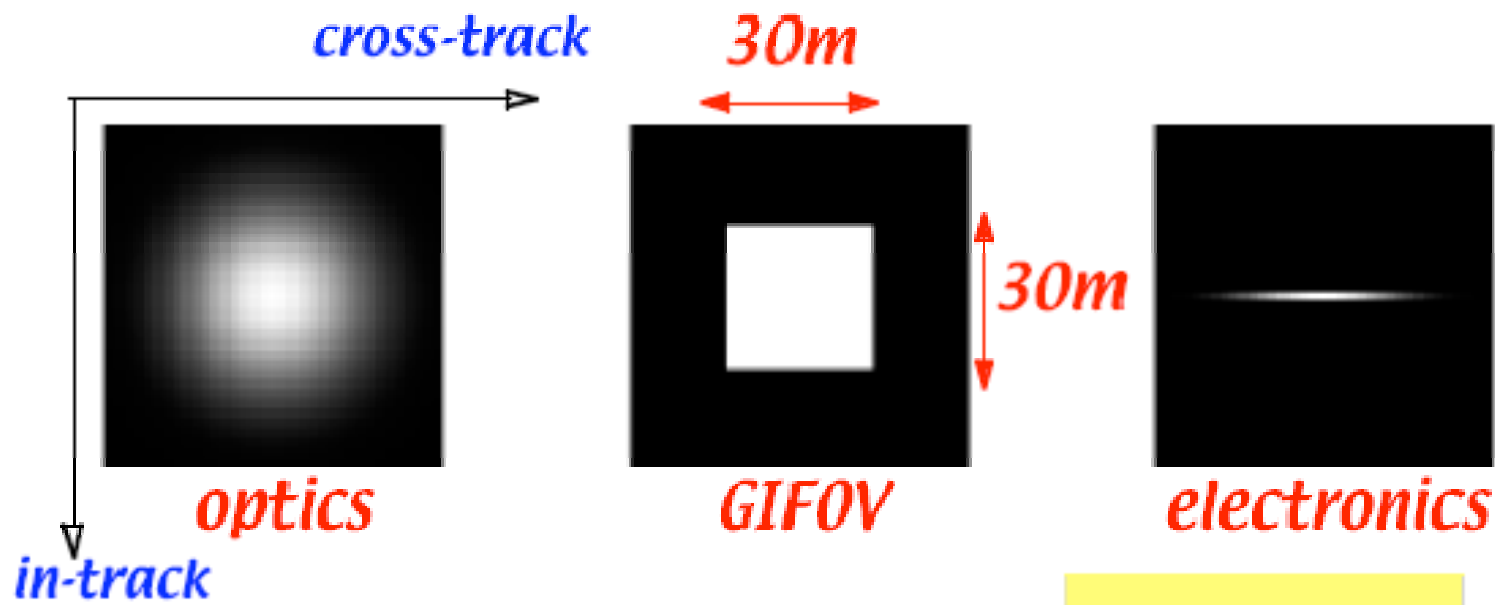
Upper: undersampled conditions,  $GSI > GIFOV$

Lower:  $GSI = GIFOV$

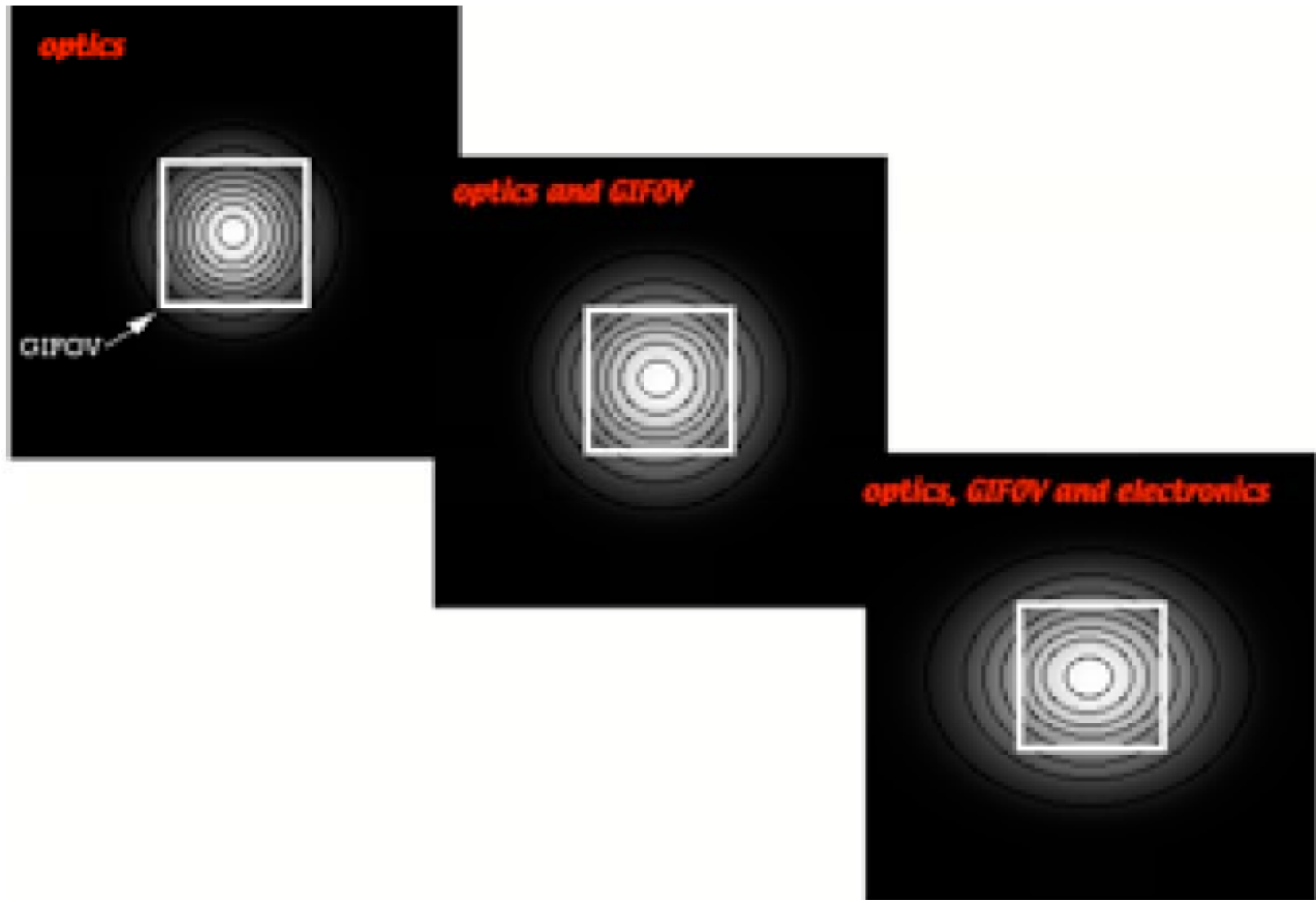


# Imaging Simulation

- Example: simulation of Landsat TM imaging
  - Model TM spatial response components (at a common scale)



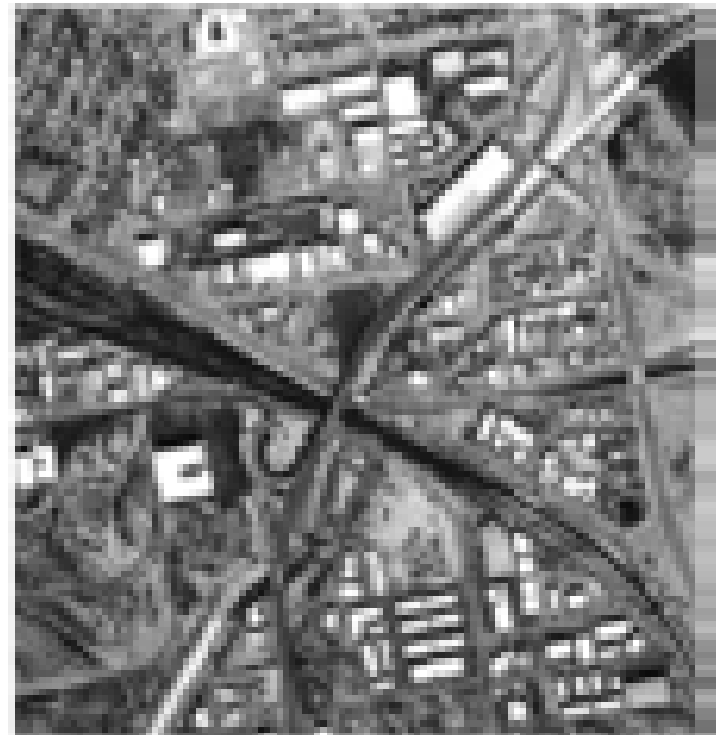
# TM Spatial Response Components



# High resolution aerial photography



**scanned aerial photograph, GSI = 2m**



**rotated and  
trim to align  
with TM orbit  
and scan  
direction**

# Imaging Simulation (cont.)

Apply each component of the spatial response and downsample to 30m



*optics*



*optics and GIFOV*



*optics, GIFOV and electronics*

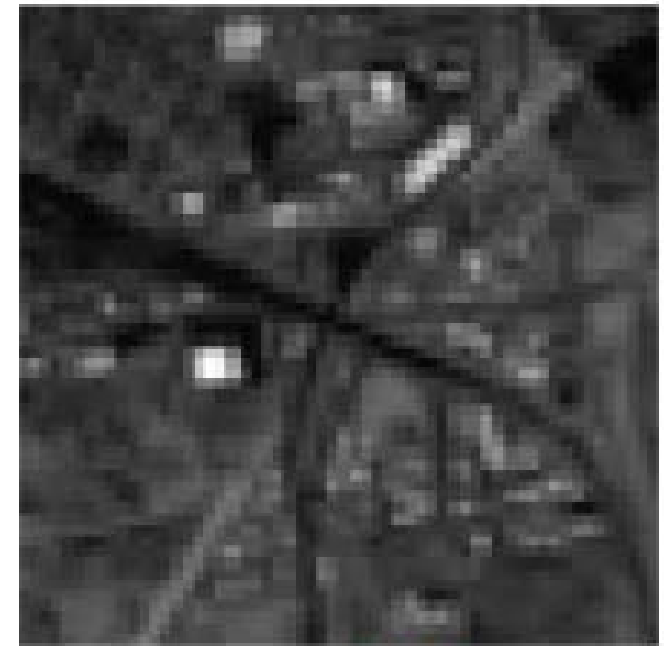
*downsample  
2m → 30m GSI*







*simulated TM*



*real TM*

Comparison  
with Real TM  
taken 4 months  
later

*real TM  
(contrast-adjusted)*



# Quiz

- How does sensor modify spatial response of scene
- What are the components of the PSFnet.
- What is optical PSF, detector PSF, image motion PSF
- Explain the MODIS design
- What contributes to electronics PSF
- What happens increasing GSI or GIFOV
- Compare effective GIFOV and geometric GIFOV

# Measurement of Sensor PSF

- Laboratory tests
  - Point sources → PSF
  - Lines sources → Line Spread Function (LSF)-1D
  - Edge sources → Edge Spread Function (ESF)-1D
- From data itself
  - Subpixel line and edge sources
  - Spatial domain representation of spatial response
  - Fourier transform domain representation is discussed in Chapter 6.

# Mathematical Relations

$$LSF_c(x) = \int_{-\infty}^{\infty} PSF(x, y) dy$$

$$LSF_i(y) = \int_{-\infty}^{\infty} PSF(x, y) dx$$

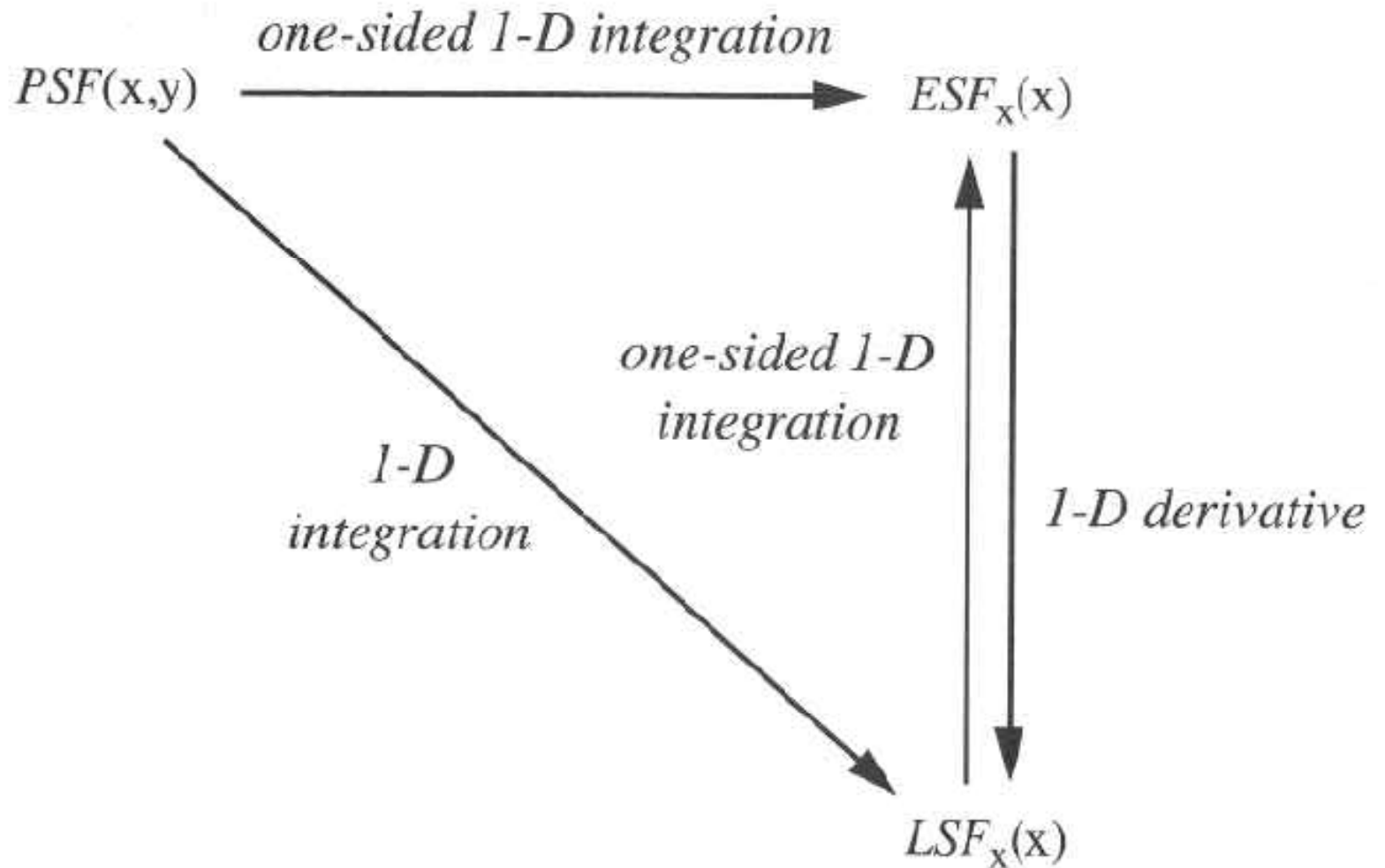
$$ESF_c(x) = \int_{-\infty}^x LSF_c(\alpha) d\alpha$$

$$LSF_c(x) = \frac{d ESF_c(x)}{dx}$$

$$ESF_i(y) = \int_{-\infty}^y LSF_i(\alpha) d\alpha$$

$$LSF_c(y) = \frac{d ESF_i(y)}{dy}$$

# Mathematical Relations



- The line or edge response is measured rather than point response
- Measure PSF, ESF and LSF using man-made targets such as mirrors or geometric patterns or targets of opportunity such as bridges
- Specular mirrors as subpixel targets, flat mirror detected in the 80m GIFOV of the first landsat MSS
- Phased array of effective point sources was used to measure the TM PSF
- Each point produces an independent, sampled PSF image

# Measurement of sensor spatial response

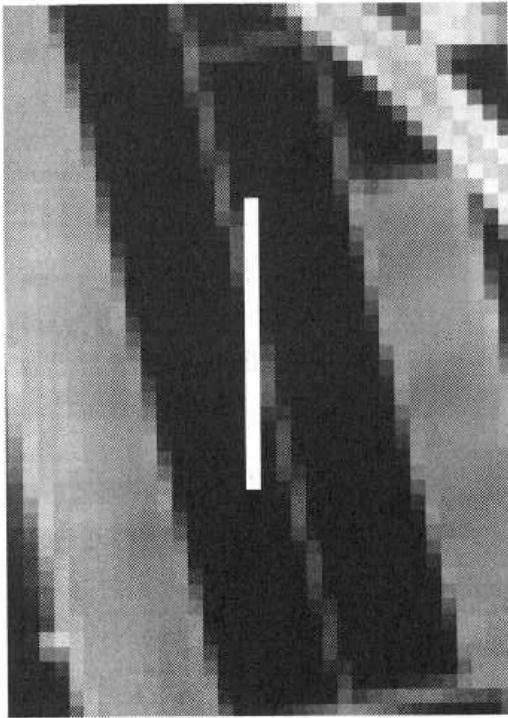
sensor	target type	reference
ADAR System 1000	edge	Blonski <i>et al.</i> , 2002
ALI	agriculture field berms	Schowengerdt, 2002
ETM+	bridge	Storey, 2001
HYDICE	bridge	Schowengerdt <i>et al.</i> , 1996
Hyperion	ice shelf edge, bridge	Nelson and Barry, 2001
IKONOS	edge	Blonski <i>et al.</i> , 2002
	parking lot stripes	Xu and Schowengerdt, 2003
	edge	Ryan <i>et al.</i> , 2003
	line	Helder <i>et al.</i> , 2004
MODIS	higher-resolution imagery	Rojas <i>et al.</i> , 2002
MSS	higher-resolution imagery	Schowengerdt and Slater, 1972
OrbView-3	edge	Kohm, 2004
QuickBird	phased-array of mirrors, edge	Helder <i>et al.</i> , 2004
simulated	non-specific	Delvit <i>et al.</i> , 2004
SPOT4 (simulated)	point source array	Robinet <i>et al.</i> , 1991
SPOT5	edge, spotlight	Leger <i>et al.</i> , 2003
TM	bridge, higher-resolution imagery	Schowengerdt <i>et al.</i> , 1985
	phased-array of subpixel targets	Rauchmiller and Schowengerdt, 1988

# ALI LSF measurement

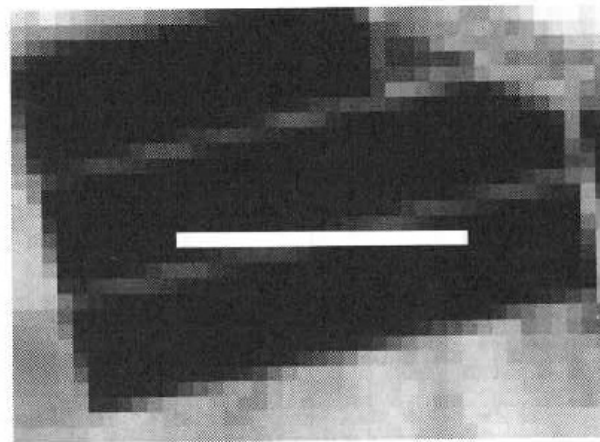
- The berm crop canopy forms a linear, high-contrast subpixel feature used to measure the MSS band LSF in the in-and cross-track directions
- Several transects were extracted, registered, and averaged in both cases to reduce noise
- If target is too narrow, result is not good due to low signal level
- If target is too wide, the estimated LSF will be broadened by the target itself



# Experimental Measurement

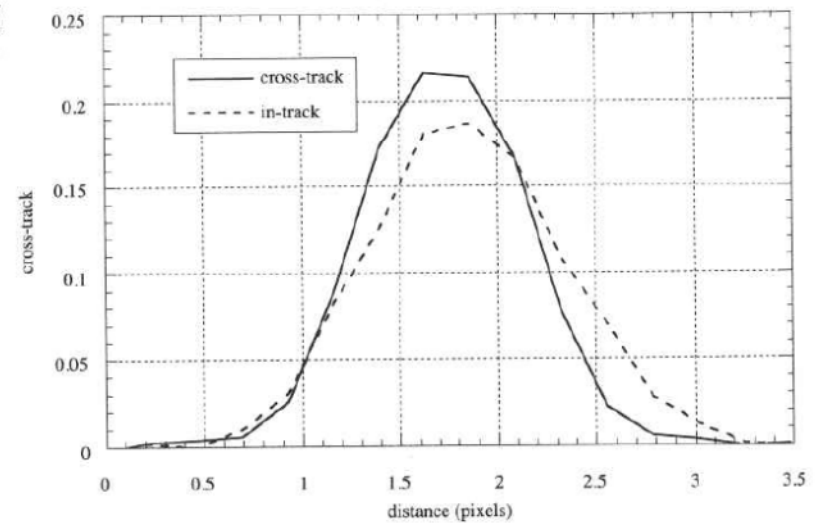


*transect used to extract subpixel samples for the cross-track LSF*



*transect used to extract subpixel samples for the in-track LSF*

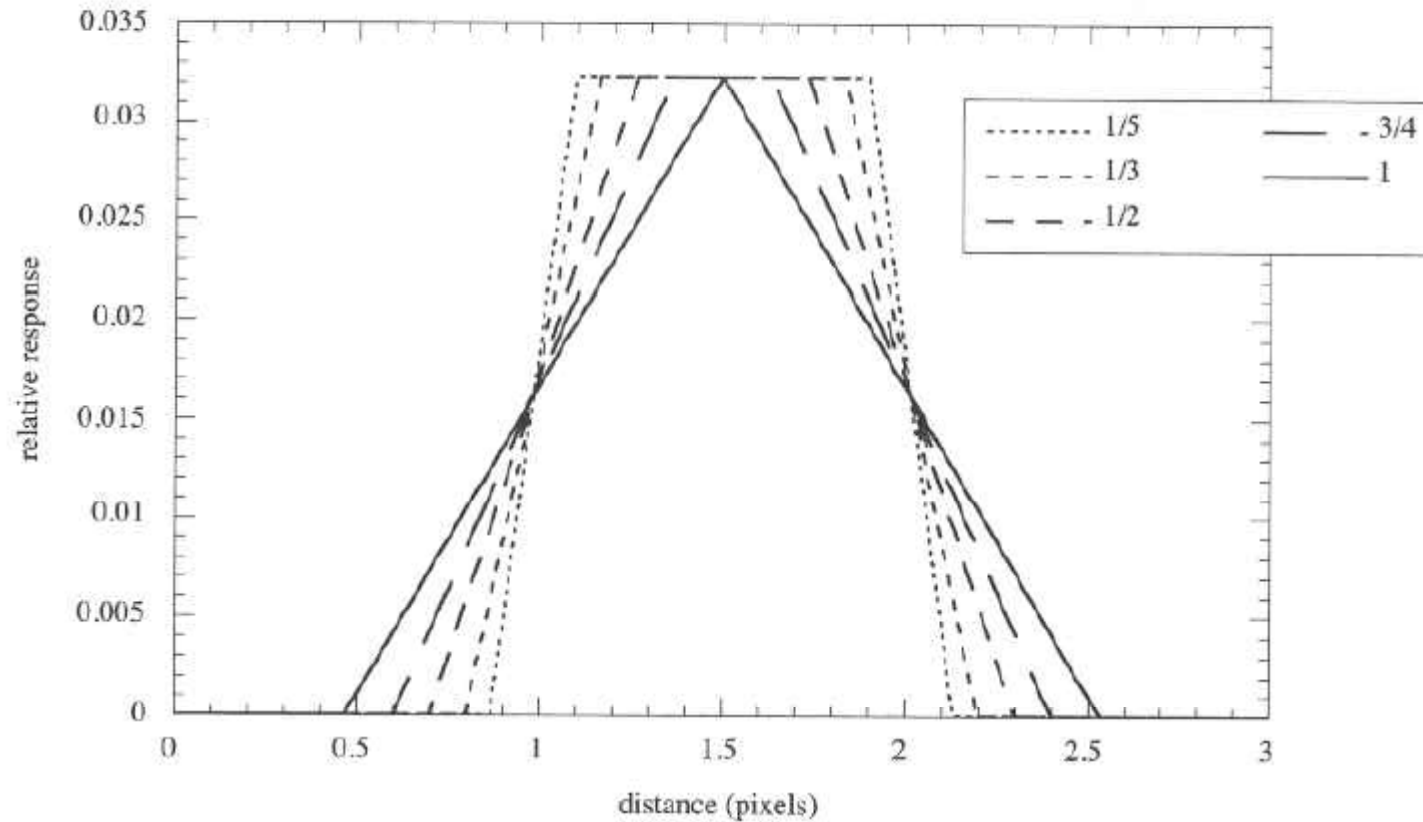
*cross-track and in-track band 3 LSFs*



# Exercise

- With angle of 13.08 deg between a line target and sensor scan direction, as in Fig. 3-18, how is the effective subpixel sample interval calculated for the extracted profiles.
- Derive equation 3-44 starting with equation 3-40.
- Calculate the convolution of a square sensor GIFOV and a square wave radiance target, either by integration using equation 3-2 or by a graphical approach. Allow the GIFOV to be  $\frac{1}{2}$ , 1 and 2 times the width of a single bar in the pattern and discuss the results in terms of sample-scene phase.

# Effect of Target Size

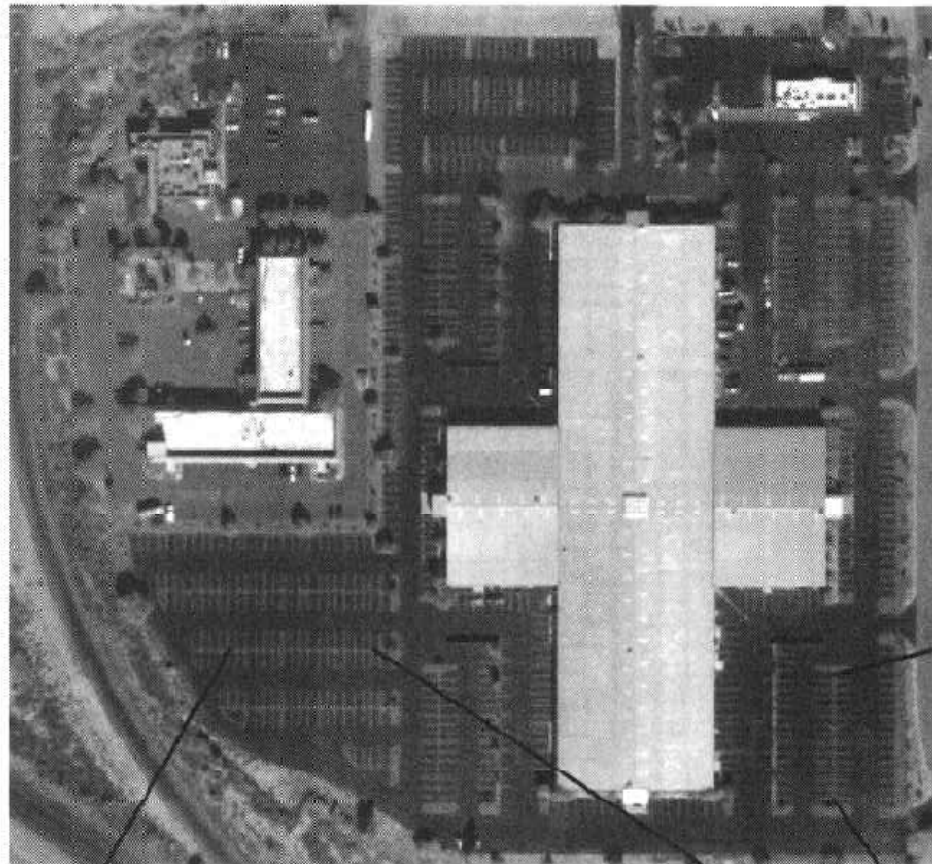


**Ratio = Target size/LSF width**

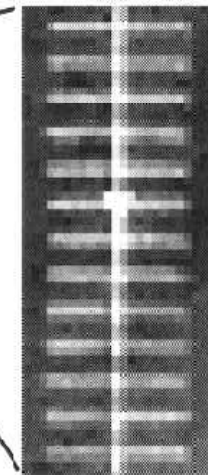
# QuickBird LSF measurement

- Trade-off using man-made targets and targets-of-opportunity that are already present on the ground
- Abundant man-made features in urban areas are good candidates
- White painted stripes in an asphalt vehicle parking lot are used to measure the QuickBird LSF
- Individual parking stripes are only about  $1/7$  GIFOV in width, but high contrast with background to yield good signal level
- Spacing is a non-integer number of pixels, each stripe is imaged with a different sample-scene phase.
- Length is several pixels, allowing averaging of several rows or columns

Estimation from data itself:  
QuickBird, Tucson Bargain Center, Nov. 4, 2002



*used for in-track  
LSF measurement*



*used for cross-track  
LSF measurement*

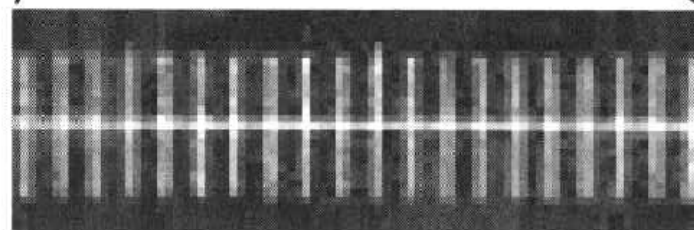
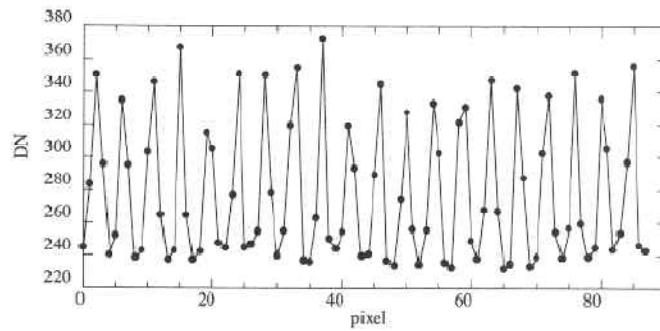
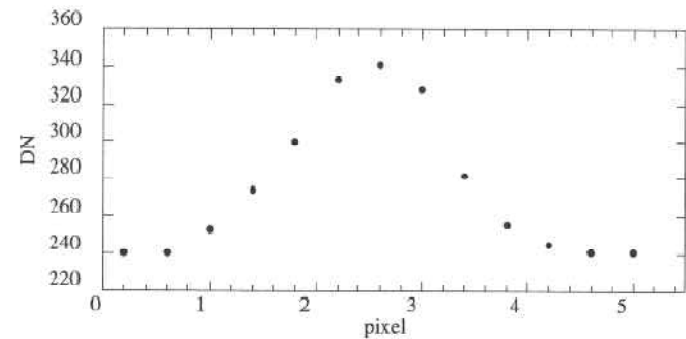


TABLE 3-2. Parking lot stripe parameters relevant to QuickBird image analysis.

parameter	size		pixels (resampled)	
	inches	meters	in-track	cross-track
width	4	0.102	0.148	0.145
spacing	120	3.05	4.42	4.40
length	240	6.10	8.84	8.80

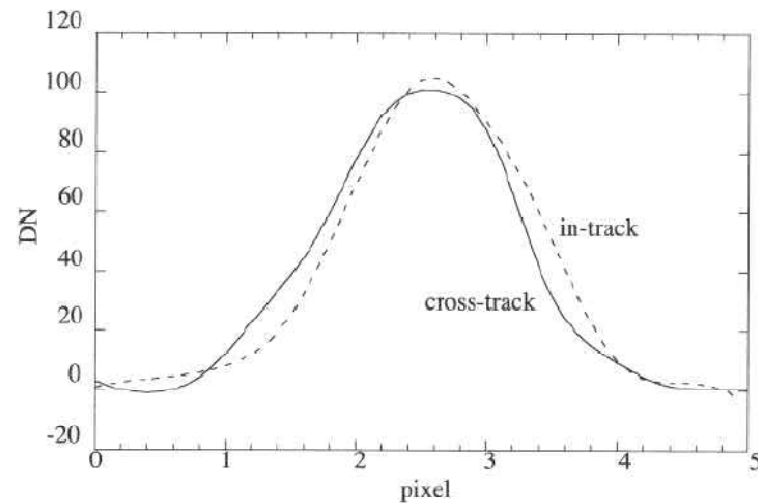


*cross-track pixel data*



*interleaved subpixel data*

*cross-track and in-track pan band LSFs*



Quickbird  
(cont.)

# Method Description (Helder '03)

- Edge Method (MTF-Modulation Transfer Function estimation method)
  - Sub-pixel edge locations were found by Fermi function fit.
  - A least-square error line was calculated through the edge locations.
  - Savitzky-Golay Helder-Choi filtering was applied on each line
  - The filtered profile was differentiated to obtain LSF
  - MTF calculated by applying Fourier transform to LSF.

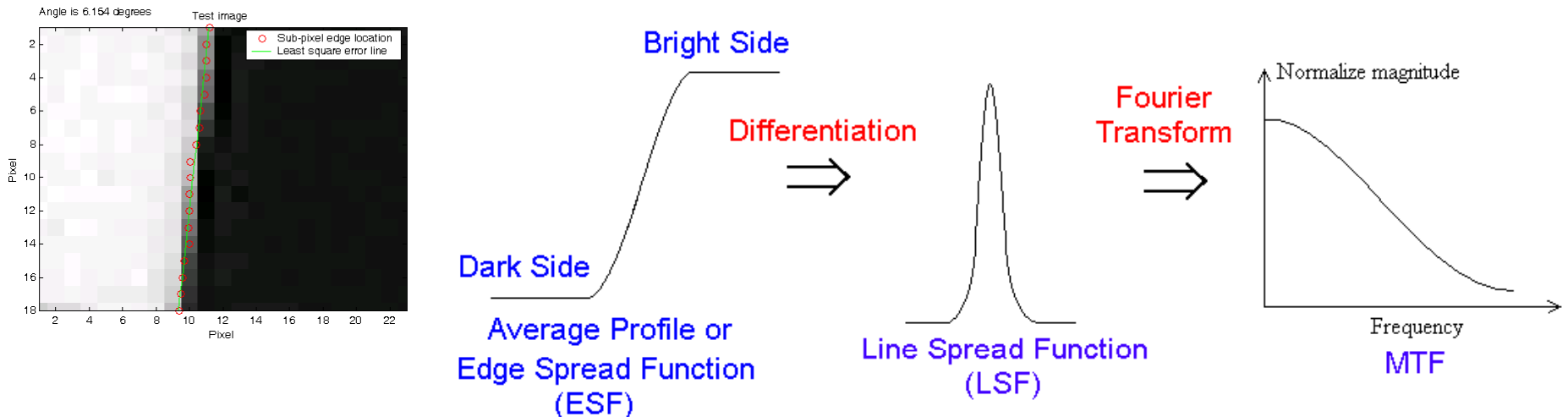


Fig 1. Edge Method

- Pulse method

- A pulse input is given to an imaging system.
- Output of the system is the resulting image.
- Edge detection and SGHC filtering was applied to get output profile.
- Take Fourier transform of the input and output.
- MTF is calculated by dividing output by input.

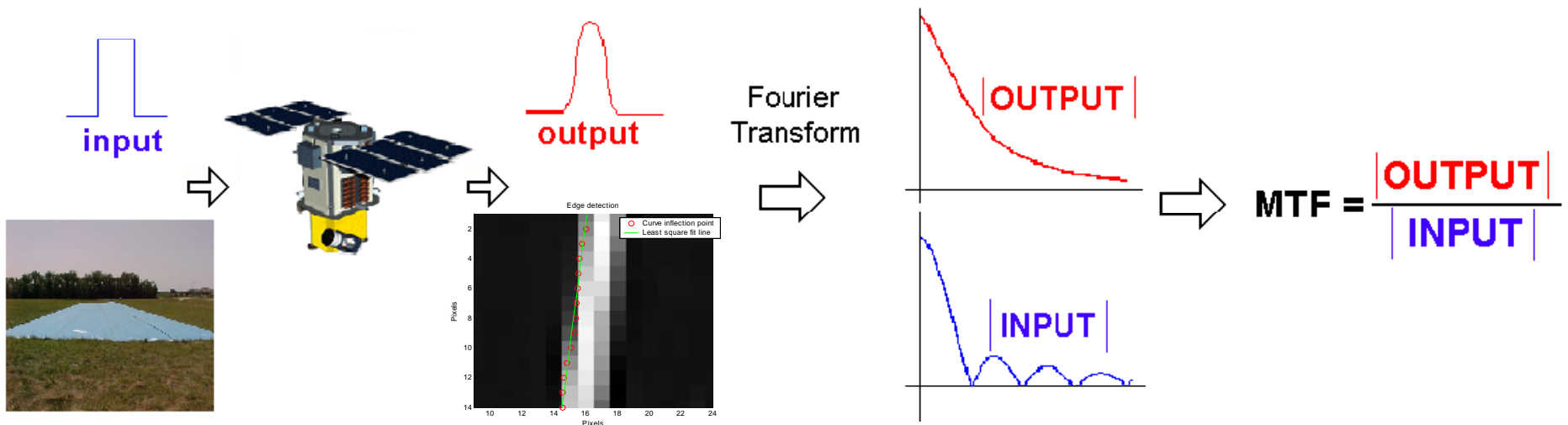


Figure 2. Pulse method



- Parametric Edge Detection

- A model based parametric method was applied to detect sub-pixel edge locations.
- The Fermi function was chosen to fit this function to the ESF for improved edge angle estimation.
- Sub-pixel edge locations were calculated on each line by finding best fitting curve's value 'b' .

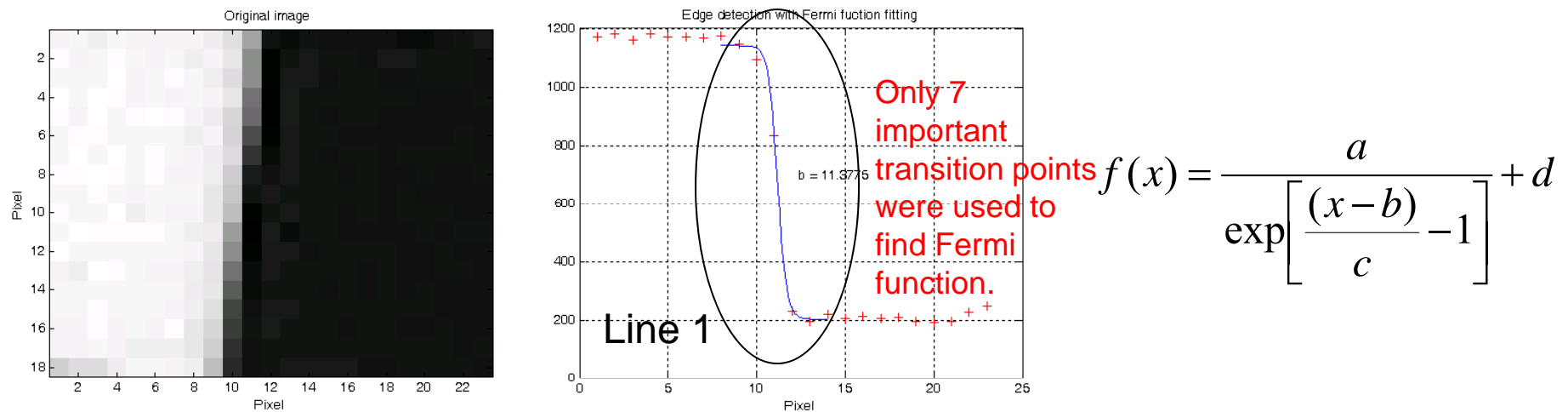


Figure 3. Parametric edge detection

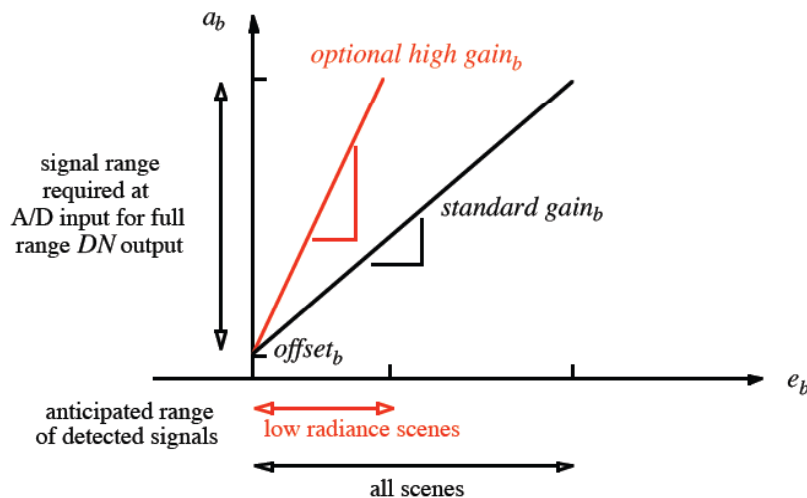
# Signal Amplification

- The electronic signal produced by the detectors is amplified

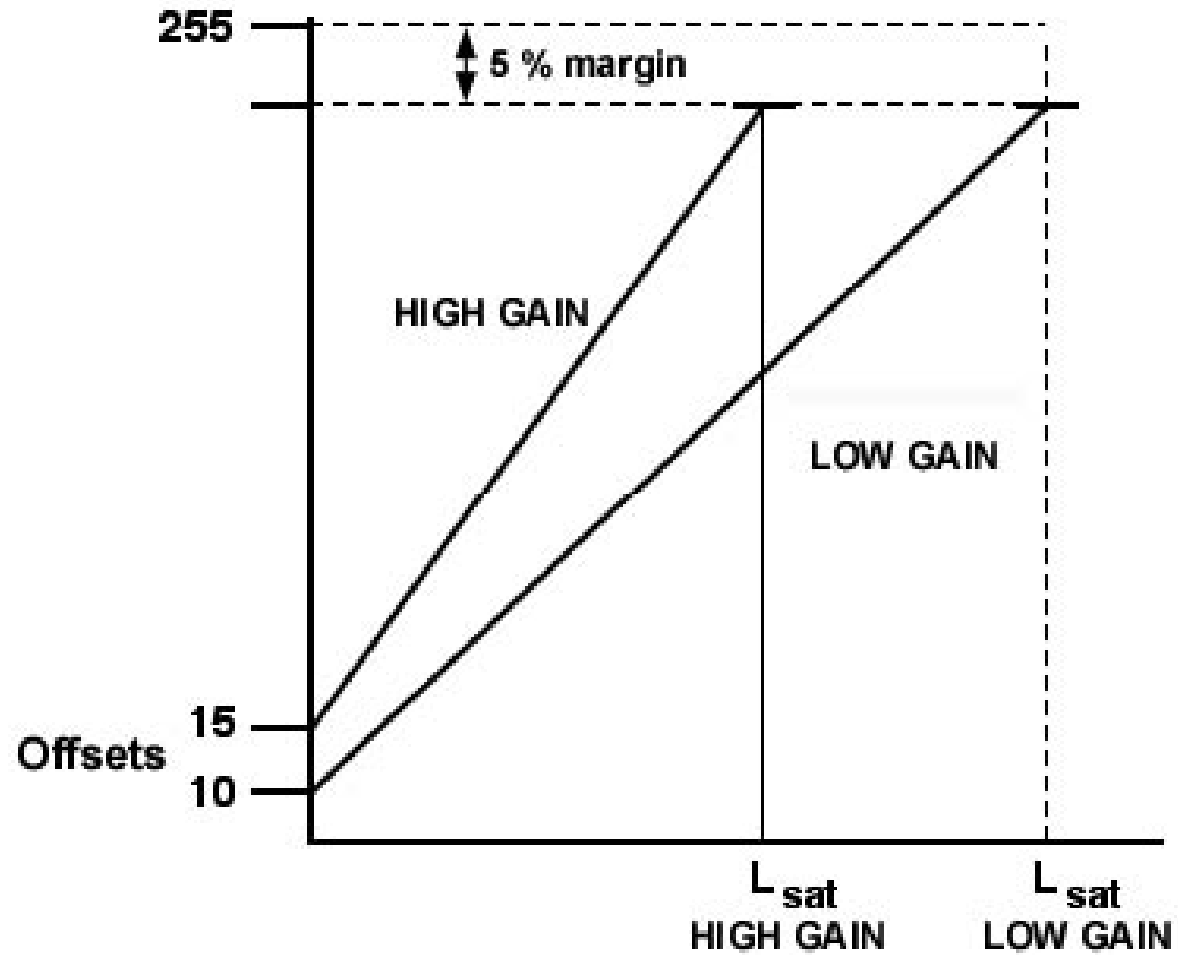
$$a_b = \text{gain}_b \times e_b(x, y) + \text{offset}_b .$$

- Some sensors have **multiple gain settings**, e.g. SPOT HRV (Chavez, 1989) and ETM thermal band, to increase signal level for dark objects

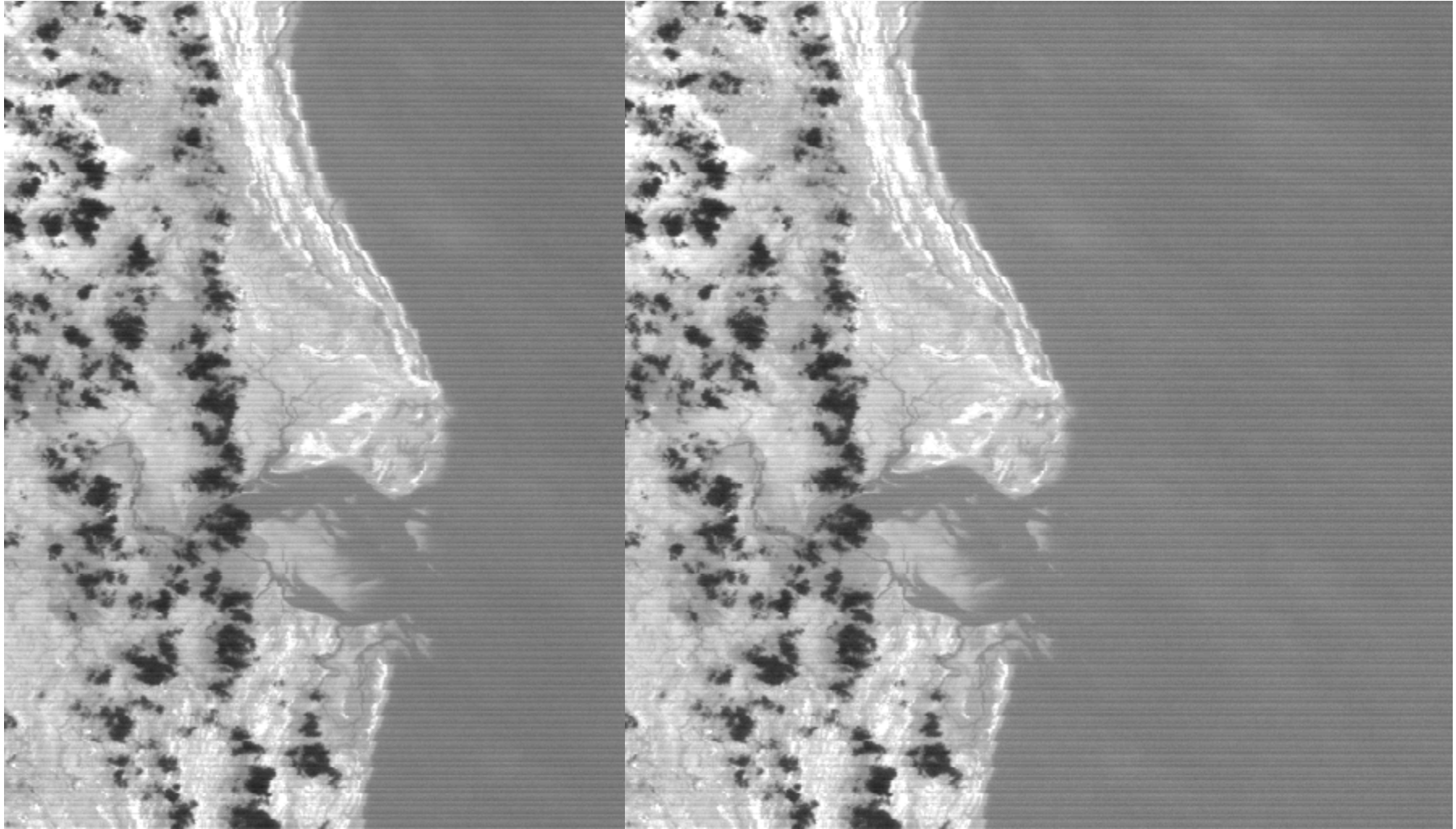
## *Linear amplification characteristics*



# Landsat ETM+



# ETM Sample Imagery

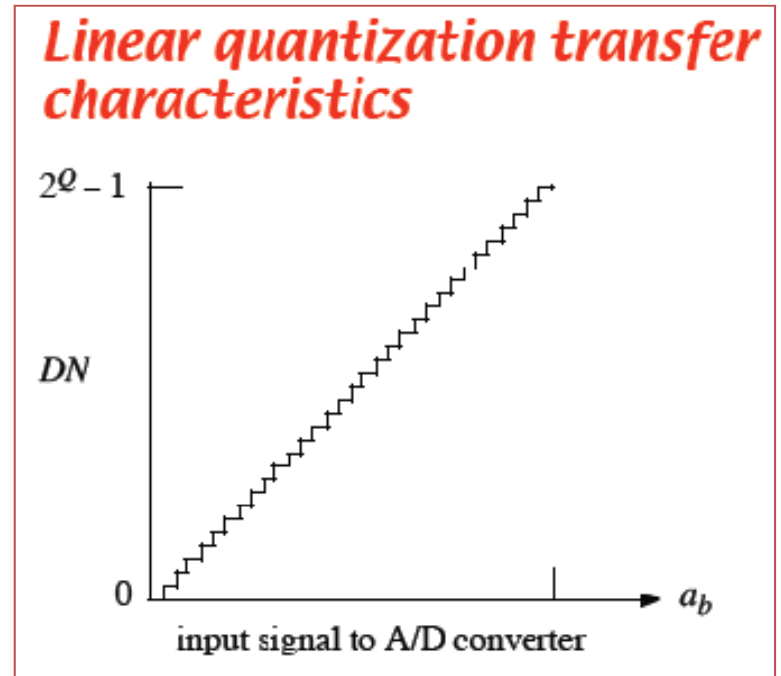


# Sampling and Quantization

- The amplified signal is sampled in time (during scan) and quantized into **Digital Numbers (DNs)**

$$\begin{aligned} DN_{pb} &= \text{int}[a_b] \\ &= \text{int}[\text{gain}_b \times e_b(x, y) + \text{offset}_b] \end{aligned}$$

- Quantization is a low-level noise superimposed on the data values
  - For Q bits/pixel quantization there are  $2^Q$  integer DNs over the range  $[0 \dots 2^Q - 1]$
- **Radiometric resolution**
  - $2^{-Q}$  dynamic-range-in-radiance



# Radiometric Resolution:

- (a) 1-bit,
- (b) 4-bits,
- (c) 8 bits

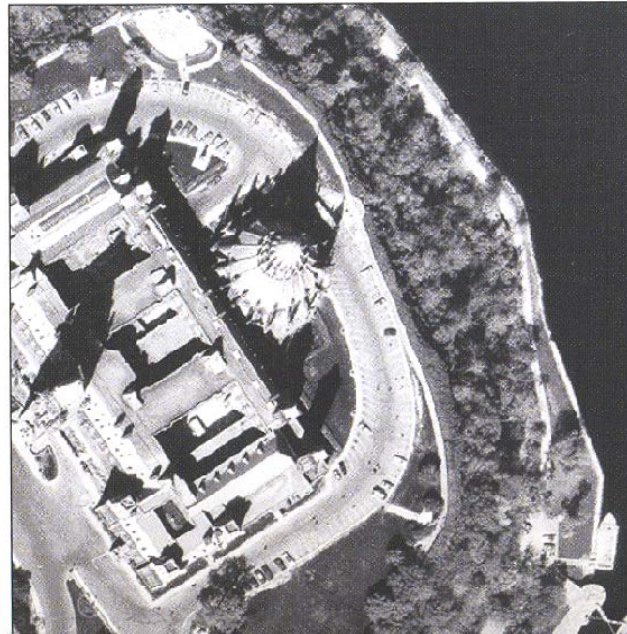
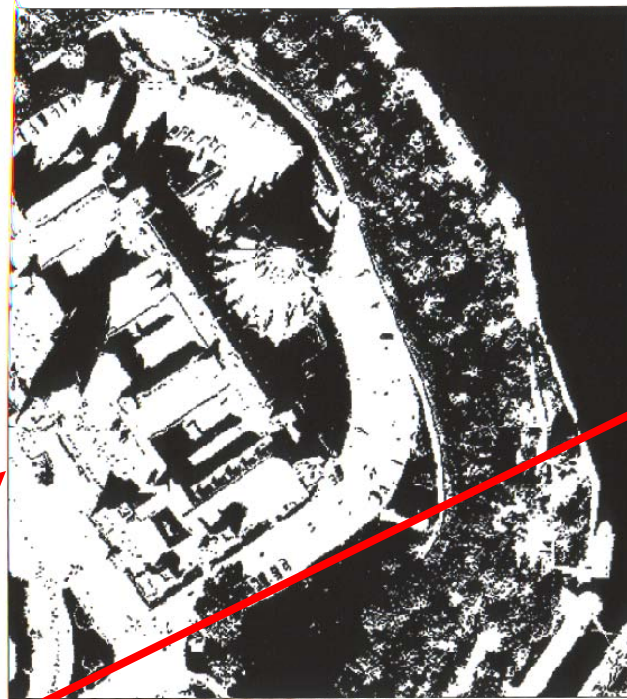


**Figure 4.20** Comparison of radiometric resolutions. The same image is displayed with (a) 2, (b) 16, and (c) 256 gray levels, which corresponds to 1-, 4-, and 8-bit radiometric resolutions. Since the human eye does not reliably distinguish more than about 30 gray levels, there is little apparent loss of image quality in the 4-bit image.  
Source: © Natural Resources Canada.

# Effective Sensor Model

- Total measured signal at pixel p in band b

$$DN_{pb} = \text{int} \left[ K_b \iiint L_\lambda(x, y) d\lambda dx dy + \text{offset}_b \right]$$

– where

- $DN_{pb}$  is the Digital Number at pixel p in band b
- $L_\lambda(x, y)$  is the at-sensor spectral radiance from scene location (x,y)
- $K_b$  is a gain coefficient for band b that includes sensor gain, detector spectral responsivity and spectral filter transmittance
- $\text{offset}_b$  is the sensor offset coefficient for band b
- the gain and offset are effective quantities, averaged over an effective spectral band

# Gain-Offset Model

- The three integrals are over:
  - the effective spectral response range of band b (spectral resolution)
  - the effective spatial response range in-track and crosstrack (spatial resolution)
- Assume a **band- and space-integrated** at-sensor radiance  $L_{pb}$  at pixel p, band b. Then,

$$DN_{pb} = K_b L_{pb} + offset_b$$

- DNs are **linearly proportional** to the total at-sensor radiance
- Ignores radiometric quantization and nonuniform response within spectral bands and the GIFOV
- Simplifies modeling and radiometric calibration of the sensor



# Sensor Calibration (DNs to radiance)

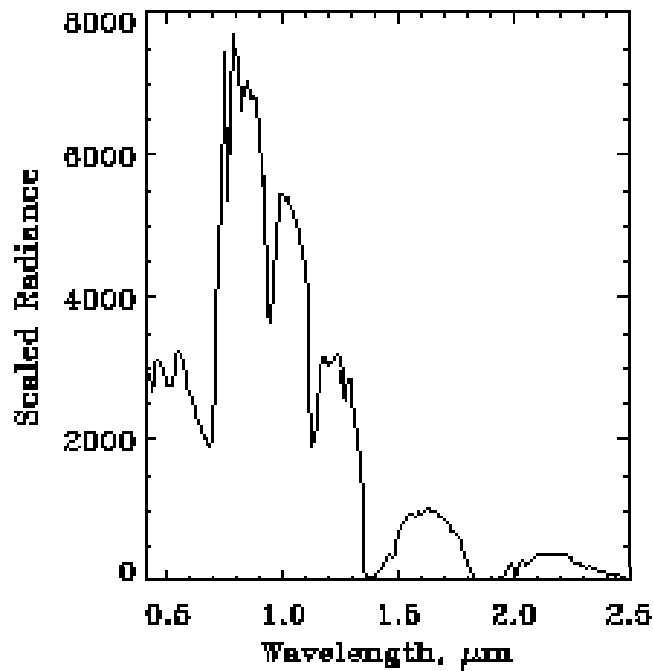
- Relating the digital number (DN) to radiance.
  - Linear relationship with radiance ( $L_\lambda$ )
  - $L_\lambda = \text{Gain (DN)} + \text{Offset}$
  - Gains and offsets provided in metadata with distribution of data

# Calibration Coefficients for LANDSAT TM

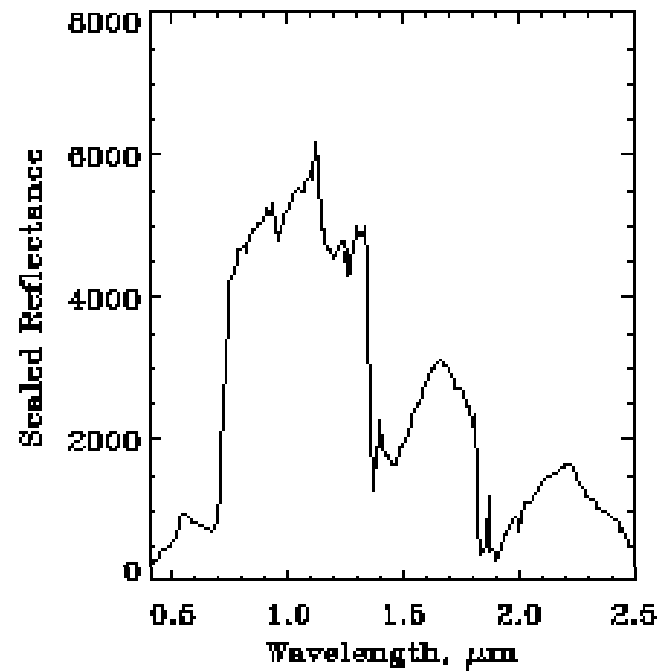
TABLE II  
L5 TM PRELAUNCH GAIN/BIAS COEFFICIENTS [8]

<b>Band</b>	<b>Prelaunch Gain</b>	<b>Prelaunch Bias</b>
1	1.555	1.8331
2	0.786	1.6896
3	1.02	1.8850
4	1.082	2.2373
5	7.875	3.2893
7	14.77	3.2117

# Scene Calibration: Radiance to Reflectance (inverse problem)



**Measured Radiance**



**Estimated Reflectance  
using ATREM**

# Geometric Distortions

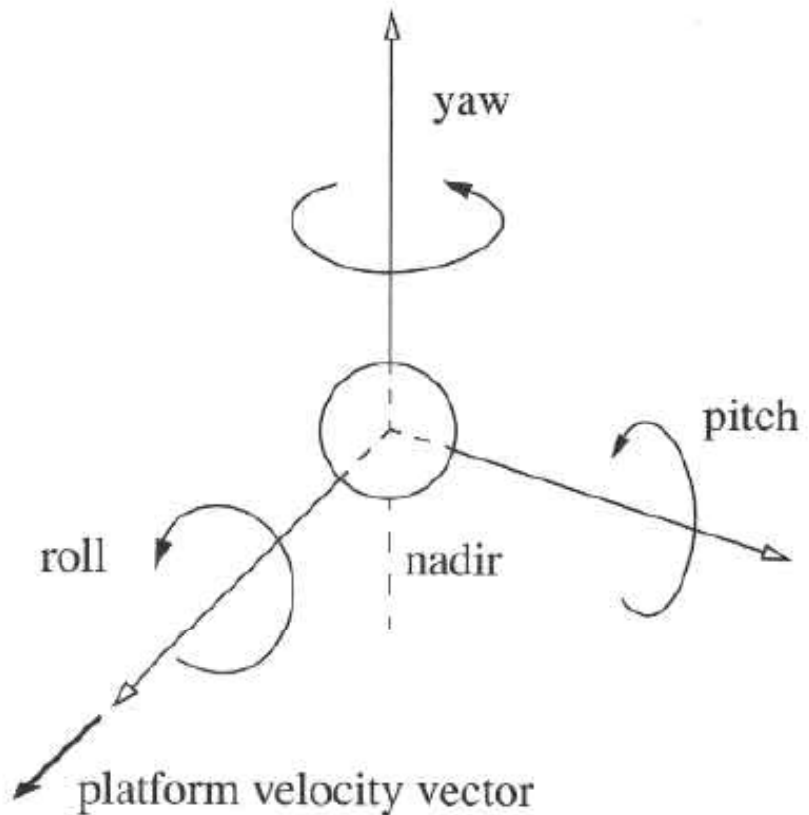
- Previous discussion focused on sensor characteristics that affected the radiometric quality of the imagery
- Here we focus on where are we looking?
  - Geometric characteristics of the imagery
    - Orbit
    - Platform attitude
    - Scanner properties
    - Earth rotation and shape

# Sources of Distortion

- All remote sensing images are distorted relative to a map
  - platform motion, especially airborne sensors
  - scanning distortion of the Ground Sample Interval (GSI)
  - topography

# Sensor attitude

- The angle(s) of an aerospace vehicle with respect to a reference such as the horizon
- Small changes in sensor attitude can result in large changes in the viewed location on the ground
- Expressed by three angles: roll, pitch and yaw.
  - Usually recorded with the image data



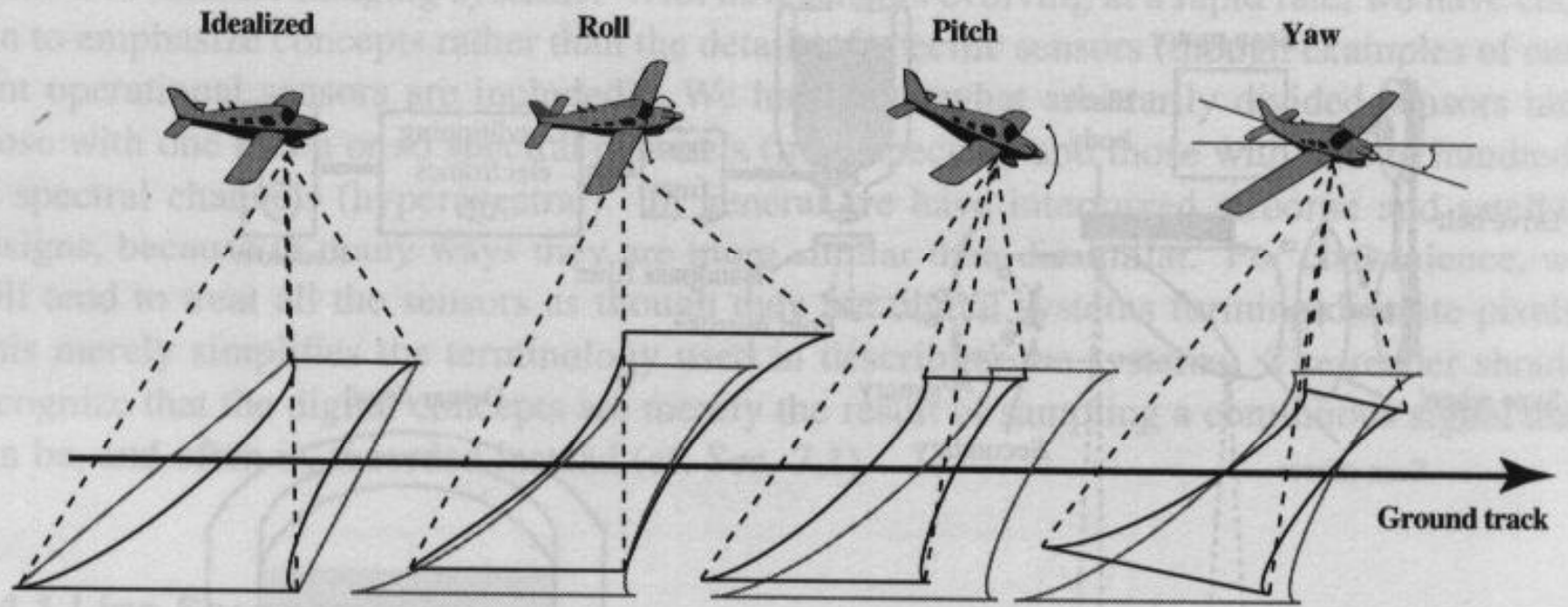
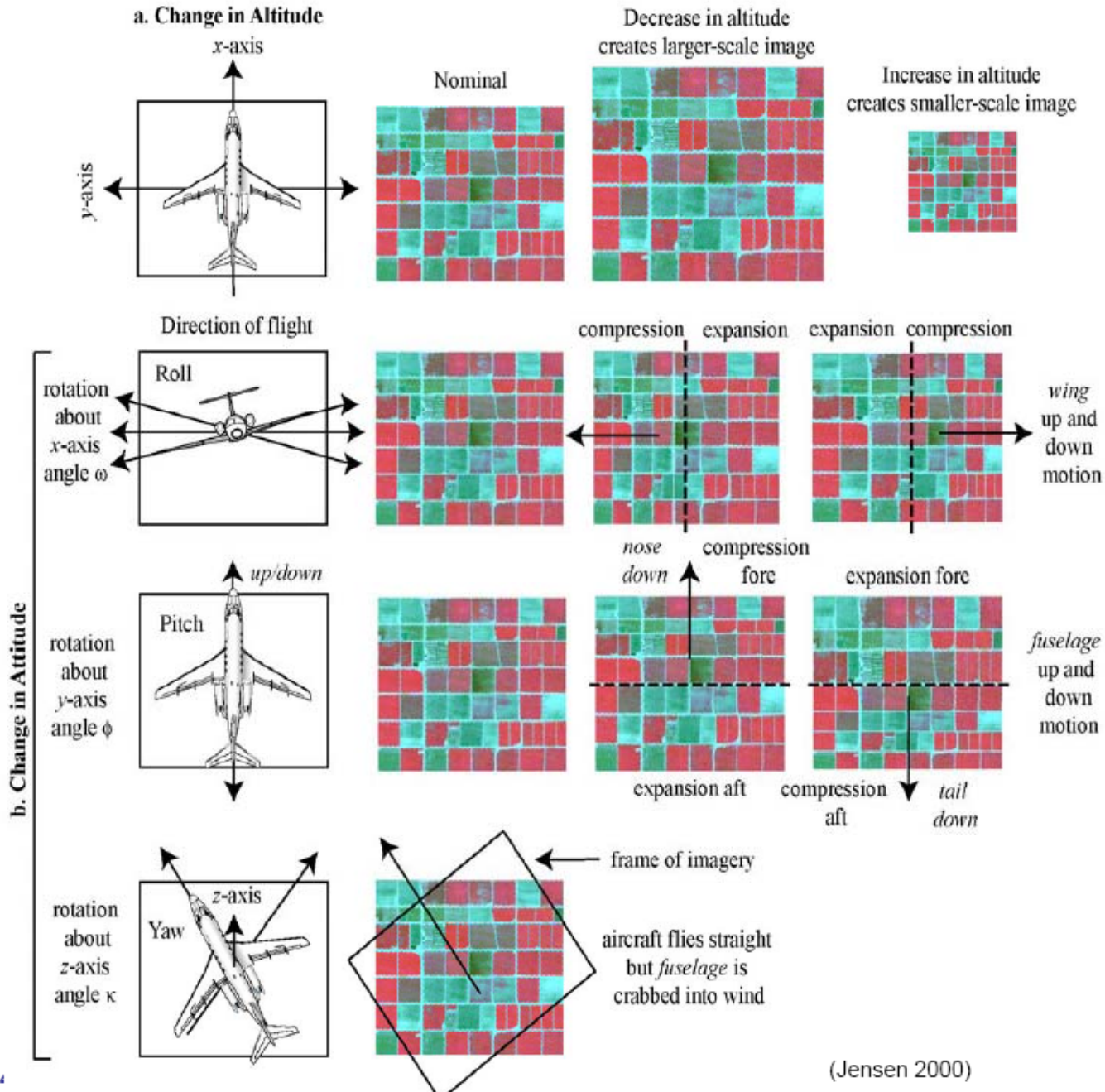


Figure 5.17 Geometric distortions due to aircraft orientation. Gray boundaries represent nominal coverage; black boundaries represent actual coverage.

# Geometric Modification of Remotely Sensed Data Caused by Changes in Platform Altitude and Attitude



(Jensen 2000)



# Angle Between Adjacent Pixels

TABLE 3-3. The angle between two adjacent pixels for a number of sensors. AVHRR and Landsat are not pointable; all the other sensors are pointable.

system	altitude (km)	in-track GSI (m)	angle (mrad)
AVHRR	850	800	0.941
Landsat-4,-5 TM (multispectral)	705	30	0.0425
SPOT-1 to -4 (multispectral)	822	20	0.0243
Landsat-7 ETM+ (panchromatic)	705	15	0.0213
SPOT-5 (multispectral)	822	10	0.0122
SPOT-5 (panchromatic)	822	5	0.00608
OrbView-3 (panchromatic)	470	1	0.00213
IKONOS (panchromatic)	680	1	0.00147
QuickBird (panchromatic)	450	0.6	0.00133

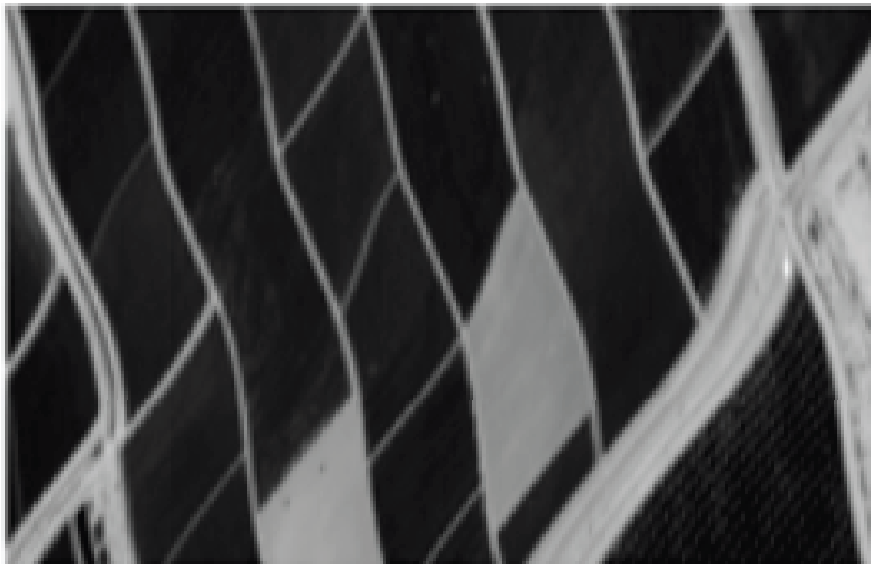
# Sensor Attitude (more)

- Satellite Sensors: it is assumed to be a slow varying function of time

$$\alpha = \alpha_0 + \alpha_1 t + \alpha_2 t^2 + \dots$$

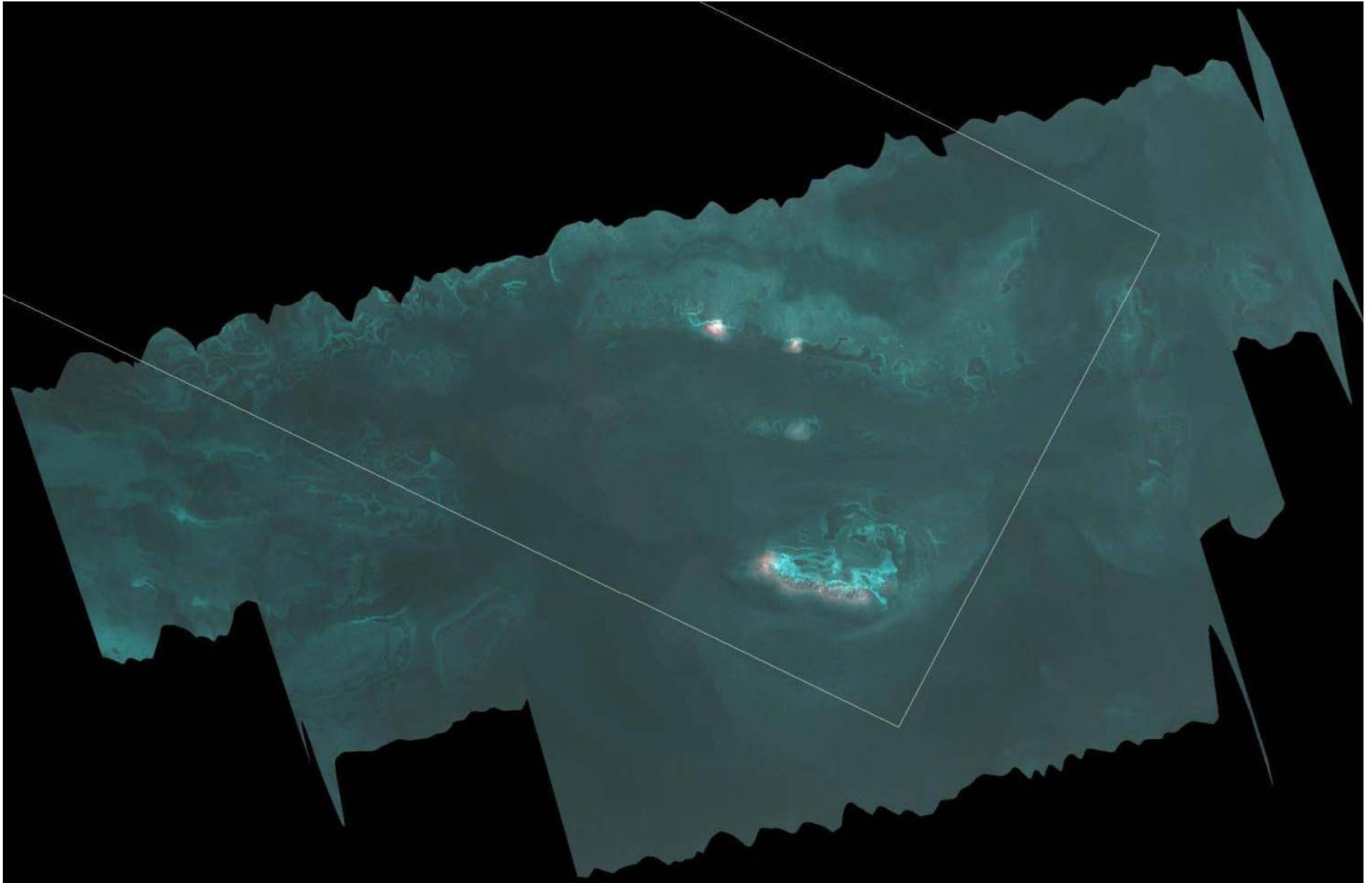
- Airborne Sensors: subject to large changes from wind and turbulence.
  - Gyro-stabilized platform is needed to avoid severe image distortions

## *Distortion caused by airplane motion (ASAS airborne sensor)*

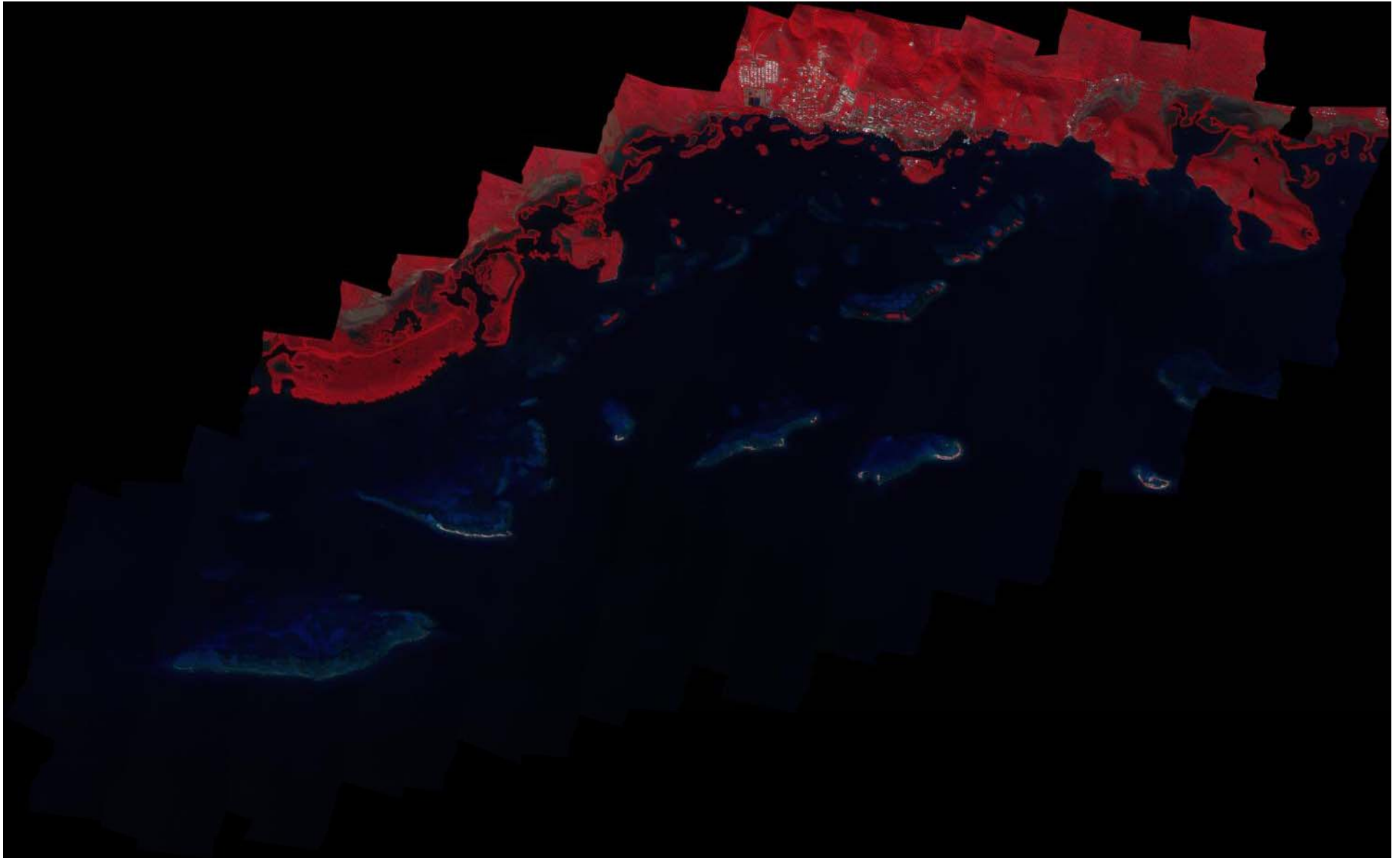


Note changes in geometric patterns (changes in attitude) and radiometric differences (non Lambertian surfaces) due to changes in view angle

# Example: Recent Campaign in PR



With some corrections



# Scanner Models

- Scanner induced distortions can be easily modeled as a function of time
  - As long as they are consistent throughout an image
- Whiskbroom scanners have more inherent distortions than pushbroom
  - Whiskbroom: moving crosstrack
  - Pushbroom: fixed crosstrack geometry
  - Pre-flight calibration is possible

TABLE 3-4. Examples of sensor-specific internal distortions. The reader is cautioned that some measurements of distortion were made from ground-processed imagery, and that a careful reading of the indicated reference is required before assuming the errors apply to all of the imagery from a given sensor. For example, the inter-focal plane misregistration in TM is given for early data; later data were found to be registered to within 0.5 pixel because of improved ground processing (Wrigley et al., 1985) .

sen- sor	source	effect on imagery	maximum error	reference(s)
MSS	non-unity aspect ratio sampling	cross-track versus in- track scale differential	1.41:1	USGS/NOAA, 1984
	nonlinear scan mirror velocity	nonlinear cross-track distortion	±6 pixels	Anuta, 1973; Steiner and Kirby, 1976
	detector offset	band-to-band misregistration	2 pixels between bands	Tilton <i>et al.</i> , 1985
TM	focal plane offset	misregistration between visible (bands 1–4) and IR (bands 5–7)	–1.25 pixels	Bernstein <i>et al.</i> , 1984; Desachy <i>et al.</i> , 1985; Walker <i>et al.</i> , 1984
SPOT	detector element misalignment	in-track and cross-track pixel-to-pixel positional error	±0.2 pixels	Westin, 1992

# Line and Whiskbroom Scan Geometry

- Flat Earth

$$\textit{flat earth: } GSI_f(\theta)/GSI(0) = [1/\cos(\theta)]^2$$

- Spherical Earth: Large IFOV

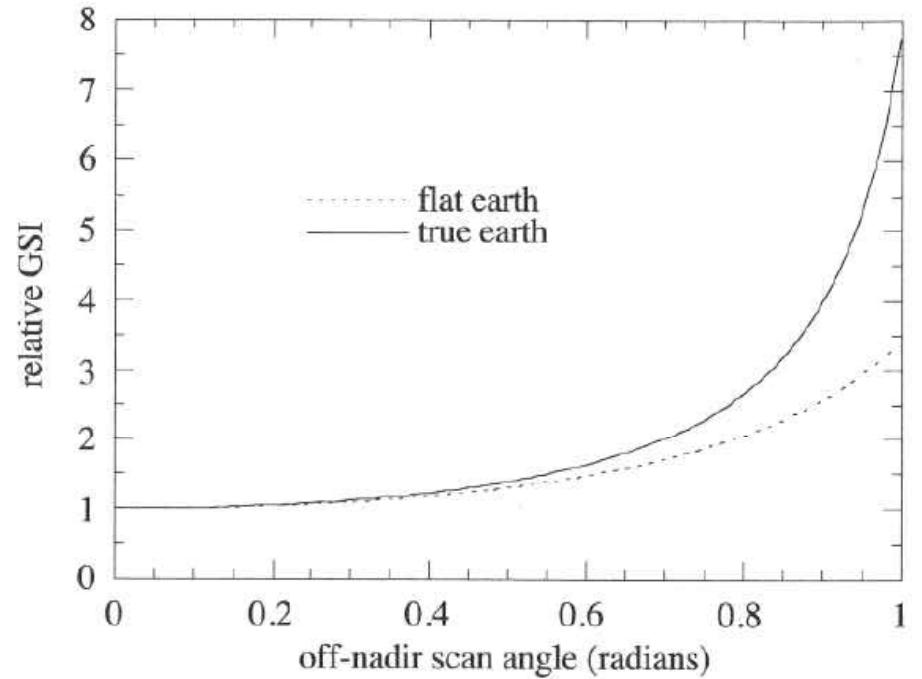
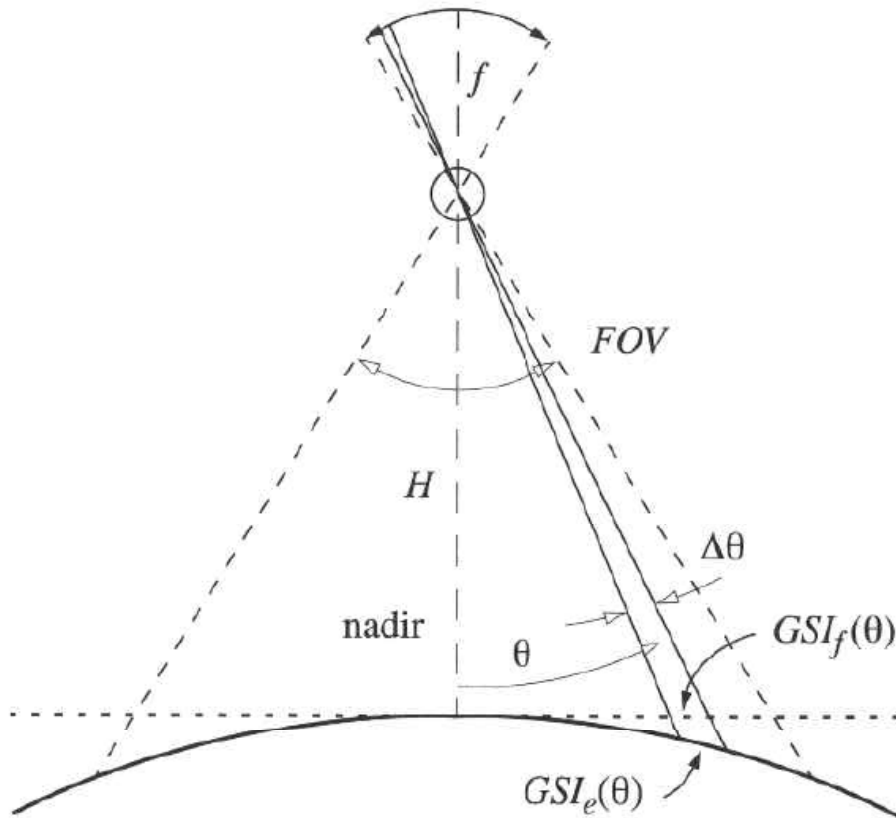
$$\textit{spherical earth: } GSI_e(\theta)/GSI(0) = \frac{[H + r_e(1 - \cos\phi)]}{H \cos(\theta) \cos(\theta + \phi)}$$

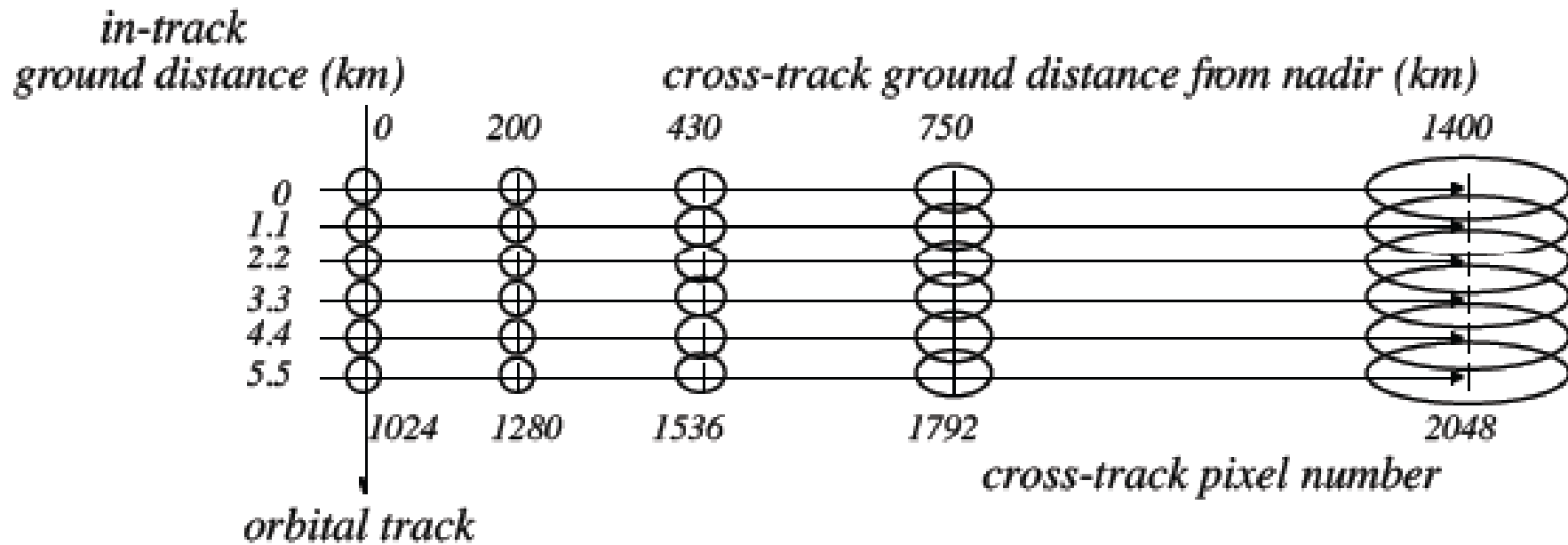
– where  $\phi$  is the geocentric angle

$$\phi = \text{asin}\{[(r_e + H)/r_e]\sin(\theta)\} - \theta$$



## Scanning Distortion: line and whiskbroom scanners

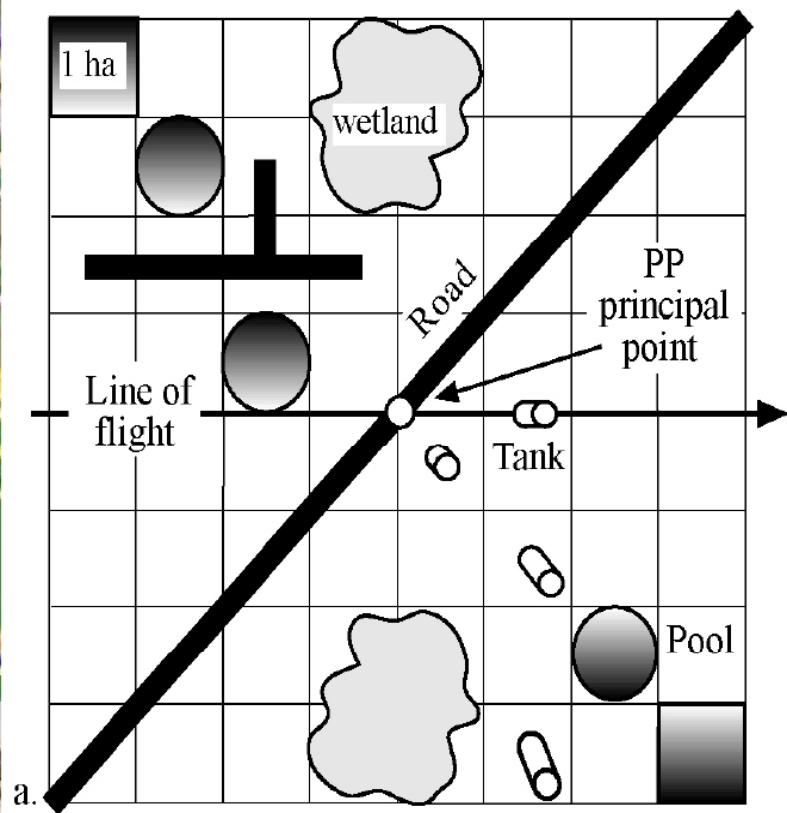




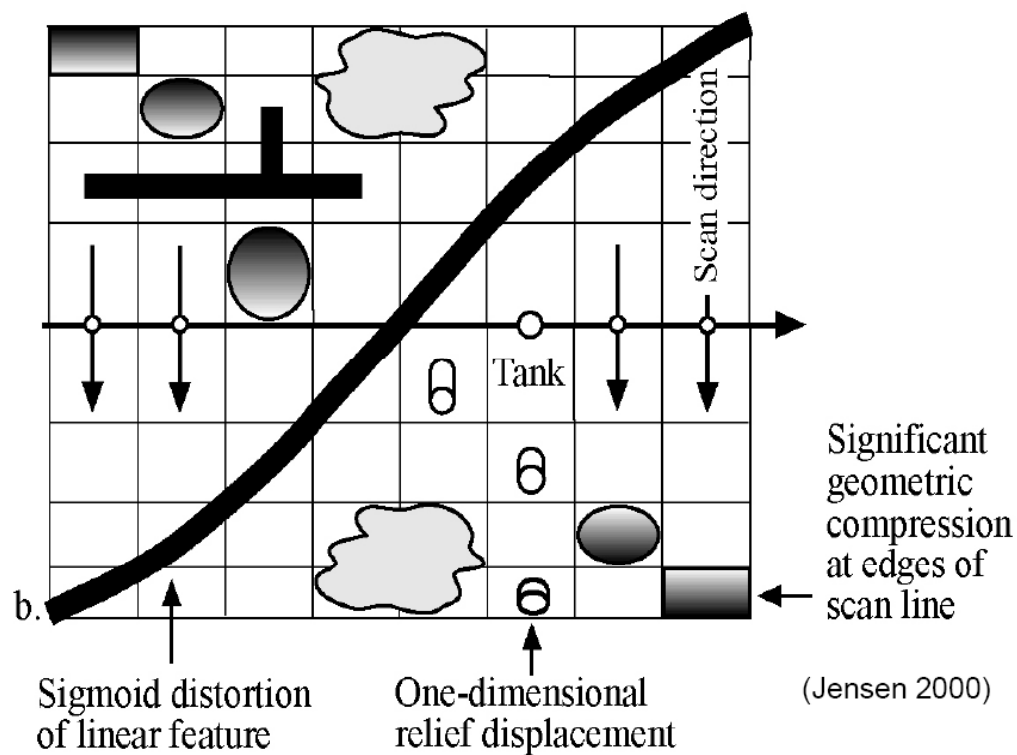
**Bow-tie distortion in AVHRR data (Fig. 3-23)**

# More on Scan Distortion

**Vertical Aerial Photography Perspective Geometry**



**Across-track Scanner Geometry with One-Dimensional Relief Displacement and Tangential Scale Distortion**



# Pushbroom Scan Geometry

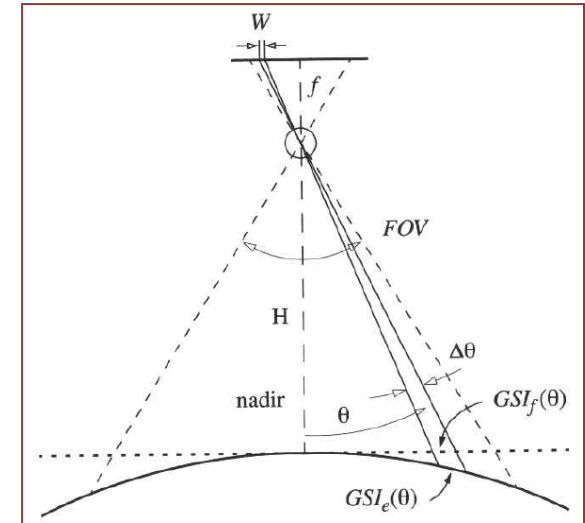
- For flat earth

$$\text{flat earth: } GSI_f = w \times \frac{H}{f}$$

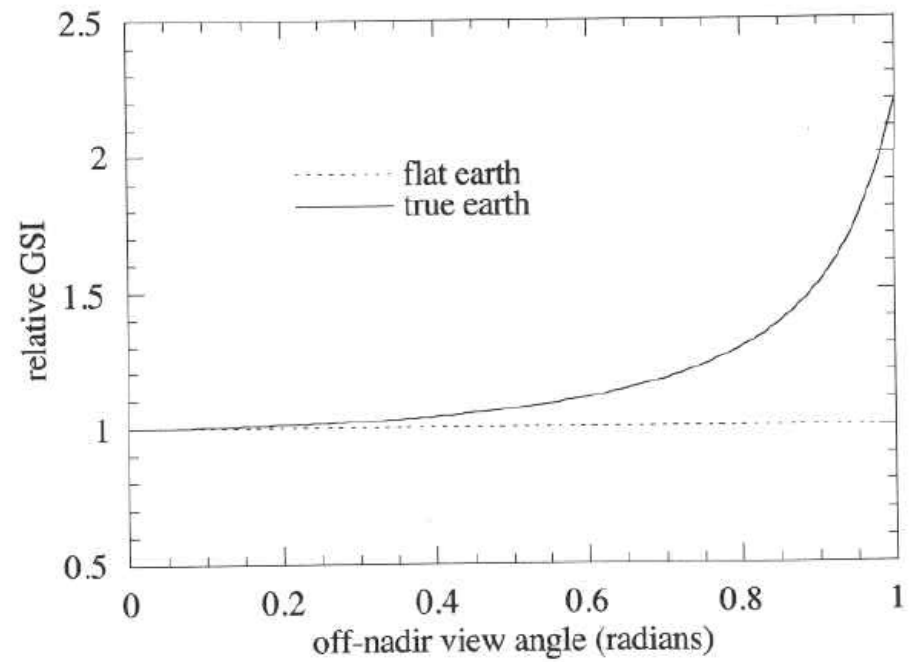
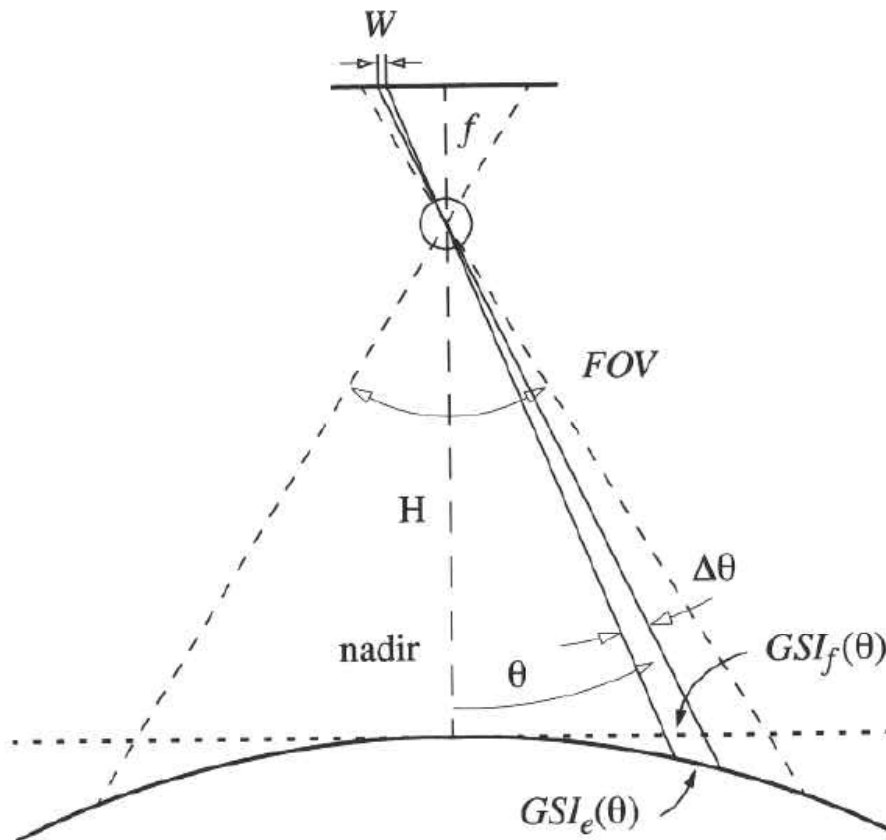
- Spherical earth

$$IFOV(\theta)/IFOV(0) = [\cos(\theta)]^2$$

$$\text{spherical earth: } GSI_e(\theta)/GSI(0) = \frac{[H + r_e(1 - \cos\phi)] \cos(\theta)}{H \cos(\theta + \phi)}$$



# Pushbroom Scan Geometry



# Earth Model

- Earth geometric properties are independent of the sensor but they affect the acquisition process via the orbital motion of the satellite.

– Earth is not an exact sphere

- Ellipsoid Equation

$$\frac{p_x^2 + p_y^2}{r_{eq}^2} + \frac{p_z^2}{r_p^2} = 1$$

where  $(p_x, p_y, p_z)$  are the geocentric coordinates of any point P in the surface of the earth,  $r_{eq}$  and  $r_p$  are the equatorial and polar radius respectively.

- $r_p < r_{eq}$

# Earth Model

- Geodetic Latitude

$$\varphi = \text{asin}(p_z/r)$$

- Geodetic longitude

$$\lambda = \text{atan}(p_y/p_x)$$

- Eccentricity

$$\varepsilon = \frac{r_{eq}^2 - r_p^2}{r_{eq}^2}$$

# Earth Model

- Earth rotates at a constant speed  $\omega_e$
- Velocity at the surface is given by

$$v_0 = \omega_e r_e \cos \varphi$$

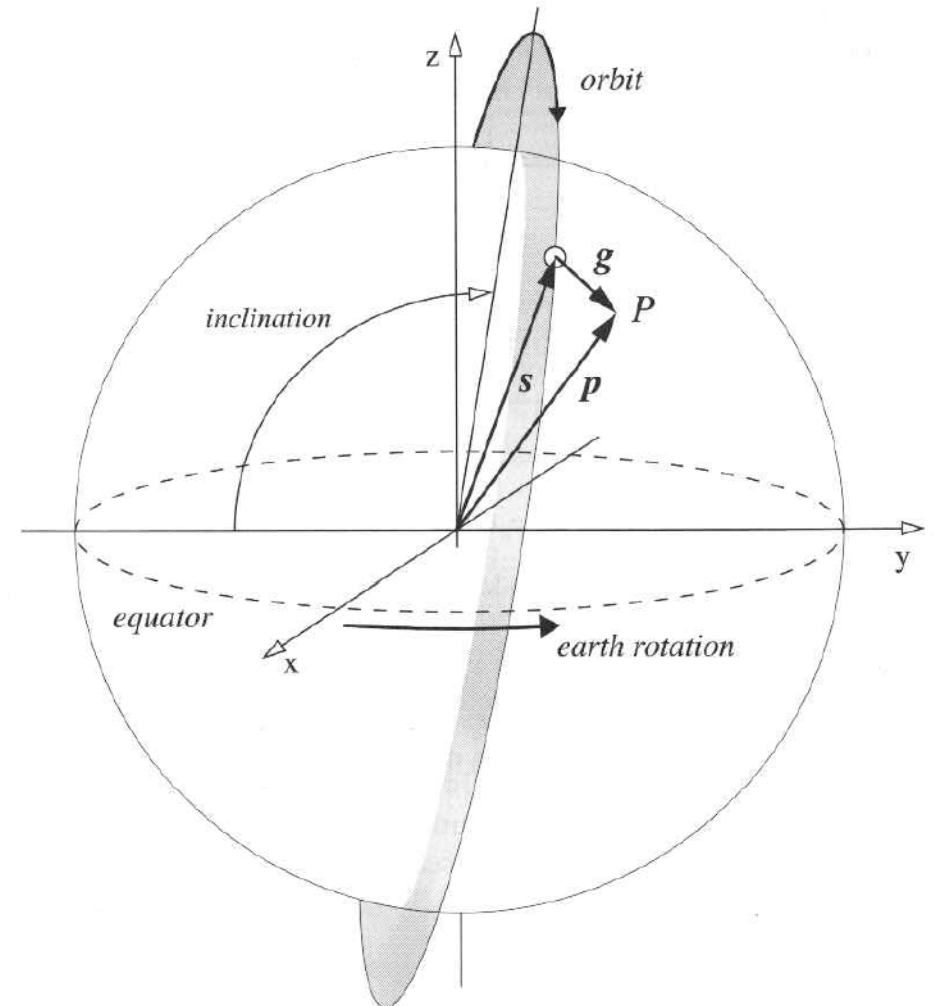
- For polar orbiting satellites

$$v_e = v_0 \cos(i)$$

where  $i$  is the orbit inclination angle

- LANDSAT,  $9.1^\circ$  w.r.t. the poles

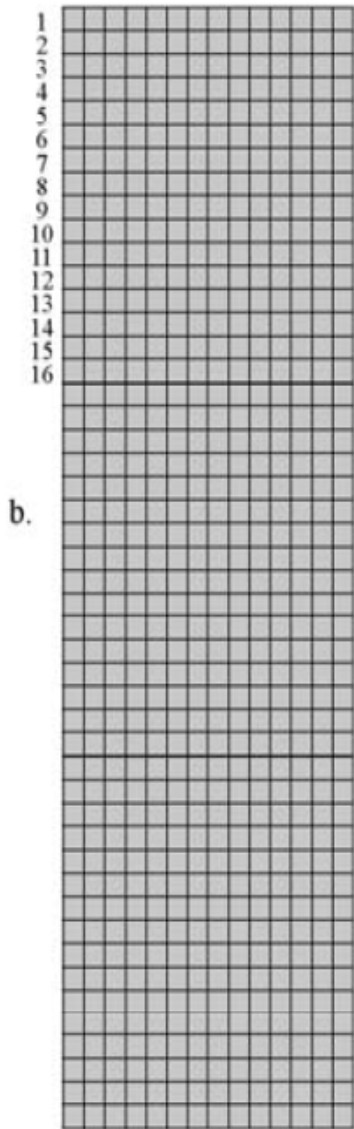
$$v_e = 0.98769 v_0$$



**s**, **g**, and **p** form the fundamental observation triangle



Pixels in a Landsat Thematic Mapper dataset *prior* to correcting for Earth rotation effects



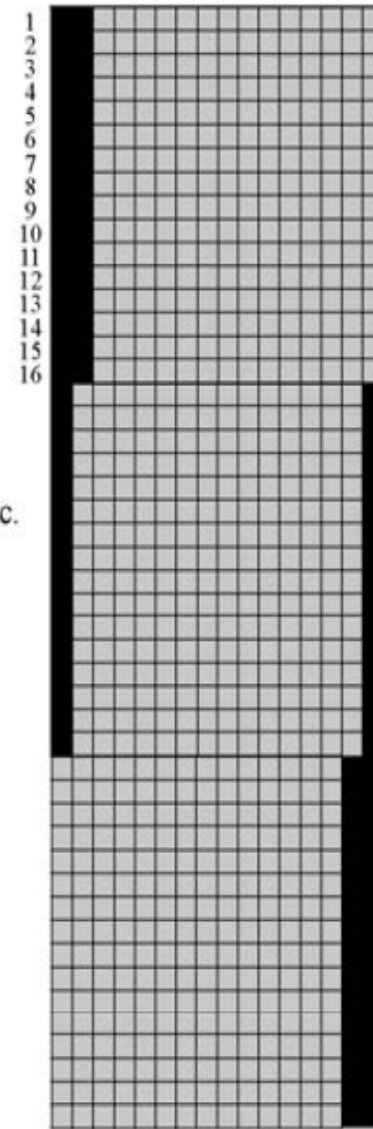
b.

continued

Landsat satellite line of flight



Pixels in a Landsat Thematic Mapper dataset corrected for Earth rotation effects



c.

continued

Earth rotates west to east



Entire scan consisting of 16 lines offset to correct for Earth rotation effects



Usually padded with null values (e.g.,  $BV_{i,j,k} = 0$ )



(Jensen 2000)

# Earth Parameters

parameter	value
equatorial radius	6,378.137km
polar radius	6,356.752km
equatorial circumference	40,075.02km
polar circumference	39,940.65 km
eccentricity	0.00669
angular velocity	$7.2722052 \times 10^{-5}$ rad/sec

# Satellite Orbits

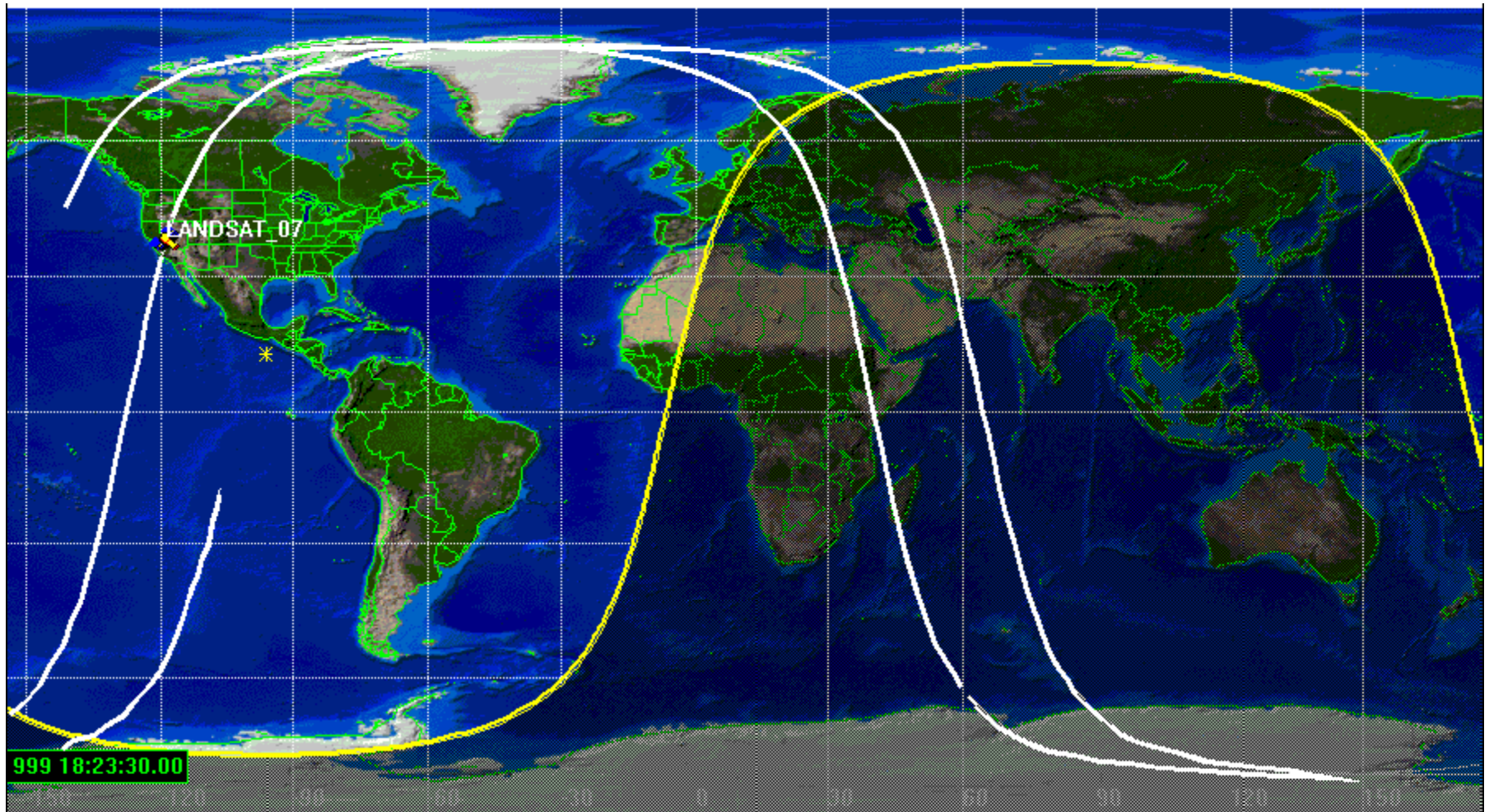
- Standard orbits depend on altitude
  - LEO – low earth orbiting satellite → Few hundreds of miles
  - Geosynchronous → Some 20,000 miles

# LEO Satellites

- Sun-synchronous
  - They cross the equator at the same local time,
  - Maintain a constant solar-illumination angle for observations.
- Ascending and descending node orbits
  - Ascending → South to north
    - NASA Aqua 1:30 PM – ascending mode
  - Descending → North to south (most common)
    - NASA Terra 10:30 AM – descending mode

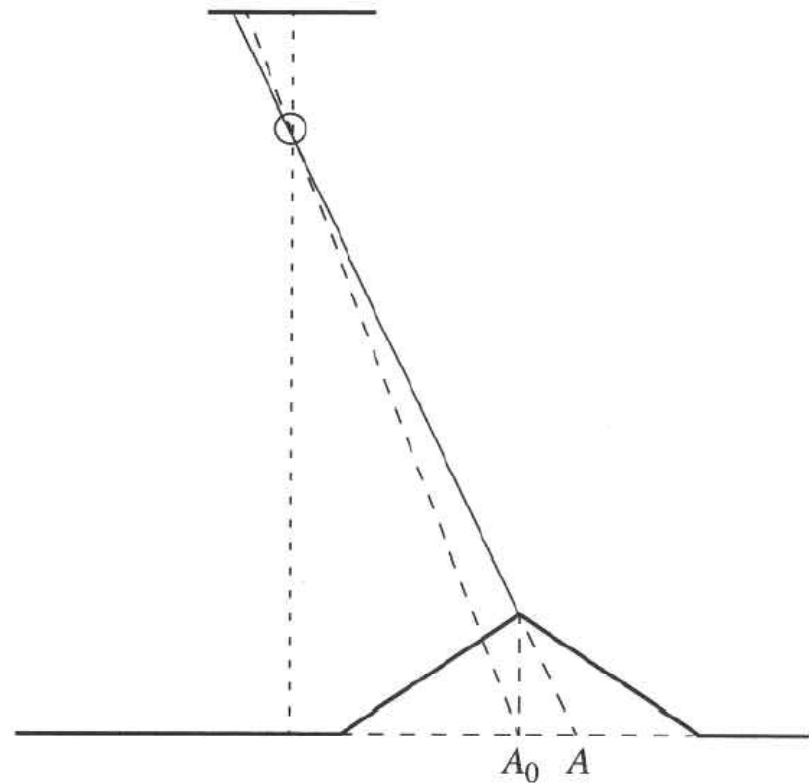
# LANDSAT 7

Descending: day, Ascending at night

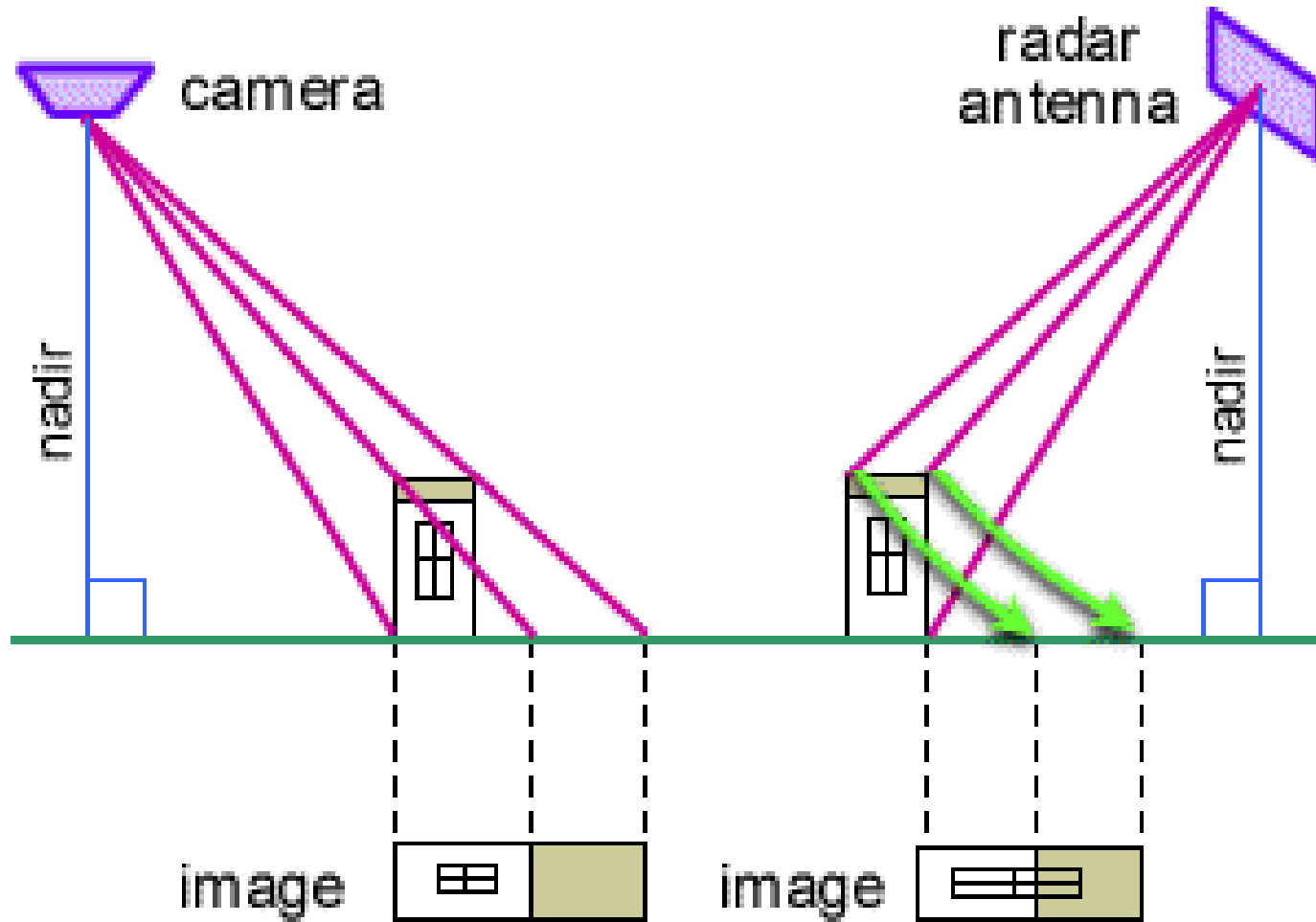


# Topographic Relief (cont.)

- ground point at A actually appears to come from  $A_0$  because of topography



# Relief Displacement



# Topographic Relief

- Image offset proportional to elevation above base plane, or “datum”
- Stereo pair of images can be used to find elevation (see book for more info)
- Imagery corrected for topographic distortion is called “orthographic”



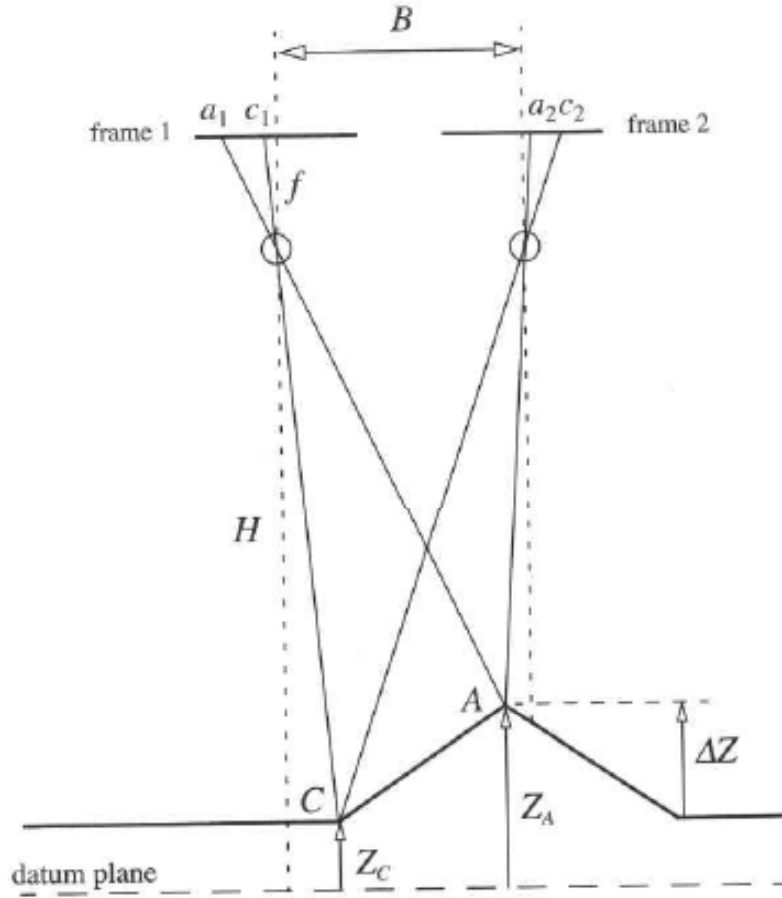


*FIGURE 3-34. Geometry of stereo imaging. The distance between the image points  $a_1$  and  $c_1$  in frame 1 is not equal to the distance between the image points  $a_2$  and  $c_2$  in frame 2 because of the elevation difference between ground points A and C and the different view points of the two frames. The distance between the two view points (called "camera stations" in aerial photography) is called the "base" B of the stereopair.*

- Image parallaxes of ground points A and C are,

$$p_a = a_1 - a_2 = \frac{fB}{H - Z_A}$$

$$p_c = c_1 - c_2 = \frac{fB}{H - Z_C}$$

- H and Z are measured relative to the datum plane, image coordinates, a1, a2, c1 and c2 are measured relative to optical center (principal point) of the respective image

$$\Delta Z \cong \Delta p \frac{H^2}{fB} = \Delta p \times \frac{H}{f} \times \frac{H}{B} = \frac{\Delta p / m}{B/H},$$

# Summary

- This chapter presents how the sensor and acquisition process modifies the signal of interest in remote sensing.
  - The sensor affects the spatial and radiometric quality of the signal.
- Important aspects
  - Spatial features weighted by sensor PSF.
  - Spectral radiance weighted by sensor spectral response
  - Imaging is an affine transform of the radiance
  - Geometric distortions arise from internal sensor and external platform and topographic factors

# Quiz

- Explain PSF, LSF and ESF. How are they related?
- What are optical PSF, detector PSF, image motion PSF.
- How are LSF and ESF measured?
- How is at sensor signal amplified, sampled and quantized.
- Is the sensor model linear? Explain.
- What is sensor calibration.
- What is geometric distortion.
- What is sensor attitude. Explain.
- Explain scanner models and their geometry
- How does earth geometry affect sensor acquisition.
- What is topographic distortion. How is it measured.